

INTERMOLECULAR POTENTIAL ENERGY FUNCTIONS FOR
PAIRS OF SIMPLE POLYATOMIC MOLECULES AND THEIR
APPLICATION TO PROPERTIES OF GASES AND LIQUIDS

by
MARVIN DEAL MARPLES

A DISSERTATION SUBMITTED TO THE FACULTY OF GRADUATE STUDIES OF
THE UNIVERSITY OF FLORIDA
IN PARTIAL FULFILLMENT OF THE REQUIREMENTS FOR THE
DEGREE OF DOCTOR OF PHILOSOPHY

UNIVERSITY OF FLORIDA
June, 1961

INTRODUCTION

There have been several attempts to calculate potential energy functions for relatively small polyatomic molecules in order to determine the precise form of their potentials. The end result of these calculations has usually been the correlation of properties of these polyatomic molecules using the calculated form of the potential energy function as the basis. These calculations, therefore, have been more qualitative than quantitative in their application.

In the present work, these calculated potential energy functions are tested in a more quantitative manner. In Part I, thermodynamic properties for equilibrium states of polyatomic molecules are calculated from both gas and dilute gas data, and are then used in the calculation of potential energy functions for the more complex polyatomic molecules considered. These calculated potential energy functions are then tested by calculating second virial coefficients and comparing with experimental data.

Most of the results of calculated potential energy functions in previous works have been applied to the gas state. In Part II of the present work, an attempt is made to determine if the calculated potential energy functions of Part I can be applied in the prediction of pure liquids. Because of the complexity of using accurate Lennard-Jones or the present work makes use of a simplified model of the liquid state, the modified potential will be used. Experimental measurements of

the thermal pressure coefficient for these compounds are presented and the other values, thermal pressure coefficient and configurational entropy- ΔS relationships are discussed in light of the predictions of this model. Also included in Part II is an investigation of the configurational entropy- ΔS relationship in liquids using the radial distribution function as the basis for discussion.

The author is indebted to the National Science Foundation for providing Cooperative Graduate Fellowships to the author for the period of this study. Grateful also of this field, this study could not have been made. The author also thanks the University of Florida Computing Center for the donation of computer time for much of the calculations. The author appreciates the cordiality help of Dr. T. M. Low, III, who directed the research and was chairman of the supervisory committee, and the contributions of Dr. T. L. Bailey, III, Dr. B. J. Braggins, Dr. J. F. Harkins, Dr. J. T. Hines, and Professor R. B. Nielsen, Jr., who served on the supervisory committee. Thanks are also due to the author's wife for her patience and support and for typing the manuscript.

Barbara Lynn Holladay

TABLE OF CONTENTS

	Page
PREFACE	ii
LIST OF SYMBOLS	vi
LIST OF TABLES	ix
PART I. POTENTIAL ENERGY FUNCTIONS AND THE SECOND VIRIAL COEFFICIENT	
Chapter I INTRODUCTION AND REVIEW	3
Potential Energy Functions for Simple Systems of Interactions	
Interactions between Polyatomic Molecules	
Bonds and Lonepairs	
Dipole and Quadrupole	
Induction	
Dispersion and Repulsion	
II THE SECOND VIRIAL COEFFICIENT AND POTENTIAL ENERGY FUNCTIONS	13
Generalized Lennard-Jones Potential	
Exponential Shell Model	
Exponential Equations for the Second Virial Coefficients	
Exponential Expansion	
Flügel's Correlation	
III EXPONENTIAL FORMS AND POTENTIAL ENERGY FUNCTION PARAMETERS FOR DIFFERENT GROUPS	20
Hydrogen H_2	
Oxygen O_2	
Fluorine F_2	
Chlorine Cl_2	
Bromine Br_2	

	Page
Chap. I I. CALCULATED FOR POLYMERIZED MONOMER	10
CH_2 CH_2 C_2H_4 CCl_4 $\text{C}(\text{CH}_3)_4$ $\text{C}_2\text{H}_5\text{C}(\text{CH}_3)_3$ CH_3 CH_3 $\text{CH}_3\text{C}(\text{CH}_3)_3$	
II. SUMMARY AND DISCUSSION	41
PART II. POTENTIAL ENERGY FUNCTIONS AND THE LIQUID STATE	
III. MEASUREMENT OF CH_3/CH_2 AT LOW TEMPERATURES	15
CH_4 CH_3 CH_2	
IV. THE SPHERICAL POTENTIAL ENERGY MODEL OF THE LIQUID STATE - Molar Volume of Liquids Thermal Expansion Coefficient of Liquids α for Liquids	19
V. CONFIGURATIONAL, SPHERE-PAIR CORRELATION IN LIQUIDS	127
VI. SUMMARY OF PART II	129
TABLES	129
APPENDIX A	147
APPENDIX B	173
APPENDIX C	185
NOTATION	201
BIBLIOGRAPHY	205
SYMBOLICAL INDEX	221

LIST OF FIGURES

	Page
1. Lennard-Jones 6-12 Potential	1
2. Derived Second Virial Coefficients for van der Waals	11
3. Derived Boyle Temperature for van der Waals Potential Energy Function	12
4. Derived Virial Coefficients from van der Waals and from the Spherical Well Potentials	13
5. Potential Energy Functions of Gaseous Hydrogen (H_2), H_2 , and Cl_2	22
6. Potential Energy Functions of Gaseous Hydrogen (H_2 and H_2)	24
7. Second Virial Coefficient of H_2	26
8. Second Virial Coefficient of H_2	27
9. Second Virial Coefficient of H_2	31
10. Second Virial Coefficient of Cl_2	42
11. Potential Energy Function of C_2H_2	46
12. Second Virial Coefficient of C_2H_2	48
13. Potential Energy Function of CO_2	54
14. Coefficients of Potential Energy of CO_2	55
15. Second Virial Coefficient of CO_2	57
16. Potential Energy Function of C_2H_4	59
17. Second Virial Coefficient of C_2H_4	60
18. Potential Energy Function of CH_4	62
19. Second Virial Coefficient of CH_4	63

	Page
139. Potential Energy Function of $\text{CH}_3\text{CH}_2\text{I}_2$	62
140. Second Virial Coefficient of $\text{CH}_3\text{CH}_2\text{I}_2$	64
141. Potential Energy Function of $\text{C}_2\text{H}_5\text{CH}_2\text{I}_2$	65
142. Second Virial Coefficient of $\text{C}_2\text{H}_5\text{CH}_2\text{I}_2$	67
143. Potential Energy Function of CH_3	70
144. Second Virial Coefficient of CH_3	71
145. Potential Energy Function of $\text{CH}_3\text{I} = 1$	72
146. Potential Energy Function of $\text{CH}_3\text{I} = 2$	74
147. Second Virial Coefficient of CH_3I	75
148. Potential Energy Function of $\text{H}_2\text{CCH}_3\text{I} = 1$	77
149. Second Virial Coefficient of $\text{H}_2\text{CCH}_3\text{I}$	79
150. Experimental Apparatus for Measuring $\text{CH}_3\text{I}/\text{CH}_3\text{I}_2$	85
151. Thermal Pressure Coefficients of CH_3	100
152. Representations of CH_3	101
153. Thermal Pressure Coefficients of CH_3	105
154. Equation of State at Zero Reduced Pressure for the Reduced Potential Well Model	111
155. Liquid Water Volume Correlation	114
156. Liquid Water Volume Correlation	114
157. Thermal Pressure Coefficients of A and CH_3	117
158. Thermal Pressure Coefficients of CH_3 and CH_2	118
159. Thermal Pressure Coefficients of CH_3 and CH_2	119
160. β from the Reduced Potential Well Model	122
161. β as a Function of Liquid Volume	123
162. β^2 from the 6-12 Potential	123

	Page
44 ∇ Over Geodesic and Riemannian Manifolds	122
45 ∇^2/ρ vs. ∇^2/ρ for the Spheroidal Shell Potential	140
46 Reduced-Order Approximation for the Spheroidal Shell Potential	149

LIST OF CONTENTS

	Page
1 Reduced Second Virial Coefficients for n - n Pairs of Gases	126
2 Reduced Triple Temperatures for n - n Pairs of Gases	127
3 Potential Energy Function Parameters from Second Virial Coefficients (I)	128
4 Bond Lengths (II)	135
5 First-Order Formations for the n - n Pairs of Gases (I)	140
6 Procedures Used in Calculating Potential Energy Functions of Gaseous States	141
7 Summary of Potential Energy Function Calculations for Gaseous States	142
8 Potential Energy Function of H_2	144
9 Potential Energy Function of H_2	145
10 Potential Energy Function of H_2	146
11 Potential Energy Function of H_2	147
12 Potential Energy Function of H_2	148
13 n - n Potential Functions for H_2	149
14 Potential Energy Function of H_2	150
15 Critical Temperatures and the Maximum Factor	151
16 Calculated Parameters for Isopropyl Alcohol	152
17 Potential Energy Function of H_2	153
18 Potential Energy Function of H_2	154
19 Potential Energy Function of H_2	155
20 Potential Energy Function of H_2	156

	Page
21. Potential Energy Function of $\text{C}_2\text{H}_2\text{H}_2$	147
22. Potential Energy Function of CH_4	148
23. Potential Energy Function of H_2O	149
24. Potential Energy Function of $\text{Si(CH}_3)_4$	150
25. Thermal Pressure Coefficients and Compressibility of CH_4	151
26. Thermal Pressure Coefficients of CH_4	152
27. Liquid Vapor Volume Correlations and Extrapolated Liquid Volume at 0°C	153
28. α for CH_4 and CH_2	154
29. Configurational Entropy and Other Volume of Liquids	155
30. Formulas Used in Figures 42 and 43	156
31. Relativistic Expressions r_{rel}^2 and r_{rel}^2/r_0^2	170
32. Spherical Shell Potential, $r_0^2 = 1.70$	171
33. Spherical Shell Potential, $r_0^2 = 1.40$	172
34. Spherical Shell Potential, $r_0^2 = 1.70$	173
35. Spherical Shell Potential, $r_0^2 = 1.60$	174
36. Spherical Shell Potential, $r_0^2 = 1.50$	175
37. Spherical Shell Potential, $r_0^2 = 1.30$	176
38. Reduced Boiling Temperature for the Spherical Shell Potential	177
39. Lennard-Jones 6-12 Potential	179
40. Lennard-Jones 6-12 Potential	180
41. Lennard-Jones 6-12 Potential	181
42. Lennard-Jones 6-12 Potential	182
43. Lennard-Jones 6-12 Potential	183
44. Lennard-Jones 7-14 Potential	184
45. Lennard-Jones 7-14 Potential	185

PART I

POTENTIAL ENERGY FUNCTIONS FOR THE SPHERICAL TRIAXIAL COORDINATE

CHAPTER 1

INTRODUCTION AND SCOPE

When considering the physical properties of pure liquids and gases and also fluids that in order to understand the observed properties, it is necessary to have some understanding of interactions in the molecular media. The simplest system in which interactions between atoms and molecules can be described is one which consists of an isolated pair of atoms (or molecules). From quantum mechanical considerations, it has been determined that a pair of atoms will interact with others at relatively large separations, and will interact with others at very small separations. In some intermediate cases there will be no net force of interaction. These interactions are described by the relative pair potential energy as a function of interatomic separation. The force acting on each particle of the isolated pair at any given separation is determined as the negative of the slope of this potential energy function at that separation. The most form of the potential energy function desired is presented in Section 1.1. From quantum mechanical theories of the simplicity of the problem. For this purpose several attempts have been made to develop a rather satisfactory atomic approximation to the potential energy function which would at least approximate physical reality.

Potential Energy Functions For Simple Systems of Interactions

The most widely used of these approximations has been the

Lennard-Jones potential and this will be the only very long-range energy function discussed here. This will allow later on to combine energy functions for the single nature of interaction and discussed by Hirschfelder, Gaildog, and Boyd (1).

The Lennard-Jones 12-6 potential has been found to be useful in the calculation of properties of the inert gases liquids and other gases with relatively small molecules. This potential energy function is not necessarily the best representation for each one of this type of pair nuclei, but it does serve quite well for now. This potential for pair-wise calculation is

$$V(r) = \epsilon \left[\left(\frac{r_0}{r} \right)^{12} - \left(\frac{r_0}{r} \right)^6 \right] + \epsilon \left[\left(\frac{r_0}{r} \right)^{12} - \left(\frac{r_0}{r} \right)^6 \right] \quad (2)$$

The meanings of the symbols can be seen in Figure 1 and are described below.

$V(r)$ = Potential energy of interaction

r = Value of r at the minimum of $V(r)$

ϵ = Value of $-V(r)$ at the minimum of $V(r)$

r_0 = Value of r when $V(r) = 0$

ϵ = Maximum attractive constant of atoms or molecules

The term which includes the short-range repulsion represents the long-range attractive forces and is presumed to be as by quantum mechanics for negative potentials. The term contains the short-range repulsion constant represents the short-range repulsive forces. This form of representation of the repulsive forces can be justified by quantum mechanics. The repulsive part is thought to arise principally for inter-nuclear separations and because the repulsive forces are known to be very large and to change rapidly at small separations.

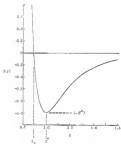


Figure 1 Landau-Lifshitz-Aldrich (LLA) function

TRANSITION-AMPLITUDE FORMULAS FOR SPIN-1

For a two nucleus molecule the operators \hat{u}^A and \hat{u}^B are given by the formulae. For this purpose it is desirable to generalize also here a two particle energy function to allow other values of the operators. With this in mind, one gets an equation of the form

$$\text{DET } \alpha \frac{d^2}{dt^2} \left[\frac{1}{2} \frac{d^2}{dt^2} \right] + \left(\frac{d^2}{dt^2} \right)^2 \quad (10)$$

where α is a transition operator.

α is a transition operator, and

α is a transition between molecular states

\hat{u}^A, \hat{u}^B are defined as before.

The transition \hat{u}_A in plane is given by \hat{u}_A^B by

$$\hat{u}_A^B = \frac{1}{2} \left(\frac{d^2}{dt^2} \right)^2 \quad (11)$$

Equation 11 contains several of these \hat{u}_A^B potentials in having form

There have been several attempts to determine the proper form of the function representing the potential energy of interaction of two isolated polyatomic molecules as a function of the electron between their nuclei. Thus these previous work influenced and were used in the present work, a total energy of two will be given here. These previous papers are discussed by Pythagoras [1].

Energy and Angular Momentum. These authors assumed that the potential energy of interaction between two spherically symmetrical polyatomic molecules could be found by summing the interactions between all possible pairs of atoms in the molecules and averaging these interactions over all orientations. It was assumed that there was no overlap

free rotation of the molecules. The intermolecular potential energy function stage is assigned molecular mass assumed to follow the same form as the 4-12 potential energy function.

The procedure of calculation was as follows: an expression was written for the energy of interaction between every pair of atoms (one free and one attached to the surrounding molecule) as a function of interatomic and distance between molecular centers. This expression was then averaged over all orientations of the free molecules, giving equal weight to all orientations. The total internal molecular pair potential energy was equal to the sum of the intermolecular energies for the atom pairs.

The assumption in the averaging process was that the atoms were rigid, which made the results better in that than the lattice series selection by Pitzer and Lippman (19) which will be discussed later.

Although the results were applicable to any two collections of the type $\delta_{\alpha}\delta_{\beta}$ and $\delta_{\alpha}\delta_{\beta}$ (Koster and Lippman) only calculations for only one case. The assumption made here was that

1. $\delta_{\alpha} = 0$ if $\alpha = 2$ or $\alpha = 3$ or $\alpha = 4$; $\delta_{\alpha} = 0$ if $\alpha = 5$; that is, intermolecular interaction collection of the form $\delta_{\alpha}\delta_{\beta}$.
2. The sum of all stages in the collection is the same, $\sum_{\alpha} \delta_{\alpha}$.
3. $\delta_{\alpha}^2 = \delta_{\beta}^2 = \delta_{\gamma}^2$.
4. The relation in the potential energy function for all pairs of atoms in the case was equal to $\delta_{\alpha}\delta_{\beta}$.
5. $\delta_{\alpha}^2 = \delta_{\beta}^2$ where δ_{α} is the distance from the center of the atom pair to the center of the paragonal stage.

Then the potential energy function is function of distance between molecules centered was calculated for this case. It was found that a

combined potential V_{ij} in the matrix could be obtained using the Lennard-Jones type of potential energy function. Equation 11 was equivalent to a $\sigma = 5$ and $\epsilon = 20$, V_{ij} is a 7-12 potential energy function. The authors described procedures for this potential energy function for several molecules from contact radial coefficients etc. This potential was found to correlate quite well the volumes such as CH_4 , C_2F_4 , SF_6 and C_6H_6 , but was found to give poor agreement for these volumes which were more compressible than those from the Lennard-Jones 6-12 potential.

Since their results for interactions between two molecules are given correctly and will be used later, their general equation will be given here. The following equations apply to interactions between two molecules i and j , assuming only that there is no overlap. This implies that the total interaction energy is the sum of all interactions between atom pairs. Equal weight is given to all interactions of the two molecules. No other assumptions were used.

$$V_{ij} = V_{ijc} + V_{ijp} + V_{ijc} + V_{ijp} \quad (12)$$

where V_{ij} = Total interaction potential energy between the two molecules

R = Distance between molecular centers

V_{ijc} = Potential energy of interaction between central atoms
(atoms i and j are at center of molecule)

V_{ijp} = Potential energy of interaction between central and all peripheral atoms

V_{ijp} = Potential energy of interaction between all peripheral atoms

$$r_{10} = -\frac{1}{2} \epsilon_{10}^2 \left[\left(\frac{f_{10}^2}{g} \right)^{12} - 2 \left(\frac{f_{10}^2}{g} \right)^9 \right] \quad (3)$$

$$r_{10} = -\frac{1}{2} \epsilon_{10}^2 \left[\frac{\left(\frac{f_{10}^2}{g} \right)^{12}}{2g^2 f_{10}} \left[\left(1 - \frac{f_{10}}{g} \right)^{-12} - \left(1 + \frac{f_{10}}{g} \right)^{-12} \right] \right.$$

$$\left. - \frac{\left(\frac{f_{10}^2}{g} \right)^9}{2g^2 f_{10}} \left[\left(1 - \frac{f_{10}}{g} \right)^{-9} - \left(1 + \frac{f_{10}}{g} \right)^{-9} \right] \right\} \quad (4)$$

$$r_{10} = -\frac{1}{2} \epsilon_{10}^2 \left[\frac{\left(\frac{f_{10}^2}{g} \right)^{12}}{2g^2 f_{10}} \left[\left(1 - \frac{f_{10}}{g} \right)^{-12} - \left(1 + \frac{f_{10}}{g} \right)^{-12} \right] \right.$$

$$\left. - \frac{\left(\frac{f_{10}^2}{g} \right)^9}{2g^2 f_{10}} \left[\left(1 - \frac{f_{10}}{g} \right)^{-9} - \left(1 + \frac{f_{10}}{g} \right)^{-9} \right] \right\} \quad (5)$$

$$r_{10} = -\frac{1}{2} \epsilon_{10}^2 \left[\frac{\left(\frac{f_{10}^2}{g} \right)^{12}}{2g^2 f_{10}} \left[\frac{f^2}{g^2} - \frac{f^2}{2g^2} + \frac{2f^2}{2g^2} - \frac{2f^2}{2g^2} + \frac{f^2}{g^2} - \frac{f^2}{g^2} \right] \right.$$

$$\left. + \frac{f^2}{g^2} - \frac{f^2}{2g^2} + \frac{2f^2}{2g^2} - \frac{2f^2}{2g^2} \right]$$

$$- \frac{4f_{10}^2}{g^2 f_{10}} \left[\frac{f^2}{2g^2} - \frac{f^2}{2g^2} + \frac{f^2}{2g^2} - \frac{f^2}{2g^2} \right] \right\} \quad (6)$$

$$\cos \theta = \frac{2}{3} \frac{1}{\sqrt{10}} \quad (2)$$

$$\cos \theta = \left(\frac{1}{3} + \frac{2}{3} \frac{1}{\sqrt{10}} \right)^{1/2} = f^2 \quad (3)$$

$$\cos \theta = \left(\frac{1}{3} - \frac{2}{3} \frac{1}{\sqrt{10}} \right)^{1/2} = f^2 \quad (4)$$

\vec{e} is chosen free vector of arbitrary magnitude from the unit sphere

$\vec{e}^T = \vec{e}^T$ is Hermitian in Limited-Order δ -Q potential for some δ .
 Similarly $\delta = \frac{1}{2}, \frac{1}{3}, \frac{1}{4}$ refer to the chain lengths.

Noting that these equations can be used directly for interactions between two isolated CH_2 radicals, where $a = a = \frac{1}{2}$, $b = b = \frac{1}{2}$ and

$$\vec{e}(\vec{e}) = \vec{e}_{12} + \vec{e}_{34} + \vec{e}_{56} \quad (5)$$

The value of \vec{e}_{12} is one in the $\delta = \frac{1}{2}$ bond length. Other members of this type include $\vec{e}_{13}, \vec{e}_{14}, \vec{e}_{23}, \vec{e}_{24}, \vec{e}_{34}$ and $\vec{e}_{45}, \vec{e}_{56}$. If CH_2 groups are considered to interact in single chains

The results of Huggins and Lenz are also applicable to molecules in which there is no chain in the center such as in the aromatic gases $\text{H}_2, \text{O}_2, \text{N}_2, \text{CO}_2$, and CH_4 . For these molecules, equation 5 gives the total interaction. The parameters for these molecules are $a = a = \frac{1}{2}$, $b = b = \frac{1}{2}$, and the value of \vec{e} is such that it satisfies the total length is made of the molecules.

There is another type of molecule for which the equations of Huggins and Lenz are also applicable. These are molecules such as CH_2F_2 and $\text{CH}_2\text{CH}_2\text{F}_2$ in which, when freely rotating the molecules, there are always found 12 distinct positions. Equation 5 can be used for all

Calculations of the electron in the potential $V(r) = -12.13/r$ eV (CCl_4 , CCl_2 and BF_3 were used by multiplying interaction momentum by the ratio r from water and using the derived equation). We use parameters for chlorine atoms in BF_3 and BF_2 . Other values and parameters (g^N and r^N) calculated from data on gas viscosity of BF_3 . They used these same conversions for water and for sulfur dioxide also. In the calculations for CCl_4 the parameters for the different stages were determined from data on the second virial coefficient of CCl_4 gas. The parameters for the nucleus stages were taken to be those of neon. These calculated values of g^N and r^N for the molecules were compared with well potential energy function parameters determined from experimental data and were found to be in reasonable agreement. In writing the code of the stages of the subsequent potential energy functions. It will be shown later that a variation of g^N and r^N values without taking two stages of the potential energy function into account is of doubtful value.

Section II.D. Potentials derived by use of dispersion potentials as the general expression for the interaction of an isolated pair of quadrupole quadrupole, quadrupole octapole, etc. In considering the importance of interaction to be in the asymptotic region, and since the longest interactions are between peripheral atoms, we considered the entire interaction between molecules to be due to interactions among peripheral atoms. We assumed that interactions between pairs of atoms would be represented by a Lennard-Jones 12-6 potential energy function and that the total intermolecular between molecules is the sum of the interactions between all pairs of atoms. The derivation is valid for the solution in a glass problem and then we attempt to give the average interactions from all orientations of the two molecules as in the

is given diagrammatically. In the present expression there are several terms which are not dependent on molecular shape, size, mass, and orientation and several terms which depend upon the shape, size, mass, and orientation of the molecule. These terms can usually be used to describe the interaction effects for polymeric solutions. These terms are of the greatest interest. The authors concluded that for asymmetric polyatomic molecules the electrostatic term was only a small contribution as long as the separation between molecules is large compared to the size of the molecule. The electrostatic term was found to govern, in agreement with intuition, which suggested that reaction of the molecules to get average potentials. From the data on the second virial coefficient of C_2H_4 and the critical temperature of this derivative, it is concluded that the London-dispersal potential interaction parameter for the chlorine chain should be

$$\begin{aligned}\epsilon_0^2 &= \epsilon_{\text{L}}^2 \\ \epsilon_0^2 &= \frac{1}{2} \epsilon_{\text{L}}^2\end{aligned}$$

For C_2H_4 it was found that $\epsilon_{\text{L}}^2 \approx \epsilon_0^2$.

The authors also show calculating interaction between methyl and ethylene molecules. The ϵ^2 values for the methyl gas of chlorine gas are probably too small for peripheral cases. For these cases must be considered as the values of the ϵ^2 values are

...available. The authors also show that the most exact method for determining potential energy functions of gases is the recording of ionization energy. Their experiments usually give the potential energy of interaction and they discuss various aspects of experimental interest. For this reason these authors, in the present case, use of electron values to

conclusion, although part of the potential energy functions of various groups, properties. It is hoped that this will not be true in the case of the. The work by Kohn and Pines has shown a large range of potential equations, but none of their calculations are similar to the work done here and should be compared.

From the existing data, potential energy functions were determined for the systems H^2-CH_4 , $H^2-C_2H_2$, $H^2-C_2H_4$, $H^2-C_2H_6$, $H^2-C_2F_4$, $H^2-C_2F_6$, and $H^2-C_2F_8$. These potential energy functions were valid at separations where the Fermi case applies. The values and the potential energy functions for CH_4 and CF_4 with the hydrogen ions, no precise potential energy functions for hydrogen ions and C_2H_2 , and C_2F_4 .

In the first series, the interaction between $H^2-C_2H_2$ and $H^2-C_2F_4$ were assumed to be the relatively no interaction between hydrogen ions and the hydrogen and chlorine atoms in C_2H_2 and C_2F_4 respectively. The interaction between the hydrogen and chlorine atoms were assumed to be as the average of their group. The same assumption was made for interaction between H^2-CH_4 and H^2-CF_4 and interaction potentials for hydrogen and chlorine atoms with H^2 were assumed from the H^2-CH_4 and H^2-CF_4 data. This was done by deriving equations for the interaction of an atom with a diatomic molecule which is the system discussed previously. These parameters for hydrogen and chlorine interaction with CH_4 and CF_4 data were then used to calculate the potential energy of interaction between $H^2-C_2H_2$ and $H^2-C_2F_4$. The calculated and experimental results agreed within a factor of two over the entire range of separations. A similar procedure was followed to calculate the potential energy functions for

$\text{CH}_3^+ = \text{C}_2\text{H}_3^+$ and $\text{CH}_3^- = \text{C}_2\text{H}_3^-$. Two-center overlap matrix elements for $\text{CH}_3^+ = \text{C}_2\text{H}_3^+$ and $\text{CH}_3^- = \text{C}_2\text{H}_3^-$. In this case, overlap matrix elements were not defined at asymptotic and the asymptotic overlap is infinite. The asymptotic eigen was within a factor of 10, too.

The other overlap case was to assume that, in CH_3H_2 and CH_3H , there were two centers of interaction. For example, atoms are considered to be two centers separated by the usual $\text{C}-\text{C}$ distance to obtain a better description was made for CH_3H_2 . The interaction energies were taken as the center of the carbon atom in CH_3H_2 and CH_3H . Parameters for CH_3 and CH_2 groups were determined as before. This data on CH_3 and CH_2 and the potential energy functions for CH_3H_2 and CH_3H were calculated. The asymptotic eigen was within a factor of ten between calculated and experimental potential energies.

CHAPTER II

THE SECOND VIRIAL COEFFICIENT AND BODILIAN EXPANSION FUNCTIONS

The equation of state for imperfect gases can be written in the form

$$\frac{P}{P_0} = 1 + \frac{B(T)}{V} + \frac{C(T)}{V^2} + \frac{D(T)}{V^3} + \dots \quad (1)$$

where P is absolute pressure,

P_0 = Tolson gas scale

T = absolute temperature

V = gas constant

The coefficients $B(T)$, $C(T)$, and $D(T)$ are called the second, third, and fourth virial coefficients, respectively, and are directly related to the interactions between the molecules of the gas.

This equation of state describes at the density of the liquid and is used primarily for gases at low to medium density. The coefficient $B(T)$ is introduced to account for interactions of pairs of molecules. $C(T)$ for interactions between three molecules. $D(T)$ for interactions between four molecules, etc. Therefore, at low density, use of the second virial coefficient is usually sufficient, but as the density increases, more virial coefficients are also to use.

There is a large volume of data available on the second virial coefficient of gases, but data on the third and higher virial coefficients must be classified as unreliable because of experimental

interactions of various quark-quark pairs. By construction, including an n quark-quark vertex from the quark self-energy diagram requires that it has different fermion-level coefficients. So in an explicit action calculation we have limited to the second virial coefficient.

For eight-component potential energy functions, the second virial coefficient is given by [1,11]

$$B(T) = -\frac{1}{2} \int_0^\infty \left(e^{-\beta U(r)} - 1 \right) r^2 dr \quad (4.1)$$

where the symbols have the same meaning as given previously.

Quark-quark Lennard-Jones Potential

For the quark-quark form of the Lennard-Jones potential energy from [14], Equation 3, the second virial coefficient is given by substituting the Lennard-Jones into (4)

$$B(T) = -\frac{4\pi m}{3} \left(\frac{a}{r_0} \right)^{12} \int_0^\infty r^{12} \sum_{l=0}^\infty \gamma^{(l)}(r) dr^3 \quad (4.2)$$

$$\text{where } \gamma^{(l)}(r) = \frac{1}{4\pi r^2} \left| \frac{\partial^l U}{\partial r^l} \right| \quad (4.3)$$

$$r = \left(\frac{a}{r_0} \right) \left(\frac{r}{r_0} \right)^{1/6} \quad (4.4)$$

$$+ \frac{r^2 \partial^2 U}{1 - \partial^2} \quad (4.5)$$

$$= 1 / \frac{2\pi^2}{3} \frac{1}{T^3} \quad (17)$$

by direct calculation, it can be shown that

$$C_V = \left(\frac{4}{3} \right) \frac{1}{T^3} \quad (18)$$

Thus for simple polycrystalline materials, the constant of integration will differ from one material from to another and be temperature, and if the potential energy function were suitably fitted by the generalised Lennard-Jones potential, the different materials would have different values of α and β . It is shown in Equation 18 that the second virial coefficient is a function of α and β as well as of temperature. Calculations of the second virial coefficient were made by hand for the present work for several values of α and β in order to determine how sensitive a function the second virial coefficient is of α and β . For convenience and to save the trouble even made, the calculations were done by computer (see The reduced second virial coefficient $B^*(T^*)$ is defined as

$$B^*(T^*) = \frac{B(T)}{\frac{3}{4} \pi \sigma^3} \quad (19)$$

and the reduced temperature T^* is defined as

$$T^* = \frac{kT}{\epsilon} \quad (20)$$

where k is Boltzmann's constant

Calculations of B^* as a function of T^* have been made for the 6-12 potential energy function and are given by Bircakofsky, Gurev and

where $\Gamma = \frac{1}{2} \frac{d\sigma}{d\Omega}$ is the cross section of π^0 in a particular π^0 decay. The π^0 decay cross section was calculated numerically for the 4-21, 4-22, 4-23, and 2-21 potential. Using the numerical values of Γ from Table I, Γ^0 values for π^0 were calculated. The Γ^0 values in Equation (1) decrease rapidly as high values of π^0 are chosen, but decrease as low Γ^0 . The calculated Γ^0 values are listed for low values of Γ^0 because of the order of them it was necessary to use the Γ^0 values in Γ^0 for low Γ^0 .

Using the general equations for Γ^0 for π^0 and potential (Equations 10-14) are given below, the final equations for calculating Γ^0 are given below for each of the potential energy functions presented above.

4-21 Potential

$$\Gamma^0 = \frac{1}{2} \frac{d\sigma}{d\Omega} \frac{1}{\Gamma^0}$$

$$\Gamma^0 = \frac{1}{2} \frac{d\sigma}{d\Omega} \frac{1}{\Gamma^0} \left[\Gamma^0 \left(\frac{1}{2} \right) \right] \frac{1}{\Gamma^0} \quad (15)$$

4-22 Potential

$$\Gamma^0 = \frac{1}{2} \frac{d\sigma}{d\Omega} \frac{1}{\Gamma^0}$$

$$\Gamma^0 = \frac{1}{2} \frac{d\sigma}{d\Omega} \left[\Gamma^0 \left(\frac{1}{2} \right) + \frac{1}{2} \sum_{j=1}^{\infty} \left[\Gamma^0 \left(\frac{j}{2} \right) \right] \frac{1}{j} \right] \quad (16)$$

$$\Gamma^0 = \frac{1}{2} \frac{d\sigma}{d\Omega} \frac{1}{\Gamma^0} \frac{1}{\Gamma^0}$$

Ex. 1.1.10 (1)

$$x_1^2 = x^{1/6} y^{1/3}$$

$$x^2 = x^{1/6} \left[\Gamma\left(\frac{1}{6}\right) + \frac{1}{2} \sum_{n=1}^{\infty} \left[\Gamma\left(\frac{3n+1}{6}\right) \frac{x^n}{n!} \right] \right] \quad (2)$$

$$x = 4(3)^{-1/6} y^{1/3} \quad x^2 y^{-1/3}$$

Ex. 1.1.10 (2)

$$x_1^2 = x^{1/7} y^{1/3}$$

$$x^2 = x^{1/7} \left[\Gamma\left(\frac{1}{7}\right) + \frac{1}{2} \sum_{n=1}^{\infty} \left[\Gamma\left(\frac{3n+1}{7}\right) \frac{x^n}{n!} \right] \right] \quad (2)$$

$$x = 4(3)^{-1/6} y^{1/3} \quad x^2 y^{-1/3}$$

Ex. 1.1.10 (3)

$$x_1^2 = x^{2/3} y^{1/3}$$

$$x^2 = x^{2/3} \left[\Gamma\left(\frac{1}{3}\right) + \frac{1}{2} \sum_{n=1}^{\infty} \left[\Gamma\left(\frac{3n+1}{3}\right) \frac{x^n}{n!} \right] \right] \quad (2)$$

$$x = 3(3)^{-1/3} y^{1/3} \quad x^2 y^{-1/3}$$

Table 1, column 6).

$$\sigma_{\frac{1}{2}}^{\frac{1}{2}} \approx 2^{0.47} r^{\frac{1}{2}}$$

$$r^{\frac{1}{2}} = r^{\frac{1}{2}} \left[\left(\frac{r}{r_0} \right)^{\frac{1}{2}} + \frac{1}{2} \sum_{n=1}^{\infty} \left(\frac{r}{r_0} \right)^{\frac{1}{2} + n} \right] \quad (2)$$

$$r = (2r_0)^{-1/2}$$

The results of these test calculations are given in Table 1, column 6. The $\sigma_{\frac{1}{2}}^{\frac{1}{2}}$ values for the 5-12 and 7-12 potentials (see below) are very different from the $\sigma_{\frac{1}{2}}^{\frac{1}{2}}$ values shown in Figure 2.

The correct virial coefficient is not a very sensitive test of the form of the potential energy function because the virial coefficient can often be correlated equally well by several new potentials. The values of the virial coefficients B^0 and B^1 of various systems give the potential to which the data are fitted. Therefore, it is of interest to consider the relationship among the B^0 and B^1 values for various new potentials. It is of special interest to consider the B^0 values alone since they are more sensitive to changes in potential energy function than B^1 values.

The relationship among B^0 values calculated from experimental second virial coefficient data for various new potentials can be determined by calculation of the Boyle point for new potentials. The Boyle temperature, T_B , is defined as the temperature at which the second virial coefficient is zero. Note that since $B^0 < 0$ when $T^0 < T^B$, T_B is less than T^0 . Note the reduced second virial coefficient plots given in Figure 3, and the T_B values for reduced Boyle temperatures for each of the 5-12, 6-12 and 7-12. This was done for the potentials shown in

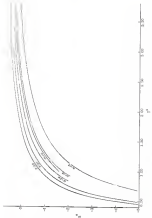


Figure 2. Reduced Viscosity (η_{sp}/c) versus Concentration (c/c_0)

Figure 2, and the related Regge trajectories are given in Table 3. The values for the $\alpha(0)$ and $T=0$ potentials were given by Hansen and Linderh (2). These results are also given in Figure 2, which can be used to determine Regge trajectories for other α trajectories.

Using these related Regge trajectories values it is possible to derive also the relationship among the \mathcal{L}^2 values for the various α potential energy functions dependent from experimental data derived around the Regge point. In the Regge point,

$$\frac{\mathcal{L}_{\alpha=0}^2}{\mathcal{L}_{T=0}^2} = \frac{\sum_{k=1,2}^n}{\mathcal{L}_{T=0}^2} \quad (22)$$

This ratio is also given in Table 4 for the various potentials. The data in Table 3 show that for a given set of experimental elastic elastic coefficients data in the neighborhood of the Regge point, the value of \mathcal{L}^2 for a $T=0$ fit to the data would be about twice that for a $\alpha=0$ fit. This immediately why it is important to specify the stage of the potential energy function when comparing \mathcal{L}^2 values with r^2 values, since \mathcal{L}^2 and r^2 are not independent.

Values for Linderh (2) have analytically extracted \mathcal{L}^2 and r^2 from several elastic coefficients around the Regge point for several simple potentials for both the $\alpha=0$ and $T=0$ potentials. These data should allow a check on the value of the ratio $\mathcal{L}_{\alpha=0}^2/\mathcal{L}_{T=0}^2$ determined above the data. Along with this ratio of \mathcal{L}^2 's are given in Table 5. It can be seen that, except for the last three columns the agreement with the value $\mathcal{L}_{\alpha=0}^2/\mathcal{L}_{T=0}^2 = 2.0$ derived from the related energy elastic coefficients is quite good.

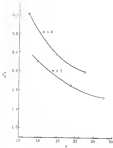


Figure 2 Reduced Spin Temperatures, for $n=2$ Principal Energy Functions

may give, in turn, a convenient way for the calculation of the potential energy function, $\Phi(\mathbf{r})$, and the primary structure, \mathbf{r}_i , of the molecule. It is of course not true that $\Phi(\mathbf{r})$ can be regarded as a function of the coordinates \mathbf{r}_i of the atoms, but this fact $\Phi(\mathbf{r}) = \Phi(\mathbf{r}_i)$ holds in what follows.

For the calculation of the vibrational frequencies by using the harmonic approximation, different potentials must be used, one for each vibrational degree of freedom. Since the atoms are assumed to occupy potential energy functions equally well, the potentials should not be quite different for the different potentials. Therefore, one should consider first as suitable the potential energy function of some equivalent central vibrational coefficient data will be fitted, especially if the potentials are to be used to calculate other properties.

Spherical Shell Model

One of the limitations upon using as the type potential energy function is the fact that the potential energy must be a function of the coordinates of the atoms. The potential energy function of the atoms is a function of the coordinates of the atoms, and the coordinates of the atoms are not available for any different are possible. Later, when, however, one of several vibrational coefficients using the type potential energy function are not really available with respect of temperature with the central vibrational coefficient data are available.

A recent work, by Debye and Hückel (11) is quite useful as a step in developing this method. They have derived equations for the central vibrational coefficient based on the spherical shell model and the central vibrational coefficient by the use of a statistical approach, which can be used in calculating equilibrium data. The spherical shell

The parameter β_{ij}^0 with values $\beta_{ij}^0 = 1$ for dihalides of the elements $\text{Ga}, \text{In}, \text{Sn}, \text{Pb}$, and $\beta_{ij}^0 = 0$ for the remaining elements, $\beta_{ij}^0 = 0$ for Ga and In , and $\beta_{ij}^0 = 1$ for Sn and Pb , is used to take into consideration the correlation of angular momentum β_{ij}^0 in the calculation, a parameter α is used to take into account the correlation of the wave function ψ for a given value of the angular momentum, $\alpha = 1$ for Ga and In , and $\alpha = 0$ for Sn and Pb . A more convenient procedure to obtain β_{ij}^0 is to use β^0 as the main parameter for the peripheral atoms and β_{ij}^0 for the atoms near the center of the molecule in the peripheral atoms. Furthermore, by calculating several spherical shell potentials one can determine the relationship between β^0/β_{ij}^0 and β^0/β_{ij}^0 . Several spherical shell potentials for different values of β_{ij}^0 were calculated in the present work, and from these calculations the relationship between β^0/β_{ij}^0 and β^0/β_{ij}^0 is obtained. This is slightly in error in Table II and Figure II of Appendix A.

There are several reasons for using the spherical shell approximation for several values of β_{ij}^0 . If it is calculated a parameter energy function for a molecule in which there is no interaction between its fragments other than that of a single spherical shell, then the spherical shell potential would not be useful. In order to determine approximately which spherical shell potential best fits the calculated potential energy function, it is necessary to have many spherical shell potentials across the molecule. Several of these spherical shell potentials were calculated in the present work by electronic computer using Equation 6 and are given in Tables I and II of Appendix A.

The radial part $\psi(r)$ is a function of r is a function of r given in Table III and Figure III of Appendix A, for the spherical shell potential in which the $\psi(r)$ is a function of r is a function of r given in the tables of de Haas and Rappaport.

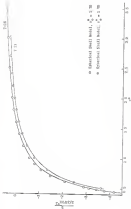


Figure 4. Reduced Viscosity Coefficients from two different models for the (Simplified Model) Reversible

Ionization limit of r^0 is taken for the ionization limit, and $g = 0$ taken for the valence, then from Equation 2 we can calculate the ratio h^0/d^0 without knowing d^0 . Overall, level 0 is the total potential energy of ionization, and d^0 is the energy parameter for the correlation, $n = 1$. The quantity g is nearly constant for the first electron between atoms in the molecule. The values of Weiss (11) correlate with valency, and all needed bond lengths are given in Table 4. The other parameters, r^0/a_0 for the atoms in these molecules should not be very much different from those for the atoms listed here. Therefore, for hydrogen atoms the r^0 value chosen will be that for lithium; for nitrogen, oxygen, and fluorine atoms, r^0 will be taken as that for neon; and for chlorine atoms, r^0 will be taken as that for argon. Parameters for the inner parts for the total potential are given in Table 4 along with the average values which were used in this work. Using these values of r^0 and g , the ratio h^0/d^0 can be calculated from Equation 2 on a function of the distance between valence electrons, R . This h^0/d^0 is plotted against R and one locates the minimum in the curve which will have the coordinates $(R^0, (h^0/d^0)^0)$ where R^0 is the minimum value of R . Using the values of the coordinates at the minimum, plots of h^0/d^0 vs. R/R^0 can be prepared. By averaging these reduced potential energy curves with those for non-polarizable ligands in Appendix B, we get that an ion potential which gives a reasonable fit to the individual potentials.

$\bar{U}_{\text{ion-ox}}^0$ (U^0 for the total potential) is available for those molecules from experimental gas viscometry and quantum virial calculations, and can be used to determine $\bar{U}_{\text{ion-ox}}^0$ by multiplying by the proper factor from Figure 3. Thus we

$$C_{\alpha} = C_{\alpha 0} \left[\frac{E_{\alpha} - E_{\alpha 0}}{E_{\alpha} - E_{\alpha 0}^{\infty}} \right] \quad (2)$$

where $C_{\alpha 0}$ and $E_{\alpha 0}^{\infty}$ are calculated previously, and E_{α} are calculated using the h - δ energy parameter E^{∞} , for the neutral atom.

The E^{∞} and q values that were used in these calculations are given in Table 4, along with the E_{α}^{∞} values for the spherical shell model. The results of the calculations are summarized in Table 7, and the calculated potential energy functions for the valence are given in reduced form in Tables 8-12 and in Figures 5 and 6. Most of these calculations have been in electronic sequence, but part of this work was done by hand.

Parameters were originally calculated only for hydrogen, fluorine, and sodium atoms, because no further calculations were planned which would require knowledge of nitrogen and oxygen atom parameters. In one recent report, not as shown in Figures 5 and 6, the variations of the calculated potential energy functions from the h - δ potential become larger as the size of the valence increases.

It perhaps seems strange that so few potentials are approximately $1/r$ and so these calculated potentials show the spherical shell model still greatly but would give the same results. The reason for using the values involving zero potentials is that these calculations were done and the resulting parameters for hydrogen, fluorine, and sodium atoms were already used in other calculations; also the paper on neutral valence calculations for the spherical shell potential was published. In order to obtain the accuracy of the spherical calculations, the parameters for

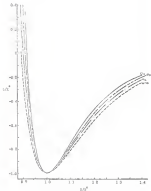


Figure 5 Potential energy functions of butadiene: Hg , Hg^+ , and Hg_2 .

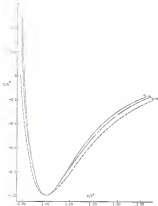


Figure 4 Potential energy dispersion of diatomic molecules (H_2 and D_2)

discrete and discrete mean were calculated using the discrete pair potential. From the spectral shift potential, the discrete pair potential was

$$|d^2 H_{0p}| \approx 30 \text{ K}$$

$$|d^2 H_{0g}| \approx 30 \text{ K}$$

The energy parameters from the pair potentials were 30.7 K for the London state and 300 K for the discrete state. This estimate is in error at about 2 percent in the energy parameters, caused by approximating the calculated spectral shift parameters with pair potentials. There seems to be no reason that the uncertainty in the k - Q parameters from which they were derived, are more or less enough to support repeating the calculations. Therefore, later calculations in which these parameters were used were not adjusted.

The values of d^2/λ for the absorption states were found to be considerably larger than those for the corresponding lower pairs as shown in Table V. This is in contradiction to the findings of Nelson (8).

If the calculated potential energy function does not differ greatly from the k - Q potential, the calculated values of \bar{h}^2 should be close to the \bar{h}^2 values for the k - Q potential calculated from experimental data. This can be seen to be true from Table V for the discrete pairs. The next step is that the values of \bar{h}^2 calculated for the discrete absorption (or to calculate spectral shifts) calculations using these values of \bar{h}^2 , from the \bar{h}^2 values used in the above calculations were taken from experimental data. The calculated values of the spectral shift constants should be compared with the experimental data. If \bar{h}^2 is used as 4000, however, the calculated values of the spectral shift constants will be considerably different from the experimental values of other temperatures.

because the second virial coefficient is proportional to \bar{v}^2 . These calculations were made and are described separately below for each of the gases. Calculations were not made for H_2 because it would have been necessary to make further corrections to the calculations.

Nitrogen (N_2)

There is a considerable volume of experimental second virial coefficient data available for N_2 . Experimental measurements were made by Tolman and Giau (14); Michels, Barmann, and de Groot (15); Raper (16); Michels, et al. (17); Haines and van Leeuwen (18); and van Leeuwen, et al. (19). These data agree very well, but all points available could not be used because of their number. Enough points were used to show clearly where the second virial coefficient curves lie. The data of Michels, et al., and of Tolman and Giau were used to locate the Boyle temperatures for N_2 , which was found to be 329°K. From r_g^2 for the nitrogen shell model was found to be 2.34 from Figure 4b the value $r_g^2 \pm 0.30$ is determined. Using these values the value of \bar{v}^2/\bar{v} for N_2 is found to be 11.5 Å^3 . \bar{v}^2 was found to be 2.41 Å thus the potential energy function of N_2 was calculated. Thus, the calculated and separate second second virial coefficient curves have been obtained at the Boyle point, and over distances of about temperatures which cover either between the values of \bar{v}^2 to one constant or the calculated potential energy function curve from set III only. The calculated second virial coefficient curve was calculated from the nitrogen shell potential values of de Boer and Reuse (20). Values of second virial coefficients at various reduced temperatures for $r_g^2 \geq 2.34$ were obtained from a comparison of these values.

Discussion: Carlini, and later (10) the k -H potential parameters found in the case of helium and neon, and Shihata, et al., (11) The average values of these parameters were used to calculate a second virial coefficient curve for the k -H potential, which is plotted in Figure 7.

The agreement of these calculations are shown in Figure 7. It can be seen in this figure that the k -H potential fits the data fairly well. The curve from the calculated k^2 and h^2 and the sphere/pole shell potential is not as good but is not badly in error. From this point it appears that the calculated value of h^2 is slightly smaller than the one that would give a best fit.

Series B_2

The second virial coefficient of B_2 has been measured by several experimenters, and their data have been cited by Myers (12) and by Shihata, et al., (13). The Boyle temperature was determined from the data of Myers to be 442°K. Presumably r_0^2 was calculated to be 6.07 and from Figure 8 the reduced Boyle temperature is 3.44. From these values T^*/ϵ was determined to be 150.4°K. h^2 was previously calculated to be 5.79 Å. Thus, the experimental and calculated second virial coefficients were again within 1% at the Boyle point. The calculated values from the extended shell potential and the experimental points are shown in Figure 8. The agreement can be seen to be excellent. Other evidence that h^2 and the shape of the potential energy function are probably nearly correct.

Series B_3

Experimental measurements of the second virial coefficient of B_3 were made by Myers, et al., (14), and their values are probably larger

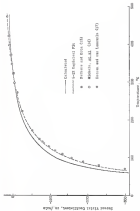
Figure 2. Reduced Viscosity Coefficient of η_0

Figure 6 Thermal Tidal Coefficient of η

in this case values than the initial second virial coefficients at low temperatures because they did not use the third virial coefficient in their calculations. From previous calculations, \bar{v}^0 was calculated to be 3.45 Å and \bar{v}^0/\bar{v} was taken as 100.4%. These values were used to calculate the second virial coefficients from the δ - δ potential tables presented earlier and from the spherical shell potential tables of de Boer and Boree for $\bar{v}_0^0 \leq 3.74$. These calculated curves are compared in Figure 8 with the experimental data and with curves calculated from Flannery's correlation and the hard-sphere equation, which were discussed earlier. It can be seen that the calculations for the spherical shell potential and the δ - δ potential are in excellent agreement with the experimental data and are considerably better than either of the curves from the hard-sphere equation or Flannery's correlation.

Calculation $\langle \bar{v}_0^0 \rangle$

From previous calculations, \bar{v}^0/\bar{v} was found to be 406% and \bar{v}^0 was 3.62 Å for ϕ_{H_2} . The value of \bar{v}_0^0 was found to be 2.56. Two of these parameters with the spherical shell potential tables of de Boer and Boree led to the calculated curve in Figure 10. In the absence of reliable second virial coefficient data, second virial coefficient curves from Flannery's correlation and the hard-sphere equation were calculated and are presented in Figure 10 for comparison. The agreement at the Boyle point is quite good for all three curves. This is especially true when one considers the steps in $\bar{v}^0/\bar{v}(\phi_{H_2-\text{D}_2})$ values that were used to calculate \bar{v}^0/\bar{v} for ϕ_{H_2} . The agreement at low temperatures is not as good but is still acceptable. If the hard-sphere equation and Flannery's correlation give the correct third coefficients, then it appears that the calculated \bar{v}^0 value for ϕ_{H_2} is slightly large.



Figure 4. Integral Viscosity Contribution of η_1

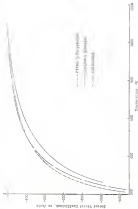


Figure 10 Broad Peak Coefficient of Eq.

From these calculations it appears that the value of calculated potential energy function is reliable and that at least the value parameter used are satisfactory. One of the energy parameters is independent from other empirical relations should indicate whether they are satisfactory or not.

CH₃CH₃

In order to calculate potential energy function of molecule containing methyl (CH₃) groups, it is necessary to have parameters for this group. In view of the studies of Gluey and Fendler¹⁰ for treating methyl groups in aliphatic chain, this approach will be used.

Brown and Lohr¹¹ demonstrate that CH₃ can be correlated with the small group and diatomic molecules which were shown to fitting a 4-12 potential better than with more complex molecules such as CH₄. Fitzer¹² in his calculations about the acoustic factor of carbon is 3.62, which indicates that the potential energy function should be given as a 4-12 potential. Therefore, it seems reasonable to treat carbon as an atom obeying the 4-12 potential. In order to obtain parameters for a CH₃ group

Gluey and Fendler¹⁰ in their calculations, assumed that a CH₃ group behaves exactly like CH₂, and this is probably nearly correct. The approach taken here is to assume that $\epsilon_{CH_3}^* \approx \epsilon_{CH_2}^*$ and then to treat carbon as though it were a diatomic gas composed of two methyl groups separated by the C - C bond distance in order to obtain the energy parameter for CH₃.

Parameters for CH₃ for the 4-12 potential are given in Table II. The value of σ^* value for CH₃ is the sum of the value is then taken

$\epsilon_{\text{CSD}}^{\text{e}} = 4.33 \text{ eV}$. Calculated $\epsilon_{\text{CSD}}^{\text{e}}$ is equal to 5.378 eV , and the potential energy function was calculated for Equation 8. These calculations give

$$r^{\text{e}} = 3.263 \text{ \AA}$$

$$\frac{\epsilon_{\text{CSD}}^{\text{e}}}{\epsilon_{\text{CSD}}^{\text{p}}} = 1.327$$

$$r_{\text{C}}^{\text{e}} = 4.33 \text{ eV}$$

The calculated potential energy function for C_2H_2 is presented in reduced form in Table 14 and in Figure 11. A 4-36 potential was found to fit the calculated curve very well, and some points are plotted in Figure 11 for this potential. From Figure 11 it was determined that

$$\frac{\epsilon_{\text{CSD}}^{\text{e}}}{\epsilon_{\text{CSD}}^{\text{p}}} = \frac{3.4}{2.56} = 1.327$$

In order to calculate $\epsilon_{\text{CSD}}^{\text{e}}$ it is necessary to have 4-36 potential constants for C_2H_2 . Wipke (1969, Section 4) and Bird (11) had parameters from both gas vibrational and second virial coefficient data, but the BSC states that the second virial coefficient data used was in error. Since then, only the parameters from gas vibrational measurements were used. These parameters for the 4-36 potential are

$$r^{\text{e}}/a = 3.263$$

$$r_{\text{C}} = 4.33 \text{ eV}$$

$$r^{\text{e}} = 4.33 \text{ eV}$$

Experimental second virial coefficient data for C_2H_2 is given by the BSC. The second virial coefficient was also calculated from Pitzer's correlation and from the Benedict-Redlich equation. These values of the second virial coefficient are given in Figure 12.

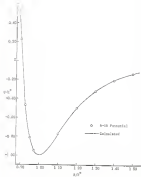


Figure 11. Potential Energy Function of $H_2^+H_2$.

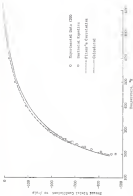


Figure 10. Based on eq. (1) Evaluation of k_p/k_0

Explicitly fitting 6-12 potential parameters to the experimental second virial coefficients, data led to parameters which were unreasonable for the following reasons:

1. The ϵ^* value was experimentally found to be approximately 7 Å (we could not expect this value to be larger than $\epsilon_{\text{O}_2}^* = \frac{1}{2} d = 1.8$ Å).
2. The calculated potential energy functions for all other color values gave ϵ^* values that were grossly out of range. This value was 4.66 Å.
3. The value of ϵ^* from gas viscosity was 4.91 Å.
4. The value of ϵ^*/h obtained explicitly was about 100% , as compared with 100% from gas viscosity data. Holmes has an ϵ^*/h value of 100% , and it does not seem reasonable that the ϵ^*/h value be about the same for N_2O .

Therefore we also fitted six parameters for the generalized still potential $\epsilon_1^* = 1.5$ and $1 \leq$. These parameters were better, but not completely satisfactory.

The difficulty in fitting parameters to these data probably results because the data cover a temperature range of only 100°K , and there are no values of the second virial coefficient near the Boyle point. Small errors in slope of the experimental curve near a steep inflex upon the side of the parameter cause large deviations.

Using Holmes's correlation gives second virial coefficients that are close to the experimental values. It probably is well to use it to calculate the second virial coefficient over a wide range of temperatures. Using the value of the Boyle point and one other point from Holmes's correlation with the calculated second virial coefficients for the 6-12 potential gave $\epsilon^*/h = 100\%$ and $\epsilon^* = 1.78$ Å. These parameters

cannot be used as a reasonable fit for the 4-12 potential. Using the 4-12 potential, the parameters are $E^*/k_B = 112^\circ\text{K}$ and $r^*/\sigma = 2.42$ Å.

Since this last set of calculations gave reasonable results, the following calculations were done using both FLANN's interpolation and the Barker's equation to estimate the Boyle temperature.

T_B , $^\circ\text{K}$	From
110	FLANN's interpolation
111	Barker's equation
790	average

$$C^*/(k_B-1) = \frac{36}{4-1} = 12^\circ\text{K}$$

Adding this value of $C^*/(k_B-1)$ with the first gas viscosity data gave the value

$$C^*/(k_B-1) = 134^\circ\text{K}$$

which was used to get the energy parameter for the 4-12 group

$$E^*/k_B-1 = 1.127 \quad C^*/(k_B-1) = 49^\circ\text{K}$$

Also it was previously found that

$$\frac{E^*/k_B-1}{E^*/k_B-2} = 2.28$$

the final result

$$C^*/(k_B-2) = \frac{36}{2-2} = 18^\circ\text{K}$$

is obtained. Therefore, the parameters good for CH_4 are

$$E^*/k_B = 120^\circ\text{K}$$

$$r^*/\sigma = 2.42 \text{ Å}$$

Use of the spherical shell model in these calculations yields the $0^+ \rightarrow 0^+$ potential well has only about 2 support differences in $1/\hbar$ from value of d^2V/dk . This certainly is well within the accuracy of the above calculations. The calculated value of d^2V/dk for $0^+ \rightarrow 0^+$ is only 18 percent less than that for $0^+ \rightarrow 0^+$. In fair agreement with Sherry and Trefethen's assumption that the two are the same.

The second related coefficient calculated from these parameters and $\sigma_0^2 \approx 0.25$ for the spherical shell potential is shown in Figure 12 and is in reasonable agreement with those determined by other methods.

CHOICE OF

PARAMETERS FOR POLYMERIZATION REACTIONS

In this section particular energy functions and related effects coefficients were calculated for polymeric molecules using as parameter for the polymeric atoms the atomic parameters calculated from the diatomic gas data. The equations of Pines and Lindqvist were applied and as solutions the potential energy functions. For all investigations reactions involving atoms, the following energy parameters were used

$$E_{AB} = \sqrt{E_A^* E_B^*}$$

$$r_{AB} = \frac{1}{2}(r_A^* + r_B^*)$$

where E_A^* and r_A^* are parameters for interaction between like molecules and E_{AB}^* is the parameter for interaction between molecules A and B. The subscripts have the same meaning with r 's r^* values.

The problem of choosing parameters for the diatomic species atom in molecules like CF_4 and SiH_4 , the correct value is SiF_4 and SiH_4 , and the correct value is SiF_4 , it has been noted only be solved by trial and error. In this attempt to use the same parameters for diatomic atoms as used for fluorine that showed calculated values of E^*/k for the r values that were most too large, not so was concluded that parameters for carbon should probably be included by those for neon and silicon. Likewise, the parameters for silicon and sulfur atoms should be included by those for argon and neon. Because of this

conveniently in choosing parameters for these targets) atoms, three calibration constants were used for each molecule in this category. In order to avoid specification of the parameters used in each calculation, the calculations were given a standardized set of scale values that can be used to determine the parameters used quite easily. The parameters for the peripheral atoms were the same for all calculations for a given molecule and were the same determined from the distance given. These parameters are

<u>Peripheral atom</u>	<u>$\bar{r}_{\text{C-H}}$</u>	<u>$\bar{r}_{\text{C-O}}/\text{\AA}$</u>
F	2.33	19.7
Cl	2.34	195
CH_3	4.33	120

For molecules involving carbon as the central atom, the following table gives the scale values and parameters used

<u>Scale value</u>	<u>$\ln^2 \lambda_1$</u>	<u>$C \bar{r}^2 / \text{\AA}^2$</u>
1	$\ln^2 \lambda_{\text{CH}_3} = 5.33 \text{ \AA}$	$C \bar{r}^2 / \lambda_{\text{CH}_3} = 26.4^\circ \text{C}$
2	$\frac{1}{2} [\ln^2 \lambda_{\text{CH}_3} + \ln^2 \lambda_{\text{CH}_2}] = 2.33 \text{ \AA}$	$\frac{1}{2} [C \bar{r}^2 / \lambda_{\text{CH}_3} + C \bar{r}^2 / \lambda_{\text{CH}_2}] = 13.4^\circ \text{C}$
3	$\ln^2 \lambda_{\text{CH}_2} = 2.33 \text{ \AA}$	$C \bar{r}^2 / \lambda_{\text{CH}_2} = 13.4^\circ \text{C}$

For amine, calculations $\text{CH}_3 = 1$ used the Clavette parameters given above and two parameters were used for the carbon atom

For molecules involving nitrogen as center or the central atom, the following table gives the scale values and parameters used

Calculation	$\langle r^2 \rangle_{\text{eq. at 25}}$	$\langle r^2 \rangle_{\text{eq. at 25}}$
1	$\langle r^2 \rangle_{\text{eq. at 25}} = 3.46 \text{ \AA}^2$	$\langle r^2 \rangle_{\text{eq. at 25}} = 3.97 \text{ \AA}^2$
2	$\frac{1}{2} [\langle r^2 \rangle_{\text{eq. at 25}} + \langle r^2 \rangle_{\text{eq. at 25}}] = 3.46 \text{ \AA}^2$	$\frac{1}{2} [\langle r^2 \rangle_{\text{eq. at 25}} + \langle r^2 \rangle_{\text{eq. at 25}}] = 4.12 \text{ \AA}^2$
3	$\langle r^2 \rangle_{\text{eq. at 25}} = 3.21 \text{ \AA}^2$	$\langle r^2 \rangle_{\text{eq. at 25}} = 3.47 \text{ \AA}^2$

For example, calculation 2: $\langle r^2 \rangle_{\text{eq. at 25}} = 3$ and the CH_2 parameters given above and other parameters are allowed.

All potential energy functions were calculated using an electronic computer and the values for each of the potential energy curves are listed by giving calculations at intervals of 0.01 Å, and the origin. Table II contains a summary of the parameters determined in these calculations. The calculations for each molecule are discussed separately below.

CH₄

Several sets of calculations were made for methane and were verified by calculated inertial vibrational frequencies that were then fitted to the experimental values. Here the $\langle r^2 \rangle_{\text{eq. at 25}}$ for methane was taken as the same as that for fluorine since the calculated $\langle r^2 \rangle_{\text{eq. at 25}}$ was so small that the calculated inertial vibrational frequencies were only about one-half the size of the experimental values. This result should not have been surprising because, as outlined before, methane behaves more like a simple diatomic molecule than like a tetrahedral molecule with large interatomic or the hydrogen atom. Here these calculations only demonstrated that methane can best be treated as a simple diatomic molecule. Some of the calculations will be given later.

Ω_4

The value of \tilde{r} for the fluxes state was the $\tilde{r} = \tilde{r}^*$ bond length, 1.303 Å.

An interesting result of these calculations was that changing the parameters for carbon changed the values of \tilde{r}^2/\hbar , but had little effect on \tilde{r}^* or on the shape of the potential energy function since it is plotted in reduced coordinates. Figure 14 shows a potential energy function plotted from the calculations of $\Omega_4 = 1$, but the other two calculated potentials differed from it by a constant amount. For this reason, only the set of values of \tilde{r}^2/\hbar and \tilde{r}^* will, adequately represent all the calculated potential energy functions. The calculated values of \tilde{r}^2/\hbar and \tilde{r}^* and the reduced potential energy function for these calculations are given in Table IV. Values plotted in Figure 15 for a T-20 potential, and for $\tilde{r}_0^2 = 3.46$ for the spherical shell potential show that either could be used as an adequate simplified representation of the calculated potential energy function of Ω_4 .

In Figure 14, the three types of interactions that add to the potential energy of Ω_4 are shown for $\Omega_4 = 1$. This figure shows that although the interactions between carbon and fluorine atoms are smaller than those between fluorine atoms, they are by no means negligible. The C - C interactions are quite small, however, and explaining them would mean little more.

These calculations show why it is possible to make calculations based upon the potential energy function of molecules such as Ω_4 , but assuming the fluorine atoms infinitely. Replacing the carbon atoms will not change the shape of the potential energy function appreciably, and as long as the parameters \tilde{r}^2/\hbar and \tilde{r}^* are calculated correctly, as

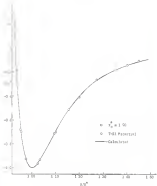


Figure 12. Potential Energy Function of SF_6 .

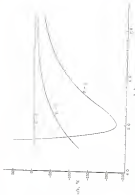


Figure 14 Comparison of Potential Energy (14-2)

nearest-neighbor energy function can be obtained. In fact, when one compares the values shown directly, the spinodal shell model parameter is 1.76 (see Table I), which also fits satisfactorily the potential energy function when surface interactions are included. This implies the success of linear and in linear's (2) calculation of nearest-neighbor coefficients using the spinodal shell model and of Clancy and Swenson's (4) calculation of potential energy functions without considering surface interactions.

In Figure 14 experimental values of the nearest-neighbor coefficient by Hansen and Lohr (5) are shown, along with calculated nearest-neighbor coefficients from linear's calculation and the Debye-Hückel equation. Also shown are the calculated nearest-neighbor parameters from calculations $CP_2 = 1$ and $CP_2 = 2$ and the value $v_0^2 \approx 1.76$ for the spinodal shell model. As can be seen, the calculation for $CP_2 = 2$ fits the data better than for $CP_2 = 1$, although both are of the right order of magnitude. It appears that the calculated value of v_0^2 is slightly larger than the best fit to the experimental data and that the value v_0^2/λ should be somewhat larger than from $CP_2 = 1$ and $CP_2 = 2$ calculations. This is borne out by the fact that a good fit to the experimental data can be obtained using $v_0^2 \approx 4.76$, $v_0^2/\lambda \approx 34.76$, and $v_0^2 \approx 1.76$ for the spinodal shell potential.

Linear's calculation seems very close to the experimental data over the entire range of temperatures, but the Debye-Hückel equation is in considerable error at high temperatures. The nearest-neighbor coefficient from calculations $CP_2 = 2$ was not as good as for $CP_2 = 1$ and $CP_2 = 2$ and it will show in diagram further.

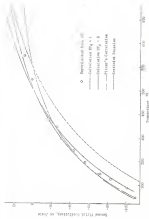


Figure 11. Reduced Viscosity vs. Temperature

$$k_B^2 P_0$$

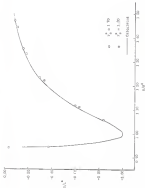
The value of $\bar{\rho}$ used for the division stems from the distance from the center of the C-C bond to the division stems, which was calculated from bond lengths and angles for the $k_B^2 P_0$ molecule. The value of $\bar{\rho}$ for the carbon stems was half the C-C bond length. The values used were

$$\bar{\rho}_P = 1.765 \text{ \AA}$$

$$\bar{\rho}_C = 0.775 \text{ \AA}$$

Again, the shape of the potential energy functions from the different set calculations differed by a multiplicative factor. The \bar{E}^P and \bar{E}^C vs r plots for each calculation and the same reduced potential energy function are given in Table 13. The reduced potential energy function is given in reduced form in Figure 14 and was previously in adequately represented by using $r_{12}^2 = 1.4$ for the spherical shell potential.

Exponential second virial coefficients for $k_B^2 P_0$ are given by Eqs. (11) and are shown in Figure 15. Also given in this figure are curves calculated from Pitzer's correlation and from the Benedict equation. Curves calculated from the parameters of $k_B^2 P_0 = 1$ and 2 using $r_{12}^2 = 1.40$ for the spherical shell potential are also shown. The calculated curve for $k_B^2 P_0 = 1$ agrees very well with the Benedict equation and Pitzer's correlation and reproduces the experimental data at lower temperatures. The calculated curve for $k_B^2 P_0 = 2$ is in better agreement with the experimental data at high temperatures, but deviates at lower temperatures. One of the calculated second virial coefficients shows possible such a rapid change in second virial coefficients as is shown by the experimental data. Although adjustment of the parameters for carbon stems could make the calculated curves pass through the experimental data, it does not appear likely that any calculated curve would fit the data over the entire temperature range.

Figure 20 Potential Energy Function of Li_2H_4

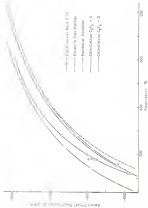


Figure 17. Derived Thermal Coefficient of C_p/T_s .

Parameters for CCl_2 for the T-10 potential calculated from gas vibratory measurements by McClellan and Blevins (22) are

$$\begin{aligned} r^0 &= 1.20 \text{ \AA} \\ k^0/r &= 22.4 \text{ N} \end{aligned}$$

Typical values of k^0/r agree fairly well, with the value 22.4 N from $\text{CCl}_2^0 = 2$ but this value of r^0 is consistently smaller than the values 1.20 \AA from $\text{CCl}_2^0 = 1$ and 1.225 \AA from $\text{CCl}_2^0 = 2$. As might be expected because of this low value of r^0 these calculations from gas vibratory data for the second virial coefficient do not so satisfactorily $\text{CCl}_2^0 = 1$ and 2.

CCl₄

The value of β used for the chlorine atom was the C = Cl bond length 1.76 \AA. Again, changing carbon parameters did not change the shape of the potential energy function. The calculated values of r^0 and k^0/r for the three calculations and the second virial potential energy function are given in Table IV. The potential energy function from these calculations is given in Figure 18 where values plotted for $r_0^0 \leq 1.8$ for the assumed atom potential show that $r_0^0 \geq 1.8$ gives a satisfactory fit to the calculated curve.

Experimental second virial coefficients of CCl_4 have been obtained by Frenkel and Hildebrand (23), and the curve representing the experimental data is their most probable curve through all the data. In Figure 19 the experimental second virial coefficient curve is shown along with curves calculated from Frenkel's correlation and the Lennard-Jones equation. Also shown are curves calculated from the parameters of calculations $\text{CCl}_4^0 = 1$ and 2 using $r_0^0 = 1.8$ for the spherical shell model.

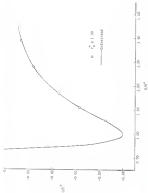


Figure 20 Potential Energy Function of D5A4

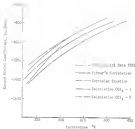


Figure 15: Second Virial Coefficient of CH_4

sets of ΔG correlation values follow the slope of the experimental data but all are close to impossible. The calculated curve for $\text{CCl}_2 = 2$ fits the experimental data at higher temperatures, but deviates at lower temperatures, not in better than Pitzer's correlation or the Barthel's equation over the range of the data. The curve calculated for $\text{CCl}_2 = 1$ approximates the experimental data at the lower temperatures. The experimental vapor liquid coefficients are available over such a narrow range of temperatures that one should not place too much importance on the difference in slope between calculated and experimental curves.

$\text{C(CH}_3)_2\text{I}_2$

The value of ρ for the CH_3 groups was the C - C bond length 1.54 Å. The calculated \bar{V}^L and \bar{V}^V/\bar{V}^L for the three calculations are given in Table III, along with the various reduced potential energy functions. The calculated potential energy function is shown in Figure 20 where it is seen that the effective shell potential for $r_{ij}^0 = 2.10$ fits the calculated curve very well.

Experimental data on the vapor liquid coefficients of $\text{C(CH}_3)_2\text{I}_2$ is given by Breen and Lohrert (2). These data are shown in Figure 21 along with curves calculated from Pitzer's correlation, and the present state from calculation $\text{C(CH}_3)_2 = 1$ and the spherical shell potential for $r_{ij}^0 = 2.10$. The Barthel equation gives a curve essentially the same as Pitzer's correlation and is not shown. The agreement among all curves shown in Figure 21 is excellent, especially when considering that a temperature range of 100°C is covered.

$\text{C}_2\text{(CH}_3)_2\text{I}_2$

The value of ρ used for the CH_3 groups was calculated from bond

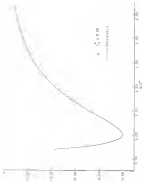


Figure 10. Normalized energy difference of $C_2H_2 + C_2H_4$.

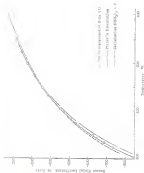


Figure 2. Effect of temperature on the acid dissociation constant of chloroacetic acid.

length and angles had was 1.425 Å. The value of \bar{p} used for the linear lattice sums was 3.775 Å. The calculated \bar{p}^2 and \bar{p}^2/\bar{h} values for the three calculations and the square reduced potential energy function are given in Table II. The potential energy function is plotted in Figure 12 along with points for the spherical shell potential for $r_0^2 = 1.7$ and 1.9. The calculated curve lies between $r_0^2 = 1.7$ and 1.9, and a good fit would probably be $r_0^2 \approx 1.85$.

In the domain of experimental second virial coefficient data, curves calculated from Flory's correlation and the restricted equation are compared with the curves for calcinations $\text{C}_6\text{H}_5\text{C}_6\text{H}_5\text{I}_2 = 1$ and 2 polymers and $r_0^2 \approx 1.85$ for the spherical shell potential as shown in Figure 13. All of these curves are in reasonable agreement.

BF_3

The value of \bar{p} used for the lattice sums was the $\text{B} - \text{F}$ bond length, 1.361 Å. Since only calcination $\text{BF}_3 = 3$ gave reasonable results the potential energy function in Figure 14 and Table II applies only to this calcination. Also shown in Figure 14 are points for the spherical shell potential for $r_0^2 = 1.7$ and 1.9, and it can be seen that $r_0^2 \approx 1.85$ for the spherical shell potential should fit the calculated curve satisfactorily.

Experimental second virial coefficients from several sources are cited by Good (21) and these points are plotted in Figure 15. The comparison of Flory's and the restricted equation gives generally identical results, as only two members of the calcination from Flory's correlation have been shown in this figure. Also given in Figure 15 is the curve for calcination $\text{BF}_3 = 3$ using $r_0^2 = 1.75$ for the spherical shell



(a) $\log r$ vs $\log T$



Figure 10: Average Turbulent Coefficients of $\gamma_1, \gamma_2, \gamma_3, \gamma_4$

Graph of $y = \sin(x)$ and $y = \cos(x)$

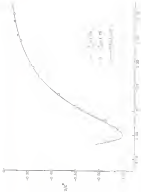


Fig. 2. Effect of temperature on the rate of polymerization of styrene.



Overall, the calculated ^{13}C NMR chemical shifts very close to the experimental data, and the calculated curve for $W_{\text{H}} = 2$ differs from the experimental data by only about 10 percent.

Since the parameters used for sulfur in the calculation that gave the only reasonable results were those for ions, not those for atoms, this should be discussed further. In all of the calculations discussed up to $W_{\text{H}} = 2$, the central atom is either distributed slightly toward chlorine in the outer shell. For $W_{\text{H}} = 2$, however, there are fewer electrons in the outer shell. This expected outer shell hole can be ascribed, for the electrons are used more closely to the chlorine atoms, giving them to the sulfur atom. If we think of these electrons in the outer shell as "belonging" to the chlorine atoms, then one less left in the center of the molecule that is essentially a lone atom, whose interactions become more and more ionic in character. This explanation is rather vague, as are all of these calculations, but nevertheless it does fit the results of the calculations.

$W_{\text{H}} = 2$

The value of g used in these calculations was the $W = 2$ band length, 1.81 Å.

Since the energy parameter for sulfur is quite large, changing this parameter had some effect on the shape of the reduced potential energy curves. The two calculations which gave reasonable results were $W_{\text{H}} = 1$ and 2, and the 1^2A and 2^2A values are shown, along with the reduced potential energy functions in Table II. The reduced potential energy curves are shown in Figures 26 and 27. The potential energy function from $W_{\text{H}} = 1.44$ is fitted reasonably well by the spherical

12 potential for $V_0^2 = 1.4$ as shown in Figure 26. The potential

Fig. 1. Dependence of the critical temperature T_c on the concentration of the impurity x for the system $\text{Pb}_{1-x}\text{Bi}_x\text{Te}$.





Graph of $\log R$ and C for a first-order reaction

Graph of $\log R$ and C

energy function for $\text{Mg}_2 = 2$ like the spherical shell potential for $r_0^2 \pm 1$ as shown in Figure 27.

Superficial measurements of the radial virial coefficient of Mg_2 have been made by Rowen, Polunsky and Pitzer (24) and are shown in Figure 28, along with calculated curves from Pitzer's correlation and the Benedict equation. Also shown are the calculated curves for $\text{Mg}_2 = 1$ and 3 using the values of r_0^2 for the spherical shell potential that are given above. Pitzer's correlation fits the data very well, and the Benedict equation does well. The calculated curves from $\text{Mg}_2 = 1$ and 3 were not very close to the experimental data, but are given high values and are given low values of the second virial coefficient. Thus the curves seem to have the same shape as the Pitzer's correlation and the experimental data, which indicates that the shape of the potential energy function and the values of r^2 are probably nearly correct. There is a very large difference in the r_0^2 's values from the two calculations which is the reason for the large difference between the curves for $\text{Mg}_2 = 1$ and 3. A value of r_0^2 's of about 100% would be more reasonable than those of the values 244 % and 102 % that were calculated. This indicates that the proper parameter for silicon is Mg_2 should be slightly smaller than those for argon, but not so small as those used for $\text{Mg}_2 = 3$.

SiMg_2Si_4

The value of \bar{q} used in these calculations was the $\text{Si} = 2$ case (Table 1, $\text{Mg}_2 = 2$). The calculated potential energy functions for $\text{SiMg}_2\text{Si}_4 = 1$ is given in Table 30 and in Figure 29. The spherical shell potential for $r_0^2 = 1.10$ is given in Figure 29 as fit the calculated potential very well.



Figure 26 Second virial coefficient of B_2

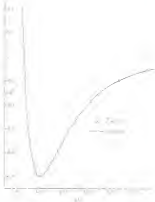


Figure 1. Example of a non-linear relationship

The calculated $\sigma_{\text{el}}(\omega)$ (solid line) of $\text{Sn(CH}_3)_4$ has been obtained by (HARRIS, LAMBERT, and TILMAN 1971) and is shown in Figure 25. The results of calculations 1, based upon the calculated free-atom σ_{el} coefficients and the Hartree-Fock atomic wave functions taken together, as only the results of the calculation from TILMAN's correlation are shown in Figure 25. Also shown in this figure is the curve calculated from the parameters of calculation $\text{Sn(CH}_3)_4 - 1$ using $r_{\text{Sn}}^2 = 1.95$. For the spherical shell model this latter curve is in reasonably fair agreement with the experimental curve, the calculated values being about 65 percent of the size of the experimental values of the atomic elastic coefficients. In view of the poor success of this type of calculation, it would appear that a complete re-view of the calculation has been made, but a careful check of this calculation and comparison with other calculations showed that no error had been made. Hence the calculated and experimental curves disagree further apart at some frequencies. It appears that both the calculated E^2 and E^2/ω values are too small for this molecule. Comparison with an estimated size of the spherical shell model is shown and done by de Haas and Houten indicating that the calculated E^2/ω should have been about 400% instead of 200 0%, and E^2 should have been about 7.5 Å instead of 3.0 Å. Evidently one of the parameters used in this calculation are not even approximately correct for this molecule, but there is no obvious reason why this should be so. One would think that the same atomic parameters that were used for SnF_4 would be correct, and that the CH_3 correction used for $\text{Sn(CH}_3)_4$ would also be the same for $\text{Sn(CH}_3)_2$. The value of q used was the average of the experimental observations and should be approximately correct. There is, of course, the possibility that this method of calculation is not suitable for this molecule.



Figure 20 Arrhenius plot of α for polypropylene

just as Flory *et al.* assume. In fact, the results of the calculations for CH_2 and CH_2CH_2 segments showed virial coefficients that were much too small. The conclusion is obvious that these calculations for CH_2CH_2 are an approximation to potential energy function for this molecule.

RESULTS AND DISCUSSION

The purpose of the calculations in Part I has been to calculate potential energy functions for several polycyclic molecules and then to test these potential energy functions by calculating several vibrational coefficients and comparing with experimental data. Since it is easy to lose sight of the progress of each step in the calculations and how it fits into the total, the following description summary is given.

1. Using the equations of Bunker and Lennard (11) and σ^2 values from Table 1, several potential energy functions for the chlorine gases Cl_2 , Cl_2 , Cl_2 , Cl_2 , Cl_2 , and Cl_2 were calculated.
2. Using these calculated potential energy functions and 9-12 potential parameters from experimental data (12) three chlorine gas energy parameters for hydrogen, fluorine, chlorine ethyl and isopropyl groups were determined. The nine parameters from the chlorine gas data calculations were tested by calculating several vibrational coefficients and comparing with experimental data.
3. Using the equations of Bunker and Lennard and the atomic parameters determined from the chlorine gas potential energy functions were calculated for Cl_2 , Cl_2 , Cl_2 , Cl_2 , Cl_2 , Cl_2 , Cl_2 , Cl_2 , and Cl_2 .
4. These latter potential energy functions were tested by calculating several vibrational coefficients and comparing with experimental data.

These calculations were made by systematically fitting calculated vibrational frequencies to the calculated potential energy functions and then using the values of the force and torque (F) to calculate second virial coefficients.

Inspection of these calculations which are in progress is now being

Calculations for the diatomic gases showed that their potential energy functions are indeed not very much different in shape from the r^{-12} potential, but this difference increases with the size of the molecule. For example, the potential energy function of hydrogen could be adequately represented by a r^{-12} potential, while that of chlorine required a r^{-10} potential. The calculated B^0 values for the diatomic gases were in good agreement with B^0 values that would be calculated from second virial coefficients data, which indicates that the size of the atom is more important in our case different from the size of the corresponding inert gas. The energy increments for the diatomic and triatomic gases depended from the diatomic gas data gave good results when used to compute molecular values, which indicates that the treatment of diatomic gases as diatomic-monomers, representing molecules in solution.

Calculations for various cases involved the assumption that there were discontinuities in the potential function and under these were compensated by giving reasonable parameters for the potential energy function. This result confirmed the findings of other workers that various can best be treated as a single case which represents strongly as a r^{-12} potential. The calculations for various and other molecules including single groups showed that treating single groups as though they were single r^{-12} centers of interaction was an adequate method of treatment. With this confirms the findings for various

The calculations for other properties indicated similarly results as the present ones. For an hydrogen atom, about that, only the $E = 0$ information could really be ignored. Changing parameters of the system wave had very little effect upon the shape of the resulting potential energy function at the value of r^* , but did have a larger effect upon the value of E^*/\hbar . This result of the calculations indicates that consideration of only the peripheral states as in the potential shell model will give a potential energy function that is approximately the correct shape. If the E^*/\hbar and r^* parameters are thus determined independently, a reasonable potential energy function should be obtained.

In these calculations it was found that reasonable results could be obtained using two parameters for each, although in some cases better results were obtained using parameter values between those of zero and infinity. In no cases were better parameters found to be infinite in any direction. The parameter estimates for the peripheral states were used for the peripheral states, and in view of the nature of these calculations, they were not thus independently varied.

There was some difficulty in getting good results for the valence nucleons which did not belong to the peripheral states because the separation lines involving the peripheral states form a large part of the total separation lines, and the choice of reasonable parameters was more important than for the states in the central zone. For BF_3 , reasonable results could only be obtained by using potentials that were softer than those for argon (probably about 50 percent softer), while for BF_4 it was necessary to use even parameters for nuclei. This latter simplification was justified by assuming that because of the lower densities in the outer shell, these elements could be considered as "belonging" to the innermost

When working with only a few data of the series. Calculations for $\beta(\text{CH}_3)_2$ were not attempted at all. Both \bar{v}^0 and \bar{v}^0/\bar{v} parameters obtained were too small.

In most cases the calculated mean vibrational coefficients did not really match the experimental ones, but for almost all of these cases some better agreement could have been obtained by arbitrarily adjusting the parameters calculated for the spectral series. It was felt that the calculations showed that reasonable approximations to the potential energy functions were obtained by using a few calculations previously, and further arbitrary adjustments could serve as useful purposes in this respect.

In an interesting study of some calculations, it was seen that PLATT's correlation yielded very good estimates of the mean vibrational coefficients of these molecules. The harmonic equation was found to give good estimates of the mean vibrational coefficients at low temperatures but not as good at temperatures around the Boyle point.

Since these calculations gave reasonable results it will not be said. It can be stated that the discrepancy between our simple potential function in the gas phase can be explained by assuming that they include multiple sources of dispersion and that this dispersion can be said to be quantitative as well as a qualitative sense.

Page 11

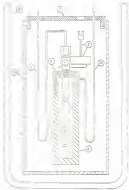
RECEIVED: 10/10/2010, 10:10 AM

MEASUREMENT OF γ RAY μ TV₀ AT LOW TEMPERATURES

Thermoelectric pressure coefficients, $(\partial P/\partial T)_{P_0}$, have been measured $(\partial P/\partial T)_{P_0}$ for several crystals available at temperatures above $^{\circ}\text{N}_2$. The thermoelectric effect used for these measurements is essentially a constant value thermoelectric coefficient in a pressure bomb. The liquid sample is placed in a sample cell and sealed in high vacuum. The temperature is then measured and the pressure coefficient has already been determined to give a suitable value of liquid density in the cell. This procedure is repeated at several temperatures without removing the sample so that a series of temperatures and pressures can be obtained at essentially constant values in standard. In general, it was found that the pressure varies linearly with temperature to give an average value of $(\partial P/\partial T)_{P_0}$. This observed value is then corrected for small changes in cell volume arising from the temperature and pressure changes.

The measurements were also made using other at just below room temperatures so that the temperature could be corrected easily by the thermal effect. In the present work, the thermal pressure coefficient for OP_4 and OP_3 were measured. The triple point of OP_4 is at $^{\circ}\text{N}_2$, and the normal boiling point is at $^{\circ}\text{N}_2$, both of which are below the freezing point of mercury and will hence not evaporate because of the low temperatures at which the apparatus can be operated in the present work. It was necessary to design the design of the apparatus.

(see Appendix B, collection record) (see Unit test by personal inspection). Figure 11 is a sketch of the initial-value cell and related apparatus. A schematic diagram of the apparatus used in the present work is shown in Figure 12. The sample cell was a 2.5-mm o.d. by 5.0-mm-long, 1/8-in. i.d. fitted with 3/16-in. o.d. collars of 1/8-in. i.d. and was not set in a specially cut block of wax. The signal bellows were fitted to the future impeller gaskets across the upper portion of the side flange of the sample tube. The initial-value cell is a closed assembly of the side flange and bellows and valve was removed. The valve was not available in an angle position, and it was necessary to have a gear reduction to provide turning the valve precisely from above. The valve was below horizontal both at the open and bellows at the factory before shipment, and the valve was installed so that the open side faced the sample cell. The bottom of the sample cell was closed by a 1/8-in. i.d. signal bellows. Three sets (two sets of one each) of bellows tubes to provide change in the cell, as a very accurate or accurate. A section was also placed that the bellows tube across at two pressure differential. The sample was connected to an indicator provided by Hils (22) which was made available that the mechanical electrical long distance. A temporary water valve was provided the sample cell to have a pressure cell. Before not used to provide pressure, and before the cell through a 1/8-in. i.d. and then stand tube. Temperature was measured on the outside of the sample cell by a thermocouple which entered the pressure cell through the pressure tap. The water to the system also entered through this tube. In addition to the sample cell, there is a glass vacuum system was also made through 1/8-in. i.d. and then stand tube. The apparatus was enclosed in a heavy metal box.



and the sealed container was suspended in a water bath maintained at 70°C. The lid to the bath was not removed until the water had cooled to a temperature below 50°C. The container was then removed from the bath and the lid was removed. The container was then sealed and the lid was removed. The container was then sealed and the lid was removed.

1. The container was suspended in the water bath as before.

2. The lid was removed and the container was sealed.

3. Liquid nitrogen was added to the water bath so that it covered the entire bath, cooling the apparatus. The apparatus was then removed from the bath and the lid was removed. The apparatus was then sealed and the lid was removed.

4. When the entire apparatus was at approximately the desired temperature and cooling had ceased to a very slow rate, a sample of liquid was distilled into the sample cell from a glass vessel placed in contact with the cell and removed.

5. After all liquid nitrogen had evaporated, and the temperature began to drift slowly upward, the valve on the side of the pressure cell was closed and the entire apparatus was removed.

6. From 50 to 100 psi of helium was admitted to the pressure cell. From a cylinder of high-pressure helium through a valve of small internal diameter could be used rather in comparison with the cell. Helium from the pressure cell. The introduction of helium compressed the helium and opened the contact rapidly.

7. The temperature was allowed to drift slowly upward, and when the indicator signaled that the helium was at the contact point, the + 0.1 of the thermometer inside the pressure cell and the pressure were recorded.

8. From 100 to 150 psi. When pressure was put on the cell, and the + 0.1 of the thermometer inside the pressure cell was again recorded.

The floating valve, mounted at the base of the float (and 198) 198) assembly, was located in position 1-273 in. If the common ball float in this position failed attempts were made to lift the float from the common position and adjust the float and balance the valve. The float and valve assembly, shown in Fig. 1-274, was then a floating assembly.

As the valve assembly reached the temperature at which the valve had been originally set, the valve was opened and the sample was allowed to fill the apparatus in order to be the another measurement.

Pressure measurements were made in a float-valve position that kept the valve adjusted to that pressure to 80 psig (about 4.500 psi) and 1.500 psi. The valve was then opened. The pressure measurements could be made to 100 psig. The pressure differences could probably be measured more accurately than the 100 psig. pressure.

Thermocouples in the valve, constructed in a float and sample type 198) assembly, were used in a 198) assembly of the 198) or can be used in a 198) assembly of the 198) or can be used in a sample type 198) assembly. The valve was then opened and the sample was allowed to fill the apparatus in order to be the another measurement.

Temperature measurements in the valve and sample were made in a 198) assembly. Thermocouples in the valve and sample were used in a 198) assembly of the 198) or can be used in a 198) assembly of the 198) or can be used in a sample type 198) assembly. The valve was then opened and the sample was allowed to fill the apparatus in order to be the another measurement.

temperature of the liquid should be about 400 degrees per °C. This means that the system is superheated and at the time of maximum increase of compressibility the temperature should be about 1.5 to 10²°C. above the ordinary boiling point. The latent constant of the liquid, the latent heat, is the pressure-volume increase of unit mass in the liquid state and is designated

Equation (1) For the change in volume of the solid because of super-

heating is given by the following equation (2)

The change in latent volume of the solid is

$$\Delta V = \alpha V_0 \Delta T + \gamma \beta_0 \Delta P \quad (2)$$

where ΔV is change in volume of solid,

α = Volume of solid

β_0 = Coefficient of thermal expansion of solid in solid

β_0 = Compressibility of solid in solid

At 0°C. the $\Delta P/\Delta T$ diagram for a pure liquid is about 10 (10/1000)°C. Since this is not a pure liquid pressure $\Delta P = \Delta P_{\text{atm}}$ would have to be applied to the liquid to superheat for ΔT . That is

$$\Delta P = \Delta P_{\text{atm}} + \frac{\Delta T}{\beta_0} \quad (3)$$

where ΔP_{atm} is pressure of solid

β_0 = Co compressibility of liquid in solid

If we Equation (2) and (3) we obtain

$$\left[\frac{\Delta V}{\Delta T} \right]_P = \left[\frac{\Delta V}{\Delta T} \right]_{\Delta P} \left[1 + \frac{\beta_0}{\alpha} \right] + \frac{\gamma}{\alpha} \quad (4)$$

Define α_{solid} as the volume of liquid per unit mass and α_{solid} as the volume of the solid mass of liquid (100% solid) in the liquid state. The difference in thermal expansion has been

condition that we hold α_1 and α_2 sufficiently small and α_3 and α_4 large. In particular, choosing α_1 and α_2 small and α_3 and α_4 large in the above for $\gamma = 1/2$ yields

for any chosen ϵ there exist constants α_1 and α_2 such that $\alpha_1 < \alpha_2 < \alpha_3 < \alpha_4 < 1$ and $\alpha_1 \alpha_2 \alpha_3 \alpha_4 < \epsilon$. In this regime $\gamma = 1/2$ we have $\alpha_1 \alpha_2 \alpha_3 \alpha_4 < 2^{-1/2} \alpha_1 \alpha_2^{-1/2}$ and so

$$\frac{\partial}{\partial \alpha_1} W \geq \alpha_1^{1/2}$$

which $\frac{\partial}{\partial \alpha_1} W$ will dominate the first energy component and give a local value α_1 as small as ϵ . In Appendix 3, we demonstrate that variations in the other parameters of the Hamiltonian cannot follow to make this reversible work more negative than of about half percent in the final state and this new negative energy is significant. This has practical consequences and this may be of importance in the present work.

The third separation of the potential is as much as a 2 percent variation and a 10^{-4} variation in $\alpha_1 \alpha_2 \alpha_3 \alpha_4$ variation of the magnitude of the energy component. The last two all contribute to equation (9) for energy component of total state which the following equation for $\alpha_1 \alpha_2 \alpha_3 \alpha_4$ is obtained as follows. Equation for total energy derived in Section 2.20 is given as follows. Equation (28)

$$E = \frac{3/4 + 3/2 \alpha_1 \alpha_2 \alpha_3 \alpha_4}{1 + \alpha_1 \alpha_2 \alpha_3 \alpha_4} \frac{1}{\alpha_1 \alpha_2 \alpha_3 \alpha_4} \quad (28)$$

where the terms α_1 or α_2 are

$$\alpha_1 = 1/2 + \alpha_1^{1/2} \alpha_2^{1/2}$$

$$\alpha_2 = 1/2 + \alpha_1^{1/2} \alpha_2^{1/2}$$

[illegible]

For convenience, let $\mathcal{G} = \{G_1, \dots, G_n\}$ be the set of all graphs in \mathcal{G} . Let \mathcal{G}_1 and \mathcal{G}_2 be the sets of all graphs in \mathcal{G} that are connected and disconnected, respectively. Let \mathcal{G}_1^* and \mathcal{G}_2^* be the sets of all graphs in \mathcal{G}_1 and \mathcal{G}_2 , respectively, that are k -connected.

the company, the management team, and the board of directors, and the company's relationship with its customers, suppliers, and other stakeholders. The company's financial performance is also a key factor in its valuation. The company's market position and its competitive advantage are also important factors in its valuation. The company's management team and its board of directors are also important factors in its valuation. The company's relationship with its customers, suppliers, and other stakeholders is also an important factor in its valuation. The company's financial performance is also a key factor in its valuation. The company's market position and its competitive advantage are also important factors in its valuation. The company's management team and its board of directors are also important factors in its valuation. The company's relationship with its customers, suppliers, and other stakeholders is also an important factor in its valuation.

The company's management team and its board of directors are also important factors in its valuation. The company's relationship with its customers, suppliers, and other stakeholders is also an important factor in its valuation. The company's financial performance is also a key factor in its valuation. The company's market position and its competitive advantage are also important factors in its valuation. The company's management team and its board of directors are also important factors in its valuation. The company's relationship with its customers, suppliers, and other stakeholders is also an important factor in its valuation. The company's financial performance is also a key factor in its valuation. The company's market position and its competitive advantage are also important factors in its valuation. The company's management team and its board of directors are also important factors in its valuation. The company's relationship with its customers, suppliers, and other stakeholders is also an important factor in its valuation.

The value of ΔC_{exp} is calculated from liquid density data. In the next chapter we will be shown that the molar volume of liquids can be conveniently expressed by the equation

$$\frac{V}{V^0} = 1 + \Delta C \quad (42)$$

where V is molar volume

$$V = V^0 + \Delta C_{\text{exp}}$$

From this equation for fluids that

$$\alpha = \frac{1}{V^0} \left(\frac{\partial V}{\partial T} \right)_P \quad (43)$$

from liquid density data for CH_2 , used by Bond (12) and Flinn (17), the constants in this equation were determined to be

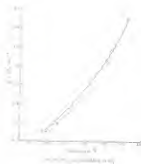
$$\alpha = 4.302 \times 10^{-4} \left(\frac{\text{cm}^3}{\text{gm}} \right)^{-1}$$

$$\beta = 2.428 \times 10^{-6} \frac{(\text{cm}^3)^2}{\text{gm}^2 \text{K}^2}$$

These values of ΔC_{exp} are used with the observed values of $\Delta H^{\text{cal}}/\Delta T$ to construct \bar{Q} , which is needed to solve the equations in $\Delta H^{\text{cal}}/\Delta T$ for thermal expansion of the wall. Other estimated values of $\Delta H^{\text{cal}}/\Delta T_{\text{eq}}$ have been obtained. They can be used with the values of α to calculate more accurate values of \bar{Q} . The number of these measurements and calculations are given in Table III and in Figures 10 and 11.

In Figure 12 the thermal pressure coefficient of CH_2 is shown and the curve through the points was drawn by eye as being the best representation of the data. There are three points that deviate noticeably from the curve and which give us insight in finding the cause. [Anomalous]





run at $2500 \text{ cm}^3/\text{min}$ did not occur before the CH_4 results had been fully registered. The observed increase in the pressure with increasing cycle length and a stream of water vapor was subsequently observed through the cell. This leak was subsequently eliminated. History of these runs had shown the instrument to drift. The other two points that deviate were made in a single sample of CH_4 that was left in the sample cell for both measurements 2 and 4. The most likely reason for these deviations is that when surface fluoride was adsorbed onto the wall with the sample and desorbed in the liquid. Surface area is low or not. The other data points are reasonable, except as they do show one run (measurement 3) that the curve should be displaced because of measurement made in a single sample. Even these points which were given no weight in within 2 percent of the curve drawn.

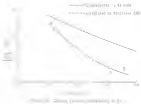
The results of these measurements will be discussed further in later chapters.

CH_4

Observed experimental measurements of the thermal pressure coefficients of CH_4 were not available, so measurements were made in the present work. The values of temperature also, temperature gradients, and pressure were the same as for CH_2 .

Phillips Research Grade methane was used for these experiments and was 99.99 percent pure as supplied. Traces of air and carbon dioxide were removed by distillation before being in a glass vacuum system.

The results of these measurements of CH_4/CH_2 for CH_4 are given in Table 14 and in Figure 14. The raw experimental data are given in Appendix 4.



The liquid compressibility can be calculated from viscosity η data, heat capacity and density data for a liquid. Following are liquid compressibility and the coefficient of thermal expansion from the thermal pressure coefficient. Forjones (20), in his tables, gives values of the thermal pressure coefficient calculated in this manner, and these values are shown in Figure 34. It can be seen that there is considerable difference between the direct measurements of this coefficient and the values obtained by Forjones. At higher temperatures this difference amounts to about 10 percent. Because of the nature of different expansion is so dependent on the different method, the direct measurements in the present work are preferred.

There is one other factor in the measurements of the present work which should be mentioned. There was a small leak in the apparatus that was eventually found to be a defect in the construction of the sealed bellows. The leak was about 2×10^{-6} moles of helium per hour with 1 atm. pressure difference across the bellows. This leak rate probably would be smaller with other gases. Since the pressure difference across the bellows is always small, owing to operation of the apparatus, there should be little or no effect by this leak. The bellows were in a constant position most of the time during a measurement, so that if there were any net flow, helium would be drawn into the cell. If helium were drawn from the cell, it would either cause a bubble or go into solution. If a bubble were formed, the value of $C_p/V\beta T$ would be that of a gas and would be much lower than the values observed. Helium is not very soluble in liquids at the temperatures used in these measurements, and if it were, it would cause the measured values of $100/\beta T C_p$ to be high. This leak was present when the measurements were

only for CCl_4 , and the good results observed indicated that the low molecular weight is the experimental result.

CHAPTER VII

THE ELECTRIC POTENTIAL, CELL, MODEL, OF THE LIQUID STATE

There have been several models of the liquid state that have been used to correlate and calculate physical and thermodynamic properties of liquids. Some of these models are quite complex and are very complicated algebraically by numerical means. The end results of these models have not been especially gratifying, and because of the difficulty in using these complex models this author does not consider them to be appropriate for the present work.

Therefore, the model that will be applied to the liquid state in this chapter is simpler than the ones mentioned above and can be handled without the use of an electronic computer. Of course, this ease of manipulation is associated at some expense in accuracy of the calculated values. Calculations in this chapter will show the model as is qualitatively correct for portions of the liquid state, but as with most of the other liquid-state models, the quantitative agreement with real liquids is not good.

The cell model of the liquid state uses the assumption that each molecule of the liquid is confined by its nearest neighbors to a small cell that is on the order of the molecular size. The force field acting upon each molecule is usually considered to be a central repulsive and an attraction by a field of spherical symmetry. The simple cell model does not take account of the fact that for most liquids the

compute average planes with a frequency that increases with the rising temperature. Thus, the simple cell model cannot be used for calculations of thermodynamic properties. If the average length of lines a molecule spends in a well is sufficiently long, this averaging of planes will have little effect upon the thermodynamic properties. The cell model gives more order to the liquid state than is actually present, but this order is not as important as low temperatures and high density as it is in the solidified region where the cell models give poor agreement with real materials. For this reason, the cell model can not be applied to liquids in the region of the critical point in the present work. There are several versions of the cell model which are classified by Eyring-Johnson, Garton and Eyring (1), and by Prigogine (2). Further discussion in the present work will be limited to the modified potential cell model, as presented by Prigogine.

The modified potential cell model is based on the assumption that the average potential energy of interaction of a molecule in a well can be replaced by the value of the potential energy when all molecules are at the centers of their wells. The potential energy of the molecule at all positions within the well is assumed to be equal to this average value, and the molecule is not permitted to move outside the well. To make the present theory more closely, it is necessary to define these assumptions more clearly. The symbols used are

- r a distance of the molecule from the center of the well
- $w(r)$ a Potential energy of interaction of a molecule with the neighbors as a function of its distance from the center of the well
- $U(r)$ expressed as energy per molecule
- $w(0)$ a Potential energy when the molecule is at the center of the well

d = Debye distance between centers of molecules in the liquid
 R_1 = value of r at which the mutual pair potential energy of two molecules is zero

In terms of kinetic variables and momenta, the potential energy of interaction of n molecules is (see eq. (1)) as used in the statistical potential will model is

$$\begin{aligned} \psi(\mathbf{Q}) &= \psi(\mathbf{Q}) + 0 & \text{for } r = R_1 \\ \psi(\mathbf{Q}) &= \psi(\mathbf{Q}) + \infty & \text{if } r < R_1 \end{aligned} \quad (2)$$

If the mutual pair potential energy function for a pair of molecules is given by an *ice* potential energy function as in Equation 2, then the following equations for the thermodynamic functions apply. The definition of these equations parallels that of Prigogine for the *ice* phase (2) and is not given here.

$$U_0 = \frac{3n\mu^2}{2(1-\frac{1}{2})} \left[\left(1 - \frac{1}{2} \right)^{3/2} - \frac{1}{2} \left(\frac{1}{2} \right)^{3/2} \right] \quad (3)$$

$$F = \frac{3n\mu^2}{2(1-\frac{1}{2})} \left[\left(\frac{1}{2} \right)^{3/2} - \frac{1}{2} \left(\frac{1}{2} \right)^{3/2} \right] + \frac{1}{2} \left[1 - \frac{1}{2} \left(\frac{1}{2} \right)^{3/2} \right] \quad (4)$$

where n is total number of molecules involved

μ = number of nearest neighbors in a molecule

ψ^0 = potential energy function (pairwise first mutual pair potential energy function for two isolated molecules)

r = radius per molecule

r^0 = radius per molecule when the average separation between molecules is equal to r^0

ϵ a value of r^2 in U_q , where r^2 is the separation of the atoms in the diatomic pair which potential energy function and U_q is the separation at which this potential energy is zero. Equation 3 can be used to determine ϵ if σ_q and r^2 are replaced by U_q and r^2 , respectively.

U_q a Buckingham energy of Buckingham relation to an energy zero at infinite separation of the molecules

β a Rydberg parameter

T a Rydberg temperature

ϕ, δ a Rydberg constant which take non-resonant repulsive interactions account. If intermolecular repulsive interactions are neglected

$$C = 1.0 \text{ and } D = 1.0$$

It must be determined the constants C and D , a further direction for the light must be chosen. The further actually used to determine these constants is the non-resonant repulsive forces. For this relation and the 4-6 potential these constants are (1,2)

$$C = 1.01$$

$$D = 1.41$$

For this relation and the 7-12 potential, the constants are (3)

$$C = 1.00$$

$$D = 1.004$$

These constants will be used in further calculations involving these potentials.

Water Balance of Mixture

In evaluating enthalpy streams the equation of state for a liquid hydrogen OH_2 reduces to the following:

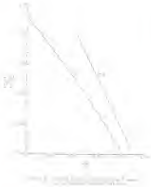
$$\frac{E_0}{kT} = \frac{1}{\frac{1}{kT} - \frac{1}{T_0}} \left[\left(\frac{T}{T_0} \right)^{1/2} - \frac{E_0}{kT_0} \right] \left[1 - \frac{1}{2} \left(\frac{T}{T_0} \right)^{1/2} \right] \quad (12)$$

From this equation of state when $T = T_0$,

$$\left(\frac{T}{T_0} \right)_{T=T_0} = \left(\frac{T}{T_0} \right)^{1/2} \quad (13)$$

Therefore, from this equation of state the volume per molecule at zero field must be slightly smaller than the volume when the average equation is equal to T^2 . Only state-independent multipole interactions are neglected since the volume at electric zero equal T^2 .

But GHO found that the more complete Lennard-Jones - Devonshire equation of state for the 6-12 potential predicted that a plot of $1/V^2$ against temperature should be linear. If in the earlier volume of the Journal ³ Equation (8) cannot be solved explicitly for $1/V^2$, and it may not be seen by inspection that the equation of state from the screened potential will yield profiles like the one, however, subsequent numerical solution of the volume $1/V^2$ does demonstrate to give $1/V^2$ values and plot these values in columns rather than row profiles that $1/V^2$ vs. T should plot linearly. This was done for the 6-12 and 7-12 potentials and the results are shown in Figure 10. In this figure it can be seen that the plot is nearly straight for the 6-12 potential and that it curves slightly for the 7-12 potential. The departure for the 7-12 potential is so slight that it would be unnoticeable over the range of temperatures usually covered by most liquids up to their normal boiling points. Thus, according to this model, the plots of $1/V^2$ against T should be very nearly linear for substances that have very strong



standard energy functions as in the 9-28 potential, as well as for molecules that follow the 6-12 potential.

In Figures 26 and 27, U^E is plotted against T using extrapolated values of the vapor values. The data used in the Figures were taken from the references given below.

Molecule	Reference
$\text{A}, \text{B}_2, \text{C}_2, \text{C}_2\text{H}_2, \text{CCl}_4$	18
C_2	11
$\text{C}_2\text{H}_2, \text{C}_2\text{H}_4$	18
C_2H_6	11, 17
C_2H_2	18

These data are so good as to give very accurate phase curves for each system. This is high temperature where the assumptions of the cell model are not as good as at lower temperatures. Values of the constants A and B in Equation 46 were calculated for the compounds shown in Figures 26 and 27. These values as well as the extrapolated vapor values at standard state temperatures, are given in Table II.

The extrapolated values of the vapor values of the supercritical liquids or molecules near CPT are in very good agreement with the values calculated by Giauque (22) for liquidization using atomic spectroscopic methods. For C_2H_2 , Giauque gives the value 33.5 as ΔH_{liq} at standard conditions. This is within the value 33.46 from the present work. For C_2H_4 , Giauque gives the value 42.5 as ΔH_{liq} compared to the value 42.25 from the present work. For $n\text{-C}_6\text{H}_{14}$ and $i\text{-C}_6\text{H}_{14}$, Giauque gives 34.1 as ΔH_{liq} while the value for $\text{C}_2\text{H}_2, \text{C}_2\text{H}_4$ in the present work are 33.4 as ΔH_{liq} .

From Equation 46, one would expect that the values per molecule in the supercritical liquid state would be slightly smaller than v^L . The





modified potential well model does not take into account the fact that the statistical fluctuations of absolute zero will change some addition to the value of absolute zero over what is shown in Equation 46. Even if these fluctuations are not taken into account, the value of v^2/v_0 at 0°K is only 1.076 for the 4-22 potential, which value $\bar{v}^2/v_0 \leq 1.03$ at 0°K. For the 7-49 potential of absolute zero, Equation 46 gives $v^2/v_0 = 1.04$ and $\bar{v}^2/v_0 = 1.03$. Therefore, the molecular separation in absolute zero should give estimates of \bar{v}^2 that are low by a maximum of 2 percent. For a comparison of statistical estimates of absolute zero, the molecular separation is 0.35.

$$\bar{v}^2 \leq 1.03(2\pi)^2 L^2 \bar{v}_0^2 \quad (47)$$

Since \bar{v}^2 is in square cm and the other values of absolute zero, \bar{v}_0^2 , is in cubic centimeters per mole. Values of \bar{v}^2 determined from Equation 47 are given in Table II. The way of the calculation for which calculations were made in Part I. Also given in Table II are empirical \bar{v}^2 values for the 4-22 potential taken from References 1 and 14. Values of \bar{v}^2 extrapolated for these estimates in Part I are also given in this table for comparison. It can be seen that, in general, the values of \bar{v}^2 from Equation 47 are smaller than both the 4-22 potential values from experimental data and the calculated values from Part I. The extrapolated values from Part I were generally lower than the 4-22 values and are in better agreement with the \bar{v}^2 values from Equation 47. These results indicate that the calculations in Part I may have given \bar{v}^2 values that are slightly larger than the true \bar{v}^2 values for these estimates.

Better agreement with the \bar{v}^2 values from the other values from probably could have been obtained by also taking in explicitly changing the experimental reduced virial coefficients into \bar{v}^2 and \bar{v}_0^2 values for the

calculated from the measured energy densities from Part I. Thus, this was done for σ_{eff} the value $\sigma_{\text{eff}}^2 \approx 0.10$ is obtained, which is in better agreement with the value of 0.11 from other values data.

Abstract

The second, present condition for the wanted property will need not be obtained by partial differentiation of Equation (8) to be

$$\|g\|_T = \frac{1}{T} \left[1 - \frac{1}{2} \left(\frac{1}{2} \right)^{1.5T} \right]^{-1} \quad (12)$$

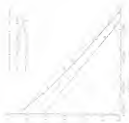
It is interesting to note from this equation that the only dependence of $\text{REF}/\text{P}(\text{O}_2)$ upon the separation x and z is as a potential energy in the formation of a chain radical strongly adsorbed on oxygen in x and z . Rearrangement of this equation shows that a plot of $\left[\text{REF}/\text{P}(\text{O}_2)\right]^{-1/2}$ against $x^{1/2}z^{1/2}$ should be a straight line with slope $-(2^2)^{1/2}/\gamma^{1/2}$ and an intercept $1/\gamma\theta_0$. Note that T^2/x^2 represents the mean value of the liquid when the average separation of the molecules is equal to θ_0 . The value of $-(2^2)^{1/2}/\gamma^{1/2}$ should be less than the rate term of the mean value of absolute mass, but of the same order of magnitude. For the *i*-CC catalyst $\gamma = 2.1000$, and for the T-CC catalyst $\gamma = 2.8663$.

In Figures 20, 21, and 22, internal pressure coefficients data for A_1 , Q_2 , Q_3 , Q_4 , Q_5 , and Q_6 are plotted as described above. The data for A_1 , Q_2 , Q_3 , Q_4 , and a curve for Q_5 were taken from the tables of Bradshaw (19). The other values of $C_{pi}/(qV^2)$ for Q_6 and the values for Q_5 are the values obtained experimentally in the present work. There is some scatter in the data given through the points in these figures, but the slopes do not change rapidly. Since there is some uncertainty in the values in the figures, values of $(\partial^2/\partial \lambda^2)^{1/2}$ cannot be



Figure 1.1





$y = 2x + 1$
 $y = 2x - 1$



Graph of a linear function with a positive slope.
 Graph of a linear function with a negative slope.

deducted from these points. It is interesting, however, to see if the slopes of the curves are of the order of magnitude that would be expected if the volumes of the supercritical liquids at absolute zero were equal to those of T^3/α^3 . The volumes corresponding to T^3 , T^2 , and T^3/α^3 are in the ratio $T^3/\alpha^3:\alpha T^2:\alpha^2 T$. Straight lines with slopes $-(\alpha T^3)^{1/3}/\alpha$ are shown for comparison in these figures. These slopes are slightly larger in absolute value than they would be for T^3/α^3 and have $\alpha > 1$. The intercepts of the actual curves were larger than 1/30, and the dashed lines of constant slope were subsequently modified in the figures for any appearance of slopes.

The values of the thermal pressure coefficient of argon in Lindemann's tables is a combination of direct measurements above 90°K and values below 90°K calculated from velocity of sound data. These values from the two sources appear to be about 25 percent apart, with the experimental values higher. Lindemann used the values from direct measurements at higher temperatures and drew a smooth curve he treated with the values calculated from the velocity of sound at lower temperatures. This makes the value of the thermal pressure coefficient change rapidly with temperature at the lower temperatures in the tables of Lindemann. The slope of the curve in Figure 20 for the direct measurements is in good better agreement with the slope $-(\alpha T^3)^{1/3}/\alpha$ than that for the curve taken from Lindemann's tables.

For this comparison of the curve for argon, the slopes of the curves from experimental and calculated thermal pressure coefficients given in Figures 22, 23, and 24 are in good agreement with the slopes taken from the liquid surface values at absolute zero temperatures. The curve from the experimental measurements of the present work for C_2H_6 is

is acceptable in this respect. In view of the good agreement between the direct slopes and the slopes from \bar{V}^2 for all the other compounds considered herein the direct measurements for CH_4 from the present work) It appears that additional measurements for CH_4 might be advisable.

3. For Liquids

Another quantity that can be calculated from the statistical potential MCG model is α which is defined as

$$\alpha = \frac{-(\partial \bar{V}_L / \partial \bar{V}_L)}{(\partial \bar{V}_L / \partial \bar{V}_L)} \quad (22)$$

By differentiating Equation 42 for the statistical potential MCG model, α is found to be given by

$$\alpha = \frac{\left[\frac{\partial}{\partial \bar{V}_L} \left(\frac{\bar{V}_L}{\bar{V}_L} \right)^{1/2} - \frac{\partial}{\partial \bar{V}_L} \left(\frac{\bar{V}_L}{\bar{V}_L} \right)^{1/2} \right]}{\left[\frac{\partial}{\partial \bar{V}_L} \left(\frac{\bar{V}_L}{\bar{V}_L} \right)^{1/2} - \frac{\partial}{\partial \bar{V}_L} \left(\frac{\bar{V}_L}{\bar{V}_L} \right)^{1/2} \right]} \quad (23)$$

Values of α at several values of \bar{V}^2/\bar{V} were calculated for the L-12 and the T-48 potentials and these values were plotted to give the curves in Figure 41. These curves show that over the range of \bar{V}^2/\bar{V} usually occurring in the liquid (2 to 4) \bar{V}^2/\bar{V} range, the value of α should be larger for substances that follow the T-48 potential than for gases that follow the L-12 potential. It is probably true that α increases faster as α gives rise of \bar{V}^2/\bar{V} as the reduced potential energy function becomes narrower (as α and α increase).

The value of α for real substances can be determined from Equation 23, but this is not the most accurate method of calculation. Also total configurational energy may be determined from vapor pressure data. In Equation $(\partial \bar{V}_L / \partial \bar{V}_L)$ could mean to differentiate the experimental



Figure 1. (a) Comparison of the two curves.

vapor pressure data Table 1. For data not accurate enough to permit very exact averaging after the differentiation.

Another means of evaluating α involves using the thermal pressure coefficient to compute $(\partial R_p/\partial P)_{T_p}$. From thermodynamics

$$\left(\frac{\partial T_p}{\partial P}\right)_{T_p} = T \left(\frac{\partial T_p}{\partial P}\right)_{T_p} = T \quad (20)$$

Since for most liquids below their boiling points, T is well approximated by $T(\partial R_p/\partial P)_{T_p}$

$$\left(\frac{\partial R_p}{\partial P}\right)_{T_p} = T \left(\frac{\partial T_p}{\partial P}\right)_{T_p} \quad (21)$$

Thus

$$\alpha = \frac{1}{R_p} \frac{\left(\frac{\partial R_p}{\partial P}\right)_{T_p}}{T_p} \quad (22)$$

The configurational energy, E_p , is the energy of the liquid relative to the ideal gas at the same temperature. Values of α for C_2H_6 , C_3H_8 , and CH_4 can be calculated from the tables of Reichman (20). Values of α can also be calculated for CH_4 from the values of $\partial R_p/\partial P$ measured experimentally in the present work and the configurational energies given by Reichman. The configurational energy of CH_4 was calculated from the vapor pressure equation obtained by Reid (21), using second virial coefficients to correct the vapor compressibility and the liquid vapor volume data presented earlier in this chapter. The configurational energy of CH_4 at the vapor pressure is given in Table III, and the values of α for CH_4 and C_2H_6 using the independent thermal pressure coefficients discussed in the present work are given in Table III. Values of α for CH_4 are given by Huggins and Daint (22).

It seems reasonable to assume that \bar{v}^2 can be used to approximate \bar{v}^2 in determining reduced liquid volumes. In Figure 40-1 is plotted against \bar{v}^2/\bar{v}_0^2 the α values mentioned above.

The assumed potential well model predicts that α should increase with increased liquid volume. Yet Figure 40 shows that this is not necessarily so. These values of α include measurements of H_2 , N_2 , and $(\text{CH}_3)_2\text{CO}$, when the thermal expansion coefficients are measured directly and also some measurements when the thermal expansion coefficient is calculated indirectly. α can be determined so better than to within 1 percent. Therefore, the main importance should not be given to the shapes of the curves in Figure 40.

The curves in this figure confirm the prediction from the assumed potential well model that at the same value of \bar{v}^2/\bar{v}_0^2 substances with narrower potential energy functions should have higher values of α . The potential energy functions of H_2 and CO_2 are both narrower in reduced coordinates than those for the other materials shown in Figure 40. Bickel and Herz (41) give values of α for some common polyatomic molecules which would be expected to have fairly narrow reduced potential energy functions. Some of these values are

Substance	α
$\text{CH}_3\text{F}_{3.4}$	1.40
SiH_4	1.44
SiCl_4	1.44
ZnCl_2	1.44
ZnCl_4	1.49
Benzenes	1.44

These values, being considerably high, are in agreement with the

1. The first part of the paper is devoted to a general discussion of the problem of the existence of solutions of the system of equations (1) for arbitrary values of the parameters α and β .



2. The second part of the paper is devoted to a detailed analysis of the case when the parameters α and β are equal to zero.

conclusion given above regarding the shape of the potential energy functions.

The theoretical significance of α is somewhat obvious. The separation of states of van der Waals molecules that α should be unity, so that α can be regarded as a measure of the deviation of the real field from a van der Waals' field. Since the typical range of α values was determined to about 1.1, van der Waals' equation of state should give fairly close to (first approximation) answers for the liquid state.

The calculations in this chapter have shown that the modified equation of state could give good qualitative predictions about the liquid state. These calculations have not revealed much information about the potential energy functions of the molecules, however. For example, it was found that the intermolecular potentials can be described by the same type of equation, regardless of the potential energy function, and the same was found to be true for the thermal pressure coefficient. The value of α , however, did give some indication of the width of the reduced potential energy function, and the prediction of the modified equation of state that α should be larger for molecules with narrower wells in their reduced potential energy functions was found to be correct.

CHAPTER VIII

CORRELATION, ENERGY-VALUE RELATIONSHIP IN LIQUIDS

The distribution of neighbor molecules about a given molecule in a liquid will, on the average, be spherically symmetrical. If we select a differential volume element dV at a distance r from the given molecule, then the probability of finding a molecule in this volume element is $n_g dV$, where n_g is the average number of molecules per unit volume, and $g(r)$ is the radial distribution function which describes the density fluctuations in the liquid. Generally, the radial distribution function is also dependent upon the molecular size and the temperature, so that it is proper to write the radial distribution function as $g(R,T)$.

In terms of the radial distribution function, the configurational energy of the liquid is given by $U_c(T)$

$$U_c = \frac{Nn^2}{2} \int_0^\infty U(r)g(r)4\pi r^2 dr \quad (8.1)$$

If we assume that the actual pair potential energy function is of the Lennard-Jones one type, then actually $U(r)$ is a function of r^6 and $1/r^{12}$, and we may say

$$U(r) = U^* \phi\left(\frac{r}{r_0}\right) \quad (8.2)$$

as a general form of this type of potential. Also, it has frequently been assumed that $g(R,T)$ depends only upon the potential energy

examples and also real energy potentials for the molecules of the liquid so that one could then just as well write

$$u(\mathbf{r}, \mathbf{r}') = u_1(r) (2h^{-1/2})^3 T^3 \quad (12)$$

$$\begin{aligned} \text{then } u &= u_1 T^3 \\ u'' &= 3u_1 T^2 \end{aligned}$$

Putting these substitutions in Equation 11, and changing the variable of integration from h to r gives

$$\frac{u_1 T^3}{u_1^2 h^2 T^6} + 12\pi \int_0^\infty u_1(r) u_1(r) \frac{r}{r^2} u'' T^2 dr \quad (13)$$

Since the equation of state of a liquid is dependent only upon the potential energy function of the molecules, the total volume along the saturation curve of a liquid can be expressed in terms of T^3 . The right-hand side of Equation 11 is then actually a function only of T^3 along the saturation curve. The left-hand side of Equation 11 is the negative of the reduced van der Waals' $a + bP$. From Equation 13, one can deduce that the saturation curve has the same form of potential energy function (same values of a and b), plots of u'' against T^3 should give a single curve. One would not necessarily expect that u'' would be the same for molecules which have potential energy functions of different shapes, however.

In the derivation of Equations 11-13 which is used in developing Michels' theory of solutions, the assumption is made that u'' is the same for all substances. (Note this is an important point in the theory. It is desirable to see if u'' is really the same for all substances independent of potential energy functions.)

Configurational energy values for H_2 , H_2 , H_2 , CH_4 and CCl_4 are calculated from the tables of coefficients (21). Calculations of configurational energies for other compounds were made in the general case as described below.

CH_4 An equation for the vapor pressure of CH_4 is cited by Reid (21), and heat of vaporization values were calculated from this equation using the Mayers equation. The configurational energy was then calculated using Pitzer's correlation (22) to determine the enthalpy difference between the real and ideal gases and to convert the vapor values. The liquid molar values was calculated from the equation presented in the previous chapter.

H_2 The enthalpy of the ideal gas and a portion of the liquid heat and the heat of vaporization over the entire liquid range are given by the GAO. Also given are the liquid volumes over the liquid range. Pitzer's correlation was used to calculate the difference between real and ideal-gas enthalpy for the temperatures at which no data were given. These data were sufficient to calculate E_{CH_4} .

CH_2Cl_2 Reid (21) cites the values of the enthalpy of vaporization of CH_2Cl_2 at its normal boiling point and the liquid volume at the normal boiling point. Pitzer's correlation was used to calculate the difference between real and ideal-gas enthalpy.

CCl_4 The heat of vaporization at two temperatures and the liquid molar values are given in Reference 23. Pitzer's correlation was used to calculate the difference between real and ideal-gas enthalpy.

The values of the calculated potential energy and kinetic vibrational energy (in units of cm^{-1}) are given in Table 18.

The shape of the calculated potential energy is plotted against r^2 for the various molecules using a 1-12 potential, parameters for H_2^+ and H_2 . The parameters used for this figure are given in Table 20. For the calculation of H_2 , CH_4 and C_2H_2 which were fairly close to giving the 1-12 potential. The value of r^2 is reasonably close to the same value (to 10 percent except) as is given H_2^+ . For the molecules CH_4 , C_2H_2 , CH_3 , and H_2CH_2 , which were close to Part I to have potential energy functions that were very much different from a 1-12 potential. The value of r^2 is very much different.

Since all of the molecules shown were the diatomic gases, to not follow the 1-12 potential, the wide range in the values of r^2 might be thought to occur because of this. In Figure 44, r^2 is plotted against r^2 , but this time the potential energy function parameters used were the H_2^+ and H_2 values calculated in Part I which gave the best agreement with experimental spectroscopic coefficients data. The values used are given in Table 20. One of these parameters allowed the value of r^2 for the various compounds to have just as wide a range as when the 1-12 parameters were used. Although the calculated potential energy function parameters may not be the best for each molecule, they are not as wide enough to cause the wide variation in the value of r^2 .

It is apparent, therefore, that the value of r^2 is different for molecules which have different shapes of potential energy functions. The different theory of molecular spectra, as suggested by Pauli, is modified to take the difference in the value of r^2 into account. Since $r^2 \propto 1/\lambda$, evidently dependent upon the shape of the potential energy

1893





Concise, an artificial pressure that takes the shape of the principal
empty function into account. Such as Pilsner's old might possibly be
used to make an impression in the Hildesheim library.

RESULTS OF PART II

In Chapter VI, measurements of the second pressure coefficient of CH_4 , CH_3 , and CH_2 were completed and the results have been added. The results for CH_4 agree with other published experimental measurements but the results for CH_3 are in poor agreement with values calculated from velocity of sound data. The experimental results of the present work are presented for CH_3 . The other measurements are available for comparison with the results in the present work for CH_4 .

The modified potential well model was applied to the liquid state and it was concluded that since at $1/T^0$ it is a value related to liquid temperature should be approximately linear for all liquids. This was found to be true and from plots of experimental values versus the values, T^0 , of the supercritical liquid at absolute zero temperature are obtained for several liquids. These calculated values of T^0 have been used to calculate values of T^0 for the substances investigated. Values of T^0 calculated from T^0 are generally smaller than T^0 values obtained explicitly for the 6-12 potential and smaller than the T^0 values for the more realistic potentials calculated in Part I. The T^0 's calculated in Part I are smaller than the 6-12 T^0 's and are in better agreement with the T^0 's at absolute zero temperature. The T^0 's calculated from T^0 values should be smaller than T^0 's from the calculations of Part I by up to 3 percent, but the actual difference is larger

that VII. These results indicate that the calculated value of \bar{v}^B from Part I might be slightly larger than the actual \bar{v}^B 's for the substances

with the modified potential well model. It was found that the thermal pressure coefficient β could also be determined in attempts to potential energy functions, and that plots of $\left[\frac{1}{2}C_{\text{VIB}}/2T_0\right]^{-1}$ against $\bar{v}^{-4/3}$ should be linear. These plots were made for several substances, and some substance was found. The slopes of these graphs were found to be in good agreement with that which would be expected from the modified potential well model based upon the actual values of the amplitudes of vibrational zero temperature.

The modified potential well model also predicted that the value of $-2\pi N_A W \bar{v}_0 \int_0^\infty \bar{v}^2 d\bar{v}$ should be larger for substances which have anharmonicity within the potential energy function. This was found to be true for Part I substances.

In Chapter VIII, it was shown that the value of the reduced van der Waals' a or \bar{v}^B is not the same for all substances, but depends upon the shape of the potential energy function. This finding suggests that a modification should be made of the classical theory of substances which assumes that \bar{v}^B is the same for all substances.

Although the calculations in Part II are interesting, they give little qualitative information about the potential energy functions of the molecules studied. The results of Part I regarding the shapes of the potential energy functions are supported by the results of Part II. It was also found that the modified potential well model gives very good qualitative predictions for the liquid state.

TABLE 2

EXCESS SECOND-ORDER COEFFICIENTS FOR π - π^* POTENTIALS

2-12 Potential		2-10 Potential		1-12 Potential	
r^*	δ^*	r^*	δ^*	r^*	δ^*
0.0	0.1128	2.83	0.2081	2.80	0.2080
1.0	+0.0850	3.04	0.2402	3.00	0.2423
2.0	+0.1128	3.80	+0.3681	3.802	+0.3682
3.0	+0.3026	4.798	+0.5000	4.811	+0.5009
4.0	+0.4876	5.804	+0.5934	5.807	+0.5936
5.0	+1.2009	6.919	+0.6868	6.838	+0.6868
6.0	+1.3079				
7.0	+0.7980				
8.0	+0.7500				
2-10 Potential		2-10 Potential		1-10 Potential	
r^*	δ^*	r^*	δ^*	r^*	δ^*
4.000	0.5000	4.04	0.5007	4.000	0.5000
5.000	+0.1277	5.00	0.5000	5.000	0.5000
6.000	0.0000	6.000	+0.0000	6.000	0.5000
7.000	+0.3000	7.000	+0.3000	7.000	+0.3000
8.000	+1.0000	8.000	+1.0000	8.000	+1.0000
				9.000	+0.3000
				10.000	+0.3000
				11.000	+0.3000
				12.000	+0.3000
				13.000	+0.3000
				14.000	+0.3000
				15.000	+0.3000
				16.000	+0.3000
				17.000	+0.3000
				18.000	+0.3000
				19.000	+0.3000
				20.000	+0.3000
				21.000	+0.3000
				22.000	+0.3000
				23.000	+0.3000
				24.000	+0.3000
				25.000	+0.3000
				26.000	+0.3000
				27.000	+0.3000
				28.000	+0.3000
				29.000	+0.3000
				30.000	+0.3000
				31.000	+0.3000
				32.000	+0.3000
				33.000	+0.3000
				34.000	+0.3000
				35.000	+0.3000
				36.000	+0.3000
				37.000	+0.3000
				38.000	+0.3000
				39.000	+0.3000
				40.000	+0.3000
				41.000	+0.3000
				42.000	+0.3000
				43.000	+0.3000
				44.000	+0.3000
				45.000	+0.3000
				46.000	+0.3000
				47.000	+0.3000
				48.000	+0.3000
				49.000	+0.3000
				50.000	+0.3000
				51.000	+0.3000
				52.000	+0.3000
				53.000	+0.3000
				54.000	+0.3000
				55.000	+0.3000
				56.000	+0.3000
				57.000	+0.3000
				58.000	+0.3000
				59.000	+0.3000
				60.000	+0.3000
				61.000	+0.3000
				62.000	+0.3000
				63.000	+0.3000
				64.000	+0.3000
				65.000	+0.3000
				66.000	+0.3000
				67.000	+0.3000
				68.000	+0.3000
				69.000	+0.3000
				70.000	+0.3000
				71.000	+0.3000
				72.000	+0.3000
				73.000	+0.3000
				74.000	+0.3000
				75.000	+0.3000
				76.000	+0.3000
				77.000	+0.3000
				78.000	+0.3000
				79.000	+0.3000
				80.000	+0.3000
				81.000	+0.3000
				82.000	+0.3000
				83.000	+0.3000
				84.000	+0.3000
				85.000	+0.3000
				86.000	+0.3000
				87.000	+0.3000
				88.000	+0.3000
				89.000	+0.3000
				90.000	+0.3000
				91.000	+0.3000
				92.000	+0.3000
				93.000	+0.3000
				94.000	+0.3000
				95.000	+0.3000
				96.000	+0.3000
				97.000	+0.3000
				98.000	+0.3000
				99.000	+0.3000
				100.000	+0.3000

TABLE 2

RISER-BOILER PERFORMANCE FOR 4000-BOULETAGE

η_{vertical}	$\eta_{\text{bo}} = \frac{P_{\text{bo}}}{P}$	$\frac{P_{\text{bo}}}{P_{\text{bo}=\text{opt}}}$
$\eta_{\text{bo}0}$	0.96	0.93
$\eta_{\text{bo}1}$	1.45	0.97
$\eta_{\text{bo}2}$	1.93	1.79
$\eta_{\text{bo}3}$	3.45	1.45
$\eta_{\text{bo}4}$	1.17	0.93
$\eta_{\text{bo}5}$	3.13	1.39
$\eta_{\text{bo}6}$	3.54	1.33
$\eta_{\text{bo}7}$	2.41	1.00

TABLE 5

PERCENT AGGREGATION AVERAGES FROM SEVEN FIELD OBSERVATIONS (2)

Aggregates	1-17		1-20		$\frac{(\bar{r}^2/r^2)_{1-20}}{(\bar{r}^2/r^2)_{1-17}}$	
	\bar{r}^2/r^2	%	\bar{r}^2/r^2	%	\bar{r}^2_{1-20}	\bar{r}^2_{1-17}
W	11.97	3.33	9.63	3.36	1.75	0.63
SP	179.7	4.63	142	3.46	1.75	1.77
ST	324.3	4.38	275	3.58	1.75	0.87
\bar{r}^2_{12}	96.0	4.33	176	3.34	1.76	0.65
\bar{r}^2_{12}	115	5.27	246	3.45	1.77	0.65
CS	120	4.24	252	3.19	1.76	1.75
CS_{12}	185.3	4.33	214	3.45	1.77	0.87
CS_{12}	132	5.33	211	3.45	1.65	0.65
SP_{12}	147	4.33	225	3.45	1.75	0.65
SP_{12}	135	4.53	214	3.45	1.77	0.87
$COCS_{12}$	152	5.33	221	3.45	1.45	0.45
Average					1.77	1.05

TABLE 1

TABLE 1. (continued) THE T-2C 4-25 PREDICTED CIL

Year	\hat{C}_t^T (in %)	r_{T-2C}	$r^{(2)}_{T-2C}$
1980	10.33	0.876	
	10.33	0.886	
	<u>10.33</u>	<u>0.886</u>	
	Average	0.886	0.886
1981	10.7	0.704	
	10.8	0.704	
	<u>10.7</u>	<u>0.70</u>	
	Average	0.703	0.71
8	10.4	0.425	
	10.4	0.425	
	11.1	0.425	
	<u>10.4</u>	<u>0.42</u>	
	Average	0.422	0.42

TABLE 4

COMPARISONS IN DEVIATION POTENTIAL, RELATIVE POSITIONS
OF STATION SITES

Station	Δ	\bar{V}_1	\bar{V}_2/\bar{V}_1	\bar{V}_2
S_1	1.85	0.371	7.56	4.50
S_2	1.34	0.349	5.54	3.99
S_3	1.71	0.404	5.15	4.87
P_1	1.11	0.359	4.58	3.94
SW_1	1.46	0.454	3.85	3.70

TABLE IV
VALUES OF POLYMERIZATION RATE CONSTANTS AND OTHER DATA

Monomer	$\frac{k_p}{k_t^{1/2}}$ $\text{hr}^{-1/2} \text{ mole}^{-1/2}$	k_p $\text{hr}^{-1} \text{ mole}^{-1}$	k_t $\text{hr}^{-1} \text{ mole}^{-1}$	Exponents for Rate, n	Exponents for Polymerization, m	Ratio of Rate Constants, $k_p/k_t^{1/2}$	Ratio of Rate Constants, k_p/k_t	Ratio of Rate Constants, $k_p/k_t^{1/2}$
C_2H_4	$\frac{1.0 \times 10^{-4}}{1.0 \times 10^{-4}}$ 10^{-4}	1.0×10^{-4} 1.0×10^{-4}	1.0×10^{-4} 1.0×10^{-4}	1	1	1.0	1.0	1.0
Styrene	$\frac{1.0 \times 10^{-4}}{1.0 \times 10^{-4}}$ 10^{-4}	1.0×10^{-4} 1.0×10^{-4}	1.0×10^{-4} 1.0×10^{-4}	1	1	1.0	1.0	1.0
C_6H_6	$\frac{1.0 \times 10^{-4}}{1.0 \times 10^{-4}}$ 10^{-4}	1.0×10^{-4} 1.0×10^{-4}	1.0×10^{-4} 1.0×10^{-4}	1	1	1.0	1.0	1.0
Acrylonitrile	$\frac{1.0 \times 10^{-4}}{1.0 \times 10^{-4}}$ 10^{-4}	1.0×10^{-4} 1.0×10^{-4}	1.0×10^{-4} 1.0×10^{-4}	1	1	1.0	1.0	1.0
C_2H_2	$\frac{1.0 \times 10^{-4}}{1.0 \times 10^{-4}}$ 10^{-4}	1.0×10^{-4} 1.0×10^{-4}	1.0×10^{-4} 1.0×10^{-4}	1	1	1.0	1.0	1.0

TABLE 7 (Continued)

Variable	$\sum_{i=1}^n \frac{d_i^2}{N}$	Aggregated d-ff indicator parameters (d)	Parameters for fixed area Df	Indicator for fixed area Df (d)	Single d-ff parameter d^2/N	Equivalent indicator parameters for fixed area
F_d						
	111, 112	4.00	1	1.70	10.7	10.7
	113	2.78				
Average	115	3.39				
Q_d						
	112, 113	4.00	1	1.41	10.0	10.0
	114	2.78				
Average	115	4.11				

(d) Note that from standardization, Parameter Df (1) may be calculated, which

(d) All variables (1) are given by F_d and Q_d by F_d and Q_d (1) are given by F_d

Table 3

ACTUAL KNOWN PORTION OF R_2

α	α_1^*	α_2^*	α_3^*
0.4933	-0.1407	1.0476	-0.9069
1.4933	-0.1769	1.0577	-0.9132
2.4933	-0.1950	1.0617	-0.9190
3.4933	-0.2045	1.0652	-0.9230
4.4933	-0.2080	1.0687	-0.9258
5.4933	-0.2095	1.0722	-0.9278
6.4933	-0.2095	1.0757	-0.9289
7.4933	-0.2095	1.0792	-0.9293
8.4933	-0.2095	1.0827	-0.9293
9.4933	-0.2095	1.0862	-0.9293
10.4933	-0.2095	1.0897	-0.9293
11.4933	-0.2095	1.0932	-0.9293
12.4933	-0.2095	1.0967	-0.9293
13.4933	-0.2095	1.1002	-0.9293
14.4933	-0.2095	1.1037	-0.9293
15.4933	-0.2095	1.1072	-0.9293
16.4933	-0.2095	1.1107	-0.9293
17.4933	-0.2095	1.1142	-0.9293
18.4933	-0.2095	1.1177	-0.9293
19.4933	-0.2095	1.1212	-0.9293
20.4933	-0.2095	1.1247	-0.9293

Table 4

POTENTIAL ENERGY FUNCTION OF H_2

r/a_0	E/V	r/a_0	E/V
0.900	-11.2579	1.0700	-0.8473
0.920	-10.3854	1.0875	-0.8952
0.940	-9.5553	1.1050	-0.9429
0.960	-8.7682	1.1225	-0.9904
0.980	-8.0257	1.1400	-0.9378
1.000	-7.3272	1.1575	-0.8849
1.020	-6.6732	1.1750	-0.8317
1.040	-6.0643	1.1925	-0.7783
1.060	-5.5008	1.2100	-0.7247
1.080	-4.9831	1.2275	-0.6709
1.100	-4.5107	1.2450	-0.6169

Table 14

POTENTIAL ENERGY FUNCTION OF H_2

r , Å	$V(r)$, eV	$V(r)$, eV	$V(r)$, eV
0.000	-0.1504	1.0707	-0.0000
0.050	-0.1795	1.0381	-0.0000
0.100	-0.2077	0.9701	-0.0000
0.150	-0.2340	0.8778	-0.0000
0.200	-0.2585	0.7640	-0.0000
0.250	-0.2812	0.6330	-0.0000
0.300	-0.3020	0.4977	-0.0000
0.350	-0.3207		
0.400	-0.3374		
0.450	-0.3527		
0.500	-0.3667		

100

TABLE 1. Summary of the results of the 1997 survey of 1000 U.S. adults

Year	Value	Year	Value
1970	1.12	1978	1.12
1971	1.12	1979	1.12
1972	1.12	1980	1.12
1973	1.12	1981	1.12
1974	1.12	1982	1.12
1975	1.12	1983	1.12
1976	1.12	1984	1.12
1977	1.12	1985	1.12
1978	1.12	1986	1.12
1979	1.12	1987	1.12
1980	1.12	1988	1.12
1981	1.12	1989	1.12
1982	1.12	1990	1.12
1983	1.12	1991	1.12
1984	1.12	1992	1.12
1985	1.12	1993	1.12
1986	1.12	1994	1.12
1987	1.12	1995	1.12
1988	1.12	1996	1.12
1989	1.12	1997	1.12
1990	1.12	1998	1.12
1991	1.12	1999	1.12
1992	1.12	2000	1.12
1993	1.12	2001	1.12
1994	1.12	2002	1.12
1995	1.12	2003	1.12
1996	1.12	2004	1.12
1997	1.12	2005	1.12
1998	1.12	2006	1.12
1999	1.12	2007	1.12
2000	1.12	2008	1.12
2001	1.12	2009	1.12
2002	1.12	2010	1.12
2003	1.12	2011	1.12
2004	1.12	2012	1.12
2005	1.12	2013	1.12
2006	1.12	2014	1.12
2007	1.12	2015	1.12
2008	1.12	2016	1.12
2009	1.12	2017	1.12
2010	1.12	2018	1.12
2011	1.12	2019	1.12
2012	1.12	2020	1.12
2013	1.12	2021	1.12
2014	1.12	2022	1.12
2015	1.12	2023	1.12
2016	1.12	2024	1.12
2017	1.12	2025	1.12
2018	1.12	2026	1.12
2019	1.12	2027	1.12
2020	1.12	2028	1.12
2021	1.12	2029	1.12
2022	1.12	2030	1.12
2023	1.12	2031	1.12
2024	1.12	2032	1.12
2025	1.12	2033	1.12
2026	1.12	2034	1.12
2027	1.12	2035	1.12
2028	1.12	2036	1.12
2029	1.12	2037	1.12
2030	1.12	2038	1.12
2031	1.12	2039	1.12
2032	1.12	2040	1.12
2033	1.12	2041	1.12
2034	1.12	2042	1.12
2035	1.12	2043	1.12
2036	1.12	2044	1.12
2037	1.12	2045	1.12
2038	1.12	2046	1.12
2039	1.12	2047	1.12
2040	1.12	2048	1.12
2041	1.12	2049	1.12
2042	1.12	2050	1.12
2043	1.12	2051	1.12
2044	1.12	2052	1.12
2045	1.12	2053	1.12
2046	1.12	2054	1.12
2047	1.12	2055	1.12
2048	1.12	2056	1.12
2049	1.12	2057	1.12
2050	1.12	2058	1.12
2051	1.12	2059	1.12
2052	1.12	2060	1.12
2053	1.12	2061	1.12
2054	1.12	2062	1.12
2055	1.12	2063	1.12

TABLE 12

SOMEWHAT PRELIMINARY RESULTS OF Φ_{12}

Φ_{12}	Φ_{12}	Φ_{12}	Φ_{12}
1. 1000	1. 1000	1. 1000	1. 1000
2. 1000	2. 1000	2. 1000	2. 1000
3. 1000	3. 1000	3. 1000	3. 1000
4. 1000	4. 1000	4. 1000	4. 1000
5. 1000	5. 1000	5. 1000	5. 1000
6. 1000	6. 1000	6. 1000	6. 1000
7. 1000	7. 1000	7. 1000	7. 1000
8. 1000	8. 1000	8. 1000	8. 1000
9. 1000	9. 1000	9. 1000	9. 1000
10. 1000	10. 1000	10. 1000	10. 1000
11. 1000	11. 1000	11. 1000	11. 1000
12. 1000	12. 1000	12. 1000	12. 1000
13. 1000	13. 1000	13. 1000	13. 1000
14. 1000	14. 1000	14. 1000	14. 1000
15. 1000	15. 1000	15. 1000	15. 1000
16. 1000	16. 1000	16. 1000	16. 1000
17. 1000	17. 1000	17. 1000	17. 1000
18. 1000	18. 1000	18. 1000	18. 1000
19. 1000	19. 1000	19. 1000	19. 1000
20. 1000	20. 1000	20. 1000	20. 1000
21. 1000	21. 1000	21. 1000	21. 1000
22. 1000	22. 1000	22. 1000	22. 1000
23. 1000	23. 1000	23. 1000	23. 1000
24. 1000	24. 1000	24. 1000	24. 1000
25. 1000	25. 1000	25. 1000	25. 1000
26. 1000	26. 1000	26. 1000	26. 1000
27. 1000	27. 1000	27. 1000	27. 1000
28. 1000	28. 1000	28. 1000	28. 1000
29. 1000	29. 1000	29. 1000	29. 1000
30. 1000	30. 1000	30. 1000	30. 1000
31. 1000	31. 1000	31. 1000	31. 1000
32. 1000	32. 1000	32. 1000	32. 1000
33. 1000	33. 1000	33. 1000	33. 1000
34. 1000	34. 1000	34. 1000	34. 1000
35. 1000	35. 1000	35. 1000	35. 1000
36. 1000	36. 1000	36. 1000	36. 1000
37. 1000	37. 1000	37. 1000	37. 1000
38. 1000	38. 1000	38. 1000	38. 1000
39. 1000	39. 1000	39. 1000	39. 1000
40. 1000	40. 1000	40. 1000	40. 1000
41. 1000	41. 1000	41. 1000	41. 1000
42. 1000	42. 1000	42. 1000	42. 1000
43. 1000	43. 1000	43. 1000	43. 1000
44. 1000	44. 1000	44. 1000	44. 1000
45. 1000	45. 1000	45. 1000	45. 1000
46. 1000	46. 1000	46. 1000	46. 1000
47. 1000	47. 1000	47. 1000	47. 1000
48. 1000	48. 1000	48. 1000	48. 1000
49. 1000	49. 1000	49. 1000	49. 1000
50. 1000	50. 1000	50. 1000	50. 1000

Table 1

4-Hz feedback, polynomial fit (1)

$\frac{1}{\sigma^2} \frac{d^2 \sigma^2}{d\lambda^2}$	$\ln_p \lambda$	$\ln_{10} \sigma$
100	0.02	0
100	1.00	1
100	2.00	2
100	3.00	3
<hr/>	<hr/>	<hr/>
100	1.00	1.00

TABLE 2
 Values of χ^2 for χ^2 test

χ^2	χ^2	χ^2	χ^2
0.00	0.00	0.00	0.00
0.01	0.01	0.01	0.01
0.02	0.02	0.02	0.02
0.03	0.03	0.03	0.03
0.04	0.04	0.04	0.04
0.05	0.05	0.05	0.05
0.06	0.06	0.06	0.06
0.07	0.07	0.07	0.07
0.08	0.08	0.08	0.08
0.09	0.09	0.09	0.09
0.10	0.10	0.10	0.10
0.11	0.11	0.11	0.11
0.12	0.12	0.12	0.12
0.13	0.13	0.13	0.13
0.14	0.14	0.14	0.14
0.15	0.15	0.15	0.15
0.16	0.16	0.16	0.16
0.17	0.17	0.17	0.17
0.18	0.18	0.18	0.18
0.19	0.19	0.19	0.19
0.20	0.20	0.20	0.20
0.21	0.21	0.21	0.21
0.22	0.22	0.22	0.22
0.23	0.23	0.23	0.23
0.24	0.24	0.24	0.24
0.25	0.25	0.25	0.25
0.26	0.26	0.26	0.26
0.27	0.27	0.27	0.27
0.28	0.28	0.28	0.28
0.29	0.29	0.29	0.29
0.30	0.30	0.30	0.30
0.31	0.31	0.31	0.31
0.32	0.32	0.32	0.32
0.33	0.33	0.33	0.33
0.34	0.34	0.34	0.34
0.35	0.35	0.35	0.35
0.36	0.36	0.36	0.36
0.37	0.37	0.37	0.37
0.38	0.38	0.38	0.38
0.39	0.39	0.39	0.39
0.40	0.40	0.40	0.40
0.41	0.41	0.41	0.41
0.42	0.42	0.42	0.42
0.43	0.43	0.43	0.43
0.44	0.44	0.44	0.44
0.45	0.45	0.45	0.45
0.46	0.46	0.46	0.46
0.47	0.47	0.47	0.47
0.48	0.48	0.48	0.48
0.49	0.49	0.49	0.49
0.50	0.50	0.50	0.50
0.51	0.51	0.51	0.51
0.52	0.52	0.52	0.52
0.53	0.53	0.53	0.53
0.54	0.54	0.54	0.54
0.55	0.55	0.55	0.55
0.56	0.56	0.56	0.56
0.57	0.57	0.57	0.57
0.58	0.58	0.58	0.58
0.59	0.59	0.59	0.59
0.60	0.60	0.60	0.60
0.61	0.61	0.61	0.61
0.62	0.62	0.62	0.62
0.63	0.63	0.63	0.63
0.64	0.64	0.64	0.64
0.65	0.65	0.65	0.65
0.66	0.66	0.66	0.66
0.67	0.67	0.67	0.67
0.68	0.68	0.68	0.68
0.69	0.69	0.69	0.69
0.70	0.70	0.70	0.70
0.71	0.71	0.71	0.71
0.72	0.72	0.72	0.72
0.73	0.73	0.73	0.73
0.74	0.74	0.74	0.74
0.75	0.75	0.75	0.75
0.76	0.76	0.76	0.76
0.77	0.77	0.77	0.77
0.78	0.78	0.78	0.78
0.79	0.79	0.79	0.79
0.80	0.80	0.80	0.80
0.81	0.81	0.81	0.81
0.82	0.82	0.82	0.82
0.83	0.83	0.83	0.83
0.84	0.84	0.84	0.84
0.85	0.85	0.85	0.85
0.86	0.86	0.86	0.86
0.87	0.87	0.87	0.87
0.88	0.88	0.88	0.88
0.89	0.89	0.89	0.89
0.90	0.90	0.90	0.90
0.91	0.91	0.91	0.91
0.92	0.92	0.92	0.92
0.93	0.93	0.93	0.93
0.94	0.94	0.94	0.94
0.95	0.95	0.95	0.95
0.96	0.96	0.96	0.96
0.97	0.97	0.97	0.97
0.98	0.98	0.98	0.98
0.99	0.99	0.99	0.99
1.00	1.00	1.00	1.00

TABLE 12

CRITICAL CONSTANTS AND THE AVERAGE FACTOR

Substance	α_f	$T_c, ^\circ K$	P_c, Atm	Sum of Critical Constants
H_2	-0.001	33.2	48.3	10
CH_4	-0.043	190.6	48.7	10
N_2	-0.040	126.2	33.5	10
C_2H_2	-0.106	308.7	49.8	10
$\text{C}(\text{OH})_2$	-0.176	423.7	31.3	10
C_2H_4	-0.071	311.3	76.1	26
H_2O	-0.047	113	21	21
CO_2	-0.149	311	37	37
C_2H_6	-0.101	305.4	37.4	37
CCl_4	-0.176	350.3	61.8	37
SO_2	-0.164	318.6	36.7	36
$\text{H}(\text{OH})_2$	-0.207	423	34	37
HF	-0.208	343.7	37.1	36
$\text{C}_2\text{H}_5\text{OH}$	-0.186	351	36.7	36

TABLE 10

CALCULATED PARAMETERS FOR POLYMERIC SELECTORS

Calculation	α_{ij}^0	$K^0/\% \text{ } ^\circ\text{C}$	K^0/A
$\text{CH}_3 = 1$	1.70	573.0	4.90
$= 2$	1.70	571.0	4.70
$= 3$	1.70	574.0	5.00
$\text{CH}_2\text{CH}_3 = 1$	1.40	570.0	5.41
$= 2$	1.40	570.0	5.00
$= 3$	1.40	570.0	5.00
$\text{CHCH}_3 = 1$	1.40	700.0	+4.0
$= 2$	1.40	570.0	+4.0
$= 3$	1.40	543.0	+4.0
$\text{CH(CH}_3)_2 = 1$	2.00	410.0	+3.0
$= 2$	2.00	410.0	+3.0
$= 3$	2.00	408.0	+4.0
$\text{CH}_2\text{(CH}_2)_2 = 1$	1.00	713.0	7.14
$= 2$	1.00	543.0	7.14
$= 3$	1.00	543.0	7.17
$\text{CH}_2 = 1$		574.0	5.45
$= 2$		470.0	5.47
$= 3$	1.70	470.0	5.51
$\text{CHCH}_2 = 1$	1.70	544.0	5.57
$= 2$	1.00	550.0	5.41
$= 3$		573.0	5.45
$\text{CH(CH}_3)_2 = 1$	1.00	567.0	7.04
$= 2$		543.0	7.07
$= 3$		550.0	7.10

TABLE 17

FORMAL, BRANCHED POLYMER OF OP_2

Designation	$\bar{M}_n \times 10^{-3}$	\bar{M}_w/\bar{M}_n
$\text{OP}_2 = 1$	4.90	1.57
$\text{OP}_2 = 2$	4.91	1.71
$\text{OP}_2 = 3$	5.00	1.84

\bar{M}_n^0	\bar{M}_w^0	\bar{M}_n^0	\bar{M}_w^0
1.4677	46.4643	1.1479	46.4674
1.4611	46.4658	1.1466	46.4666
1.4600	46.4671	1.1458	46.4664
1.4594	46.4684	1.1451	46.4661
1.4591	46.4694	1.1447	46.4660
1.4587	46.4704	1.1441	46.4658
1.4586	46.4694	1.1439	46.4656
1.4587	46.4684	1.1436	46.4655
1.4579	46.4664	1.1434	46.4653
1.4584	46.4666	1.1436	46.4657
1.4589	46.4666	1.1437	46.4657
1.4590	46.4666	1.1437	46.4657

TABLE 25

POTENTIAL ENERGY FUNCTION OF C_2F_4

Calculation	R^0 , Å	R^0/r_h , %
$\text{C}_2\text{F}_4^{\text{I}} = 1$	0.41	240.7
$\text{C}_2\text{F}_4^{\text{I}} = 2$	0.403	239.1
$\text{C}_2\text{F}_4^{\text{I}} = 3$	0.394	236.1

R_1/r^0	$\text{C}_2\text{F}_4^{\text{I}}$	R_2/r^0	$\text{C}_2\text{F}_4^{\text{I}}$
2 8233	no 5244	2 4875	no 2807
2 9142	no 5477	2 4977	no 1174
2 9207	no 5454	2 5002	no 1074
2 9710	no 5434	2 5127	no 1703
2 9797	no 5414	2 5152	no 2507
2 9862	no 5402	2 5177	no 3497
2 9917	no 5379	2 5202	no 4704
2 9953	no 5358	2 5227	no 6070
2 9977	no 5332	2 5252	no 7646
2 9999	no 5302	2 5277	no 9364
2 9997	no 5271	2 5302	no 2024

TABLE 17

POTENTIAL ENERGY FUNCTION OF CCl_4

Rotations		$r^2, \text{\AA}$	$r^2/r_0, \text{\AA}$
$\text{CCl}_4 - 1$		1.44	792.1
$\text{CCl}_4 - 2$		1.442	879.4
$\text{CCl}_4 - 3$		1.44	1112.3
r_1/r^2	r_2/r^2	r_1/r^2	r_2/r^2
1.4554	no. 1545	1.4571	no. 1571
1.4566	no. 1546	1.4583	no. 1573
1.4598	no. 1551	1.4595	no. 1575
1.4635	no. 1556	1.4607	no. 1577
1.4677	no. 1571	1.4611	no. 1580
1.4685	no. 1564	1.4634	no. 1602
1.4699	no. 1558	0.4635	no. 1605
1.4714	no. 1557	0.4636	no. 1612
1.4740	no. 1554	0.4637	no. 1617
1.4766	no. 1551	0.4638	no. 1622
1.4792	no. 1550		

TABLE III

RADIAL INHERENT PARTS OF $\langle r^2 \rangle_{\text{inh}}^2$

Calculation	$\bar{r}^2 / \text{\AA}$	$\bar{r}^2 / \text{\AA}$	\bar{r}_0^2
$\langle r^2 \rangle_{\text{inh}}^2 = 1$	6.39		499.1
$\langle r^2 \rangle_{\text{inh}}^2 = 2$	6.39		499.4
$\langle r^2 \rangle_{\text{inh}}^2 = 3$	6.40		499.4
r_0^2	r_0^2	r_0^2	r_0^2
1.0076	+0.0154	1.4498	+0.1248
1.0104	+0.0096	1.4507	+0.1295
1.0140	+0.0054	1.4515	+0.1346
1.0181	+0.0016	1.4524	+0.1397
1.0227	+0.0000	1.4531	+0.1447
1.0277	-0.0016	1.4537	+0.1496
1.0330	-0.0037	1.4543	+0.1545
1.0385	-0.0064	1.4548	+0.1594
1.0442	-0.0098	1.4554	+0.1643
1.0500	-0.0137	1.4559	+0.1692
1.0559	-0.0180	1.4565	+0.1741
1.0619	-0.0229	1.4570	+0.1790
1.0680	-0.0285	1.4575	+0.1839
1.0741	-0.0350	1.4580	+0.1888
1.0803	-0.0423	1.4585	+0.1937
1.0865	-0.0500	1.4590	+0.1986
1.0927	-0.0587	1.4595	+0.2035
1.0990	-0.0687	1.4600	+0.2084

TABLE 11

POLYNOMIAL APPROXIMATION OF $\zeta_2(\alpha_2)/\zeta_2$

Calculation	τ^2	τ^2/α_2	τ^2/α_2
$\zeta_2(\alpha_2)/\zeta_2 = 1$	1.14	71.2	1
$\zeta_2(\alpha_2)/\zeta_2 = 0$	1.34	103.4	0
$\zeta_2(\alpha_2)/\zeta_2 = 2$	1.11	69.6	2
α_2/τ^2	α_2/τ^2	α_2/τ^2	α_2/τ^2
0.0000	-0.0019	1.0000	-0.0019
1.7900	-0.0019	1.0000	-0.0019
1.8700	-0.0019	1.0000	-0.0019
1.8900	-0.0019	1.0000	-0.0019
1.7900	-0.0019	1.0000	-0.0019
1.6900	-0.0019	1.0000	-0.0019
1.5900	-0.0019	1.0000	-0.0019
1.4900	-0.0019	1.0000	-0.0019
1.3900	-0.0019	1.0000	-0.0019
1.2900	-0.0019	1.0000	-0.0019
1.1900	-0.0019	1.0000	-0.0019
1.0900	-0.0019	1.0000	-0.0019
0.9900	-0.0019	1.0000	-0.0019

TABLE II

POTENTIAL ENERGY FUNCTION OF BF_3 Calculation: $3F_{12} = 3$ $\text{R}^0 = 0.21 \text{ \AA.}$ $\text{R}^0/\text{R} = 423.0 \text{ \%}$

R/R^0	V/R^0	R/R^0	V/R^0
1.0000	-0.0000	1.0000	-0.0000
1.0010	-0.0010	1.0020	-0.0020
1.0020	-0.0020	1.0040	-0.0040
1.0030	-0.0030	1.0060	-0.0060
1.0040	-0.0040	1.0080	-0.0080
1.0050	-0.0050	1.0100	-0.0100
1.0060	-0.0060	1.0120	-0.0120
1.0070	-0.0070	1.0140	-0.0140
1.0080	-0.0080	1.0160	-0.0160
1.0090	-0.0090	1.0180	-0.0180
1.0100	-0.0100	1.0200	-0.0200
1.0110	-0.0110	1.0220	-0.0220
1.0120	-0.0120	1.0240	-0.0240
1.0130	-0.0130	1.0260	-0.0260
1.0140	-0.0140	1.0280	-0.0280
1.0150	-0.0150	1.0300	-0.0300

TABLE XX

STRUCTURAL WEIGHT FUNCTIONS OF W_4

$W_4 = 1$ $\sigma^2 = 0.27 \text{ A}$ $\sigma^2/\tau_0 = 264 \text{ g} \cdot \text{cm}^2$		$W_4 = 2$ $\sigma^2 = 0.41 \text{ A}$ $\sigma^2/\tau_0 = 378 \text{ g} \cdot \text{cm}^2$	
λ/τ_0	ψ/τ_0^2	λ/τ_0	ψ/τ_0^2
0.000	+0.0000	0.0000	+0.0000
0.010	+0.0009	0.0010	+0.0009
0.020	+0.0036	0.0020	+0.0037
0.030	+0.0080	0.0030	+0.0080
0.040	+0.0140	0.0040	+0.0140
0.050	+0.0216	0.0050	+0.0216
0.060	+0.0308	0.0060	+0.0308
0.070	+0.0416	0.0070	+0.0416
0.080	+0.0540	0.0080	+0.0540
0.090	+0.0680	0.0090	+0.0680
0.100	+0.0836	0.0100	+0.0836
0.110	+0.1008	0.0110	+0.1008
0.120	+0.1196	0.0120	+0.1196
0.130	+0.1400	0.0130	+0.1400
0.140	+0.1620	0.0140	+0.1620
0.150	+0.1856	0.0150	+0.1856
0.160	+0.2108	0.0160	+0.2108
0.170	+0.2376	0.0170	+0.2376
0.180	+0.2660	0.0180	+0.2660
0.190	+0.2960	0.0190	+0.2960
0.200	+0.3276	0.0200	+0.3276
0.210	+0.3608	0.0210	+0.3608
0.220	+0.3956	0.0220	+0.3956
0.230	+0.4320	0.0230	+0.4320
0.240	+0.4696	0.0240	+0.4696
0.250	+0.5084	0.0250	+0.5084
0.260	+0.5484	0.0260	+0.5484
0.270	+0.5896	0.0270	+0.5896
0.280	+0.6320	0.0280	+0.6320
0.290	+0.6756	0.0290	+0.6756
0.300	+0.7204	0.0300	+0.7204
0.310	+0.7664	0.0310	+0.7664
0.320	+0.8136	0.0320	+0.8136
0.330	+0.8620	0.0330	+0.8620
0.340	+0.9116	0.0340	+0.9116
0.350	+0.9624	0.0350	+0.9624
0.360	+1.0144	0.0360	+1.0144
0.370	+1.0676	0.0370	+1.0676
0.380	+1.1220	0.0380	+1.1220
0.390	+1.1776	0.0390	+1.1776
0.400	+1.2344	0.0400	+1.2344
0.410	+1.2924	0.0410	+1.2924
0.420	+1.3516	0.0420	+1.3516
0.430	+1.4120	0.0430	+1.4120
0.440	+1.4736	0.0440	+1.4736
0.450	+1.5364	0.0450	+1.5364
0.460	+1.6004	0.0460	+1.6004
0.470	+1.6656	0.0470	+1.6656
0.480	+1.7320	0.0480	+1.7320
0.490	+1.7996	0.0490	+1.7996
0.500	+1.8684	0.0500	+1.8684
0.510	+1.9384	0.0510	+1.9384
0.520	+2.0096	0.0520	+2.0096
0.530	+2.0820	0.0530	+2.0820
0.540	+2.1556	0.0540	+2.1556
0.550	+2.2304	0.0550	+2.2304
0.560	+2.3064	0.0560	+2.3064
0.570	+2.3836	0.0570	+2.3836
0.580	+2.4620	0.0580	+2.4620
0.590	+2.5416	0.0590	+2.5416
0.600	+2.6224	0.0600	+2.6224
0.610	+2.7044	0.0610	+2.7044
0.620	+2.7876	0.0620	+2.7876
0.630	+2.8720	0.0630	+2.8720
0.640	+2.9576	0.0640	+2.9576
0.650	+3.0444	0.0650	+3.0444
0.660	+3.1324	0.0660	+3.1324
0.670	+3.2216	0.0670	+3.2216
0.680	+3.3120	0.0680	+3.3120
0.690	+3.4036	0.0690	+3.4036
0.700	+3.4964	0.0700	+3.4964
0.710	+3.5904	0.0710	+3.5904
0.720	+3.6856	0.0720	+3.6856
0.730	+3.7820	0.0730	+3.7820
0.740	+3.8796	0.0740	+3.8796
0.750	+3.9784	0.0750	+3.9784
0.760	+4.0784	0.0760	+4.0784
0.770	+4.1796	0.0770	+4.1796
0.780	+4.2820	0.0780	+4.2820
0.790	+4.3856	0.0790	+4.3856
0.800	+4.4904	0.0800	+4.4904
0.810	+4.5964	0.0810	+4.5964
0.820	+4.7036	0.0820	+4.7036
0.830	+4.8120	0.0830	+4.8120
0.840	+4.9216	0.0840	+4.9216
0.850	+5.0324	0.0850	+5.0324
0.860	+5.1444	0.0860	+5.1444
0.870	+5.2576	0.0870	+5.2576
0.880	+5.3720	0.0880	+5.3720
0.890	+5.4876	0.0890	+5.4876
0.900	+5.6044	0.0900	+5.6044
0.910	+5.7224	0.0910	+5.7224
0.920	+5.8416	0.0920	+5.8416
0.930	+5.9620	0.0930	+5.9620
0.940	+6.0836	0.0940	+6.0836
0.950	+6.2064	0.0950	+6.2064
0.960	+6.3304	0.0960	+6.3304
0.970	+6.4556	0.0970	+6.4556
0.980	+6.5820	0.0980	+6.5820
0.990	+6.7096	0.0990	+6.7096
1.000	+6.8384	0.1000	+6.8384

TABLE 24

ADDITIONAL BOND LENGTHS OF $\text{H}_2\text{C}_2\text{H}_2\text{H} - 1$

$$R^0 = 1.04 \text{ \AA}$$

$$R^0/\lambda = 200.2 \text{ }^\circ$$

λ/R^0	R/R^0	λ/R^0	R/R^0
1.0597	+0.0702	1.0930	+0.0933
1.0593	+0.0700	1.0926	+0.0931
1.0589	+0.0698	1.0922	+0.0929
1.0585	+0.0696	1.0918	+0.0927
1.0581	+0.0694	1.0914	+0.0925
1.0577	+0.0692	1.0910	+0.0923
1.0573	+0.0690	1.0906	+0.0921
1.0569	+0.0688	1.0902	+0.0919
1.0565	+0.0686	1.0898	+0.0917
1.0561	+0.0684	1.0894	+0.0915
1.0557	+0.0682	1.0890	+0.0913
1.0553	+0.0680	1.0886	+0.0911
1.0549	+0.0678	1.0882	+0.0909
1.0545	+0.0676	1.0878	+0.0907
1.0541	+0.0674	1.0874	+0.0905
1.0537	+0.0672	1.0870	+0.0903
1.0533	+0.0670	1.0866	+0.0901
1.0529	+0.0668	1.0862	+0.0899
1.0525	+0.0666	1.0858	+0.0897
1.0521	+0.0664	1.0854	+0.0895
1.0517	+0.0662	1.0850	+0.0893
1.0513	+0.0660	1.0846	+0.0891
1.0509	+0.0658	1.0842	+0.0889
1.0505	+0.0656	1.0838	+0.0887
1.0501	+0.0654	1.0834	+0.0885
1.0497	+0.0652	1.0830	+0.0883
1.0493	+0.0650	1.0826	+0.0881
1.0489	+0.0648	1.0822	+0.0879
1.0485	+0.0646	1.0818	+0.0877
1.0481	+0.0644	1.0814	+0.0875
1.0477	+0.0642	1.0810	+0.0873
1.0473	+0.0640	1.0806	+0.0871
1.0469	+0.0638	1.0802	+0.0869
1.0465	+0.0636	1.0798	+0.0867
1.0461	+0.0634	1.0794	+0.0865
1.0457	+0.0632	1.0790	+0.0863
1.0453	+0.0630	1.0786	+0.0861
1.0449	+0.0628	1.0782	+0.0859
1.0445	+0.0626	1.0778	+0.0857
1.0441	+0.0624	1.0774	+0.0855
1.0437	+0.0622	1.0770	+0.0853
1.0433	+0.0620	1.0766	+0.0851
1.0429	+0.0618	1.0762	+0.0849
1.0425	+0.0616	1.0758	+0.0847
1.0421	+0.0614	1.0754	+0.0845
1.0417	+0.0612	1.0750	+0.0843
1.0413	+0.0610	1.0746	+0.0841
1.0409	+0.0608	1.0742	+0.0839
1.0405	+0.0606	1.0738	+0.0837
1.0401	+0.0604	1.0734	+0.0835
1.0397	+0.0602	1.0730	+0.0833
1.0393	+0.0600	1.0726	+0.0831
1.0389	+0.0598	1.0722	+0.0829
1.0385	+0.0596	1.0718	+0.0827
1.0381	+0.0594	1.0714	+0.0825
1.0377	+0.0592	1.0710	+0.0823
1.0373	+0.0590	1.0706	+0.0821
1.0369	+0.0588	1.0702	+0.0819
1.0365	+0.0586	1.0698	+0.0817
1.0361	+0.0584	1.0694	+0.0815
1.0357	+0.0582	1.0690	+0.0813
1.0353	+0.0580	1.0686	+0.0811
1.0349	+0.0578	1.0682	+0.0809
1.0345	+0.0576	1.0678	+0.0807
1.0341	+0.0574	1.0674	+0.0805
1.0337	+0.0572	1.0670	+0.0803
1.0333	+0.0570	1.0666	+0.0801
1.0329	+0.0568	1.0662	+0.0799
1.0325	+0.0566	1.0658	+0.0797
1.0321	+0.0564	1.0654	+0.0795
1.0317	+0.0562	1.0650	+0.0793
1.0313	+0.0560	1.0646	+0.0791
1.0309	+0.0558	1.0642	+0.0789
1.0305	+0.0556	1.0638	+0.0787
1.0301	+0.0554	1.0634	+0.0785
1.0297	+0.0552	1.0630	+0.0783
1.0293	+0.0550	1.0626	+0.0781
1.0289	+0.0548	1.0622	+0.0779
1.0285	+0.0546	1.0618	+0.0777
1.0281	+0.0544	1.0614	+0.0775
1.0277	+0.0542	1.0610	+0.0773
1.0273	+0.0540	1.0606	+0.0771
1.0269	+0.0538	1.0602	+0.0769
1.0265	+0.0536	1.0598	+0.0767
1.0261	+0.0534	1.0594	+0.0765
1.0257	+0.0532	1.0590	+0.0763
1.0253	+0.0530	1.0586	+0.0761
1.0249	+0.0528	1.0582	+0.0759
1.0245	+0.0526	1.0578	+0.0757
1.0241	+0.0524	1.0574	+0.0755
1.0237	+0.0522	1.0570	+0.0753
1.0233	+0.0520	1.0566	+0.0751
1.0229	+0.0518	1.0562	+0.0749
1.0225	+0.0516	1.0558	+0.0747
1.0221	+0.0514	1.0554	+0.0745
1.0217	+0.0512	1.0550	+0.0743
1.0213	+0.0510	1.0546	+0.0741
1.0209	+0.0508	1.0542	+0.0739
1.0205	+0.0506	1.0538	+0.0737
1.0201	+0.0504	1.0534	+0.0735
1.0197	+0.0502	1.0530	+0.0733
1.0193	+0.0500	1.0526	+0.0731
1.0189	+0.0498	1.0522	+0.0729
1.0185	+0.0496	1.0518	+0.0727
1.0181	+0.0494	1.0514	+0.0725
1.0177	+0.0492	1.0510	+0.0723
1.0173	+0.0490	1.0506	+0.0721
1.0169	+0.0488	1.0502	+0.0719
1.0165	+0.0486	1.0498	+0.0717
1.0161	+0.0484	1.0494	+0.0715
1.0157	+0.0482	1.0490	+0.0713
1.0153	+0.0480	1.0486	+0.0711
1.0149	+0.0478	1.0482	+0.0709
1.0145	+0.0476	1.0478	+0.0707
1.0141	+0.0474	1.0474	+0.0705
1.0137	+0.0472	1.0470	+0.0703
1.0133	+0.0470	1.0466	+0.0701
1.0129	+0.0468	1.0462	+0.0699
1.0125	+0.0466	1.0458	+0.0697
1.0121	+0.0464	1.0454	+0.0695
1.0117	+0.0462	1.0450	+0.0693
1.0113	+0.0460	1.0446	+0.0691
1.0109	+0.0458	1.0442	+0.0689
1.0105	+0.0456	1.0438	+0.0687
1.0101	+0.0454	1.0434	+0.0685
1.0097	+0.0452	1.0430	+0.0683
1.0093	+0.0450	1.0426	+0.0681
1.0089	+0.0448	1.0422	+0.0679
1.0085	+0.0446	1.0418	+0.0677
1.0081	+0.0444	1.0414	+0.0675
1.0077	+0.0442	1.0410	+0.0673
1.0073	+0.0440	1.0406	+0.0671
1.0069	+0.0438	1.0402	+0.0669
1.0065	+0.0436	1.0398	+0.0667
1.0061	+0.0434	1.0394	+0.0665
1.0057	+0.0432	1.0390	+0.0663
1.0053	+0.0430	1.0386	+0.0661
1.0049	+0.0428	1.0382	+0.0659
1.0045	+0.0426	1.0378	+0.0657
1.0041	+0.0424	1.0374	+0.0655
1.0037	+0.0422	1.0370	+0.0653
1.0033	+0.0420	1.0366	+0.0651
1.0029	+0.0418	1.0362	+0.0649
1.0025	+0.0416	1.0358	+0.0647
1.0021	+0.0414	1.0354	+0.0645
1.0017	+0.0412	1.0350	+0.0643
1.0013	+0.0410	1.0346	+0.0641
1.0009	+0.0408	1.0342	+0.0639
1.0005	+0.0406	1.0338	+0.0637
1.0001	+0.0404	1.0334	+0.0635

TABLE 15

THERMAL FREQUENCY COEFFICIENT AND CORRELATION OF σ_{H}

Frequency	Observed $\Delta \sigma_{\text{H}} / \Delta T$, cm ⁻¹ /°C	$\sigma_{\text{H}} / \bar{\rho}_{\text{H}}$, cm ⁻¹	$1.27 \times 10^4 / T$, cm ⁻¹ /°C	$\bar{\rho}_{\text{H}}$ (m ³) cm ⁻³	Frequency °C
1	16.71	0.17	16.74	1.934	151.4
2	13.82	0.14	13.91	1.780	159.4
3	12.00	0.10	12.76	1.670	161.7
4	14.33	0.17	14.00	0.977	160.4
5	17.43	0.10	17.41	1.317	155.1
6	16.67	0.17	15.56	1.410	162.4
7	22.51	0.16	14.07	0.770	167.4
8	22.11	0.10	20.77	0.707	99.2
9	13.36	0.14	15.54	1.037	156.1
10	16.45	0.17	15.44	1.470	158.9
11	13.13	0.10	16.17	1.514	164.1
12	16.49	0.10	15.11	1.299	153.4
13	11.37	0.10	11.65	1.370	177.7
14	14.73	0.17	14.07	0.977	167.4
15	22.34	0.10	17.44	0.700	97.1

TABLE 26

THERMAL EXPANSION COEFFICIENT OF Cu_2S

Temperature, °C.	Observed $\Delta L/L\Delta T$, °C. ⁻¹	$\alpha_{\text{Cu}_2\text{S}}^{\text{obs}}/\alpha_{\text{Cu}_2\text{S}}^{\text{ref}}$	LPTC (PTC) ₂ , °C. ⁻¹	Temperature, °C.
0	14.64	0.94	14.79	101.4
5	14.47	0.93	14.71	102.1
10	14.34	0.94	14.67	103.4
15	14.40	0.93	14.59	104.8
20	14.56	0.94	14.54	106.0
25	14.58	0.94	14.54	107.0
30	14.44	0.93	14.56	107.7
35	14.39	0.93	14.47	108.9
40	14.39	0.94	14.44	110.0

TABLE 27

SOLUBLE POLYMER CONCENTRATIONS AND KINETICALLY DERIVED RESULTS AT 25°C

Monomer	$A_p \left(\frac{\text{min}^2}{\text{cm}^2} \right)$	$A_p \frac{\pi \rho^2}{\omega \Gamma_p \eta}$	$\tau^2 \frac{\omega}{\pi \Gamma_p}$	From Kilmer Equation τ^2	(calculated) τ^2_{calc}	Extrapolated to Pure P τ^2
A	3.333×10^{-3}	3.333×10^{-3}	31.33	3.33	3.33	—
CH_3	1.667×10^{-3}	1.667×10^{-3}	26.25	3.45	3.33	3.33
CH_2	1.667×10^{-3}	1.667×10^{-3}	26.25	3.45	3.33	2.50
CH_3	1.667×10^{-3}	1.667×10^{-3}	26.25	3.34	3.33	3.33
CH_2	1.333×10^{-3}	1.333×10^{-3}	20.27	4.23	4.23	—
CH_3	1.333×10^{-3}	1.333×10^{-3}	40.53	4.36	4.33	3.33
CH_2	1.333×10^{-3}	1.333×10^{-3}	20.27	4.24	3.33	4.33
CH_3	1.333×10^{-3}	1.333×10^{-3}	73.37	5.33	5.33	5.44
CH_2	1.429×10^{-3}	1.429×10^{-3}	33.33	3.33	3.33	3.33

TABLE 26

n-Propyl Chloride and CF_3Cl

CF_3Cl		CF_3Cl	
Temperature, °C	n	Temperature, °C	n
120.5	1.424	120.1	0.773
120.7	0.784	120.7	0.769
121.0	1.030	120.8	0.771
120.4	1.020	120.3	0.775
120.0	0.886	120.0	0.766
120.6	0.760	120.0	0.763
120.4	0.780	77.7	0.608
77.5	0.680	76.7	0.677
120.0	1.003	120.0	0.770
120.0	1.000	76.0	0.603
120.0	0.763		
120.0	0.680		
121.7	0.760		
120.0	0.660		
77.0	0.664		

TABLE 24

COMPOSITIONAL EFFECTS AND SOLAR VALUES OF LIQUID

$T, ^\circ\text{C}$	R_2	$\frac{\Delta H_f}{\text{cal/g}}$	$T, ^\circ\text{C}$	R_2	$\frac{\Delta H_f}{\text{cal/g}}$
100	-0.002	45.50	90	-0.026	45.75
110	-0.011	45.48	100	-0.059	45.79
120	-0.020	45.70	110	-0.091	45.71
130	-0.027	45.91	120	-0.125	45.66
140	-0.077	45.60	130	-0.153	45.54
150	-0.055	45.91	140	-0.185	45.56
160-8	-0.045	44.43	150	-0.221	45.50
160	-0.067	44.23	160	-0.250	45.49
	$R_2^{\text{C}_2\text{H}_5}$		170	-0.271	45.47
170-9	-0.062	44.4	180	-0.323	44.83
170-7	-0.050	44.7	190	-0.331	44.83
	$\text{C}_2\text{H}_5\text{C}_2\text{H}_5$		200	-0.377	45.33
200-44	-0.004	171.6	210	-0.391	45.37
200-13	-0.006	223.11	220	-0.403	44.93
			230	-0.417	44.90
			240	-0.423	44.83
			250	-0.430	44.80
			260	-0.447	44.80
			270	-0.450	44.84
			280	-0.450	44.84
			290	-0.450	44.84

TABLE 60
 TRANSITION STATE IN CYCLES 43 AND 44

Experimental 4-32 Potential Parameters			
Substance	E^0/V_s , %	E^0 , V	Source
P	120	3.44	5
H_2	80.1	4.32	5
H_2	114	3.95	5
OH_2	140	4.32	5
C_2H_2	104	3.645	Waka work
CH_4	146.8	3.94	H_2 , 42
C_2H_2	148	4.34	23
CO_2	107	4.40	5
C_2H_2	106	3.95	23
Calculated Parameters			
H_2	125.4	3.41	
H_2	182.4	3.70	
C_2H_2	270	3.080	
CH_4	270.5	4.10	
C_2H_2	328.5	3.810	
CO_2	470.4	4.440	
C_2H_2	498.5	4.38	



1. The first part of the document is a list of names and titles, including "The Hon. Mr. Justice" and "The Hon. Mr. Justice".

2. The second part of the document is a list of names and titles, including "The Hon. Mr. Justice" and "The Hon. Mr. Justice".



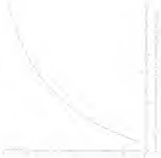


TABLE 41

CALCULATED VALUES α'_0 AND α''/α'_0

α'_0	α''/α'_0	α''/α'_0
1.040	7.740	0.40
0.950	5.400	0.30
0.850	3.747	0.18
0.750	2.697	0.10
0.650	2.063	0.06
0.550	1.611	0.03
0.450	1.231	0.02
1.000	1.000	0.00
1.050	1.050	0.00
1.100	1.100	0.00
1.150	1.150	0.00
1.200	1.200	0.00
1.250	1.250	0.00
1.300	1.300	0.00
1.350	1.350	0.00
1.400	1.400	0.00

TABLE 33

SPHERICAL WAVE POTENTIAL

$$k_0^2 = 1.75$$

$$r^2/k_0 = 1.50$$

z/k_0	u_1/r^2	u_2/r^2	u_3/r^2
1.0000	-0.0000	1.4137	-0.0000
1.0001	-0.0000	1.3999	-0.0000
1.0004	-0.0001	1.3841	-0.0000
1.0010	-0.0001	1.3553	-0.0000
1.0020	-0.0002	1.3199	-0.0000
1.0040	-0.0004	1.2591	-0.0000
1.0080	-0.0008	1.1557	-0.0000
1.0160	-0.0016	1.0000	-0.0000
1.0320	-0.0032	0.7913	-0.0000
1.0640	-0.0064	0.5834	-0.0000

1000

1998, 1999, 2000, 2001, 2002, 2003, 2004, 2005, 2006, 2007, 2008, 2009, 2010, 2011, 2012, 2013, 2014, 2015, 2016, 2017, 2018, 2019, 2020, 2021, 2022, 2023, 2024, 2025, 2026, 2027, 2028, 2029, 2030, 2031, 2032, 2033, 2034, 2035, 2036, 2037, 2038, 2039, 2040, 2041, 2042, 2043, 2044, 2045, 2046, 2047, 2048, 2049, 2050, 2051, 2052, 2053, 2054, 2055, 2056, 2057, 2058, 2059, 2060, 2061, 2062, 2063, 2064, 2065, 2066, 2067, 2068, 2069, 2070, 2071, 2072, 2073, 2074, 2075, 2076, 2077, 2078, 2079, 2080, 2081, 2082, 2083, 2084, 2085, 2086, 2087, 2088, 2089, 2090, 2091, 2092, 2093, 2094, 2095, 2096, 2097, 2098, 2099, 2100, 2101, 2102, 2103, 2104, 2105, 2106, 2107, 2108, 2109, 2110, 2111, 2112, 2113, 2114, 2115, 2116, 2117, 2118, 2119, 2120, 2121, 2122, 2123, 2124, 2125, 2126, 2127, 2128, 2129, 2130, 2131, 2132, 2133, 2134, 2135, 2136, 2137, 2138, 2139, 2140, 2141, 2142, 2143, 2144, 2145, 2146, 2147, 2148, 2149, 2150, 2151, 2152, 2153, 2154, 2155, 2156, 2157, 2158, 2159, 2160, 2161, 2162, 2163, 2164, 2165, 2166, 2167, 2168, 2169, 2170, 2171, 2172, 2173, 2174, 2175, 2176, 2177, 2178, 2179, 2180, 2181, 2182, 2183, 2184, 2185, 2186, 2187, 2188, 2189, 2190, 2191, 2192, 2193, 2194, 2195, 2196, 2197, 2198, 2199, 2200, 2201, 2202, 2203, 2204, 2205, 2206, 2207, 2208, 2209, 2210, 2211, 2212, 2213, 2214, 2215, 2216, 2217, 2218, 2219, 2220, 2221, 2222, 2223, 2224, 2225, 2226, 2227, 2228, 2229, 2230, 2231, 2232, 2233, 2234, 2235, 2236, 2237, 2238, 2239, 2240, 2241, 2242, 2243, 2244, 2245, 2246, 2247, 2248, 2249, 2250, 2251, 2252, 2253, 2254, 2255, 2256, 2257, 2258, 2259, 2260, 2261, 2262, 2263, 2264, 2265, 2266, 2267, 2268, 2269, 2270, 2271, 2272, 2273, 2274, 2275, 2276, 2277, 2278, 2279, 2280, 2281, 2282, 2283, 2284, 2285, 2286, 2287, 2288, 2289, 2290, 2291, 2292, 2293, 2294, 2295, 2296, 2297, 2298, 2299, 2300, 2301, 2302, 2303, 2304, 2305, 2306, 2307, 2308, 2309, 2310, 2311, 2312, 2313, 2314, 2315, 2316, 2317, 2318, 2319, 2320, 2321, 2322, 2323, 2324, 2325, 2326, 2327, 2328, 2329, 2330, 2331, 2332, 2333, 2334, 2335, 2336, 2337, 2338, 2339, 2340, 2341, 2342, 2343, 2344, 2345, 2346, 2347, 2348, 2349, 2350, 2351, 2352, 2353, 2354, 2355, 2356, 2357, 2358, 2359, 2360, 2361, 2362, 2363, 2364, 2365, 2366, 2367, 2368, 2369, 2370, 2371, 2372, 2373, 2374, 2375, 2376, 2377, 2378, 2379, 2380, 2381, 2382, 2383, 2384, 2385, 2386, 2387, 2388, 2389, 2390, 2391, 2392, 2393, 2394, 2395, 2396, 2397, 2398, 2399, 2400, 2401, 2402, 2403, 2404, 2405, 2406, 2407, 2408, 2409, 2410, 2411, 2412, 2413, 2414, 2415, 2416, 2417, 2418, 2419, 2420, 2421, 2422, 2423, 2424, 2425, 2426, 2427, 2428, 2429, 2430, 2431, 2432, 2433, 2434, 2435, 2436, 2437, 2438, 2439, 2440, 2441, 2442, 2443, 2444, 2445, 2446, 2447, 2448, 2449, 2450, 2451, 2452, 2453, 2454, 2455, 2456, 2457, 2458, 2459, 2460, 2461, 2462, 2463, 2464, 2465, 2466, 2467, 2468, 2469, 2470, 2471, 2472, 2473, 2474, 2475, 2476, 2477, 2478, 2479, 2480, 2481, 2482, 2483, 2484, 2485, 2486, 2487, 2488, 2489, 2490, 2491, 2492, 2493, 2494, 2495, 2496, 2497, 2498, 2499, 2500, 2501, 2502, 2503, 2504, 2505, 2506, 2507, 2508, 2509, 2510, 2511, 2512, 2513, 2514, 2515, 2516, 2517, 2518, 2519, 2520, 2521, 2522, 2523, 2524, 2525, 2526, 2527, 2528, 2529, 2530, 2531, 2532, 2533, 2534, 2535, 2536, 2537, 2538, 2539, 2540, 2541, 2542, 2543, 2544, 2545, 2546, 2547, 2548, 2549, 2550, 2551, 2552, 2553, 2554, 2555, 2556, 2557, 2558, 2559, 2560, 2561, 2562, 2563, 2564, 2565, 2566, 2567, 2568, 2569, 2570, 2571, 2572, 2573, 2574, 2575, 2576, 2577, 2578, 2579, 2580, 2581, 2582, 2583, 2584, 2585, 2586, 2587, 2588, 2589, 2590, 2591, 2592, 2593, 2594, 2595, 2596, 2597, 2598, 2599, 2600, 2601, 2602, 2603, 2604, 2605, 2606, 2607, 2608, 2609, 2610, 2611, 2612, 2613, 2614, 2615, 2616, 2617, 2618, 2619, 2620, 2621, 2622, 2623, 2624, 2625, 2626, 2627, 2628, 2629, 2630, 2631, 2632, 2633, 2634, 2635, 2636, 2637, 2638, 2639, 2640, 2641, 2642, 2643, 2644, 2645, 2646, 2647, 2648, 2649, 2650, 2651, 2652, 2653, 2654, 2655, 2656, 2657, 2658, 2659, 2660, 2661, 2662, 2663, 2664, 2665, 2666, 2667, 2668, 2669, 2670, 2671, 2672, 2673, 2674, 2675, 2676, 2677, 2678, 2679, 26

Year	WT ^a	WT ^b	WT ^c
1990	-0.163	1.000	-0.163
1991	-0.097	1.000	-0.097
1992	-0.097	1.000	-0.097
1993	-0.097	1.000	-0.097
1994	-0.097	1.000	-0.097
1995	-0.097	1.000	-0.097
1996	-0.097	1.000	-0.097
1997	-0.097	1.000	-0.097
1998	-0.097	1.000	-0.097
1999	-0.097	1.000	-0.097
2000	-0.097	1.000	-0.097
2001	-0.097	1.000	-0.097
2002	-0.097	1.000	-0.097
2003	-0.097	1.000	-0.097
2004	-0.097	1.000	-0.097
2005	-0.097	1.000	-0.097
2006	-0.097	1.000	-0.097
2007	-0.097	1.000	-0.097
2008	-0.097	1.000	-0.097
2009	-0.097	1.000	-0.097
2010	-0.097	1.000	-0.097
2011	-0.097	1.000	-0.097
2012	-0.097	1.000	-0.097
2013	-0.097	1.000	-0.097
2014	-0.097	1.000	-0.097
2015	-0.097	1.000	-0.097
2016	-0.097	1.000	-0.097
2017	-0.097	1.000	-0.097
2018	-0.097	1.000	-0.097
2019	-0.097	1.000	-0.097
2020	-0.097	1.000	-0.097
2021	-0.097	1.000	-0.097
2022	-0.097	1.000	-0.097
2023	-0.097	1.000	-0.097
2024	-0.097	1.000	-0.097
2025	-0.097	1.000	-0.097
2026	-0.097	1.000	-0.097
2027	-0.097	1.000	-0.097
2028	-0.097	1.000	-0.097
2029	-0.097	1.000	-0.097
2030	-0.097	1.000	-0.097
2031	-0.097	1.000	-0.097
2032	-0.097	1.000	-0.097
2033	-0.097	1.000	-0.097
2034	-0.097	1.000	-0.097
2035	-0.097	1.000	-0.097
2036	-0.097	1.000	-0.097
2037	-0.097	1.000	-0.097
2038	-0.097	1.000	-0.097
2039	-0.097	1.000	-0.097
2040	-0.097	1.000	-0.097
2041	-0.097	1.000	-0.097
2042	-0.097	1.000	-0.097
2043	-0.097	1.000	-0.097
2044	-0.097	1.000	-0.097
2045	-0.097	1.000	-0.097
2046	-0.097	1.000	-0.097
2047	-0.097	1.000	-0.097
2048	-0.097	1.000	-0.097
2049	-0.097	1.000	-0.097
2050	-0.097	1.000	-0.097
2051	-0.097	1.000	-0.097
2052	-0.097	1.000	-0.097
2053	-0.097	1.000	-0.097
2054	-0.097	1.000	-0.097
2055	-0.097	1.000	-0.097
2056	-0.097	1.000	-0.097
2057	-0.097	1.000	-0.097
2058	-0.097	1.000	-0.097
2059	-0.097	1.000	-0.097
2060	-0.097	1.000	-0.097
2061	-0.097	1.000	-0.097
2062	-0.097	1.000	-0.097
2063	-0.097	1.000	-0.097
2064	-0.097	1.000	-0.097
2065	-0.097	1.000	-0.097
2066	-0.097	1.000	-0.097
2067	-0.097	1.000	-0.097
2068	-0.097	1.000	-0.097
2069	-0.097	1.000	-0.097
2070	-0.097	1.000	-0.097
2071	-0.097	1.000	-0.097
2072	-0.097	1.000	-0.097
2073	-0.097	1.000	-0.097
2074	-0.097	1.000	-0.097
2075	-0.097	1.000	-0.097
2076	-0.097	1.000	-0.097
2077	-0.097	1.000	-0.097
2078	-0.097	1.000	-0.097
2079	-0.097	1.000	-0.097
2080	-0.097	1.000	-0.097
2081	-0.097	1.000	-0.097
2082	-0.097	1.000	-0.097
2083	-0.097	1.000	-0.097
2084	-0.097	1.000	-0.097
2085	-0.097	1.000	-0.097
2086	-0.097	1.000	-0.097
2087	-0.097	1.000	-0.097
2088	-0.097	1.000	-0.097
2089	-0.097	1.000	-0.097
2090	-0.097	1.000	-0.097
2091	-0.097	1.000	-0.097
2092	-0.097	1.000	-0.097
2093	-0.097	1.000	-0.097
2094	-0.097	1.000	-0.097
2095	-0.097	1.000	-0.097
2096	-0.097	1.000	-0.097
2097	-0.097	1.000	-0.097
2098	-0.097	1.000	-0.097
2099	-0.097	1.000	-0.097
2100	-0.097	1.000	-0.097

TABLE 4

SPHERICAL BELL FUNCTION

$$r^2 \leq 1$$

$$r^2/\eta = 0.25$$

η/r^2	S_1/r^2	S_2/r^2	S_3/r^2
0.950	-0.874	1.302	+0.010
0.900	-0.867	1.277	+0.008
0.850	-0.861	1.252	+0.007
0.800	-0.856	1.228	+0.005
0.750	-0.850	1.204	+0.004
0.700	-0.846	1.181	+0.003
0.650	-0.841	1.158	+0.002
0.600	-0.837	1.135	+0.001
0.550	-0.833	1.113	+0.000
0.500	-0.830	1.091	+0.000
0.450	-0.826	1.069	+0.000
0.400	-0.823	1.047	+0.000
0.350	-0.820	1.025	+0.000
0.300	-0.817	1.003	+0.000
0.250	-0.814	0.981	+0.000

TABLE 10

SPHERICAL ORBIT PROPERTIES

$$r_0^2 = 1.00$$

$$r_0^2 \bar{q} = 3.44$$

u/r_0^2	u_1/r_0^2	u/r_0^2	u_1/r_0^2
1.0000	-0.8000	1.4000	-0.8000
1.7000	-0.8076	1.5000	-0.8080
1.8000	-0.8090	1.5500	-0.8090
1.8500	-0.8095	1.5800	-0.8095
1.8750	-0.8096	1.6000	-0.8097
1.8900	-0.8096	1.6100	-0.8097
1.9000	-0.8096	1.6200	-0.8098
1.9100	-0.8096	1.6300	-0.8098
1.9200	-0.8096	1.6400	-0.8098
1.9300	-0.8096	1.6500	-0.8098
1.9400	-0.8096	1.6600	-0.8098
1.9500	-0.8096	1.6700	-0.8098
1.9600	-0.8096	1.6800	-0.8098
1.9700	-0.8096	1.6900	-0.8098
1.9800	-0.8096	1.7000	-0.8098
1.9900	-0.8096	1.7100	-0.8098

TABLE A5

SPHERICAL HARMONIC POLYNOMIALS

$$r_0^2 = 2.00$$

$$r^2/r_0^2 = 1.00$$

	Y_0^0		Y_2^0	Y_2^2
0	0.0000	-0.0148	1.4895	-0.1590
1	0.0000	-0.0148	1.7919	-0.1740
2	0.0000	-0.0148	0.8898	-0.1337
3	0.0075	-0.0148	1.2877	-0.1770
4	0.0000	-0.0148	1.8011	-0.1600
5	0.0148	-0.0148	0.7769	-0.1687
6	0.0000	-0.0148	1.1427	-0.1606
7	0.0148	-0.0148	1.0730	-0.1737
8	0.0170	-0.0148	0.9476	-0.1669
9	0.0148	-0.0148	1.0070	-0.1600
10	0.0000	-0.0147	0.7324	-0.1506
11	0.0148	-0.1477	0.9540	-0.1444

TABLE 19

SPHERICAL BELL POTENTIAL

$$r_0^3 = 1.10$$

$$r_0^3/p = 1.11$$

r/r_0	$2V/r^2$	$1/r^3$	$2V/r^2$
0.9000	-0.0475	1.4276	-0.1408
0.9125	-0.0470	1.4076	-0.1409
0.9250	-0.0465	1.3882	-0.1410
0.9375	-0.0460	1.3691	-0.1411
0.9500	-0.0455	1.3503	-0.1412
0.9625	-0.0450	1.3318	-0.1413
0.9750	-0.0445	1.3134	-0.1414
0.9875	-0.0440	1.2952	-0.1415
1.0000	-0.0435	1.2771	-0.1416
1.0125	-0.0430	1.2592	-0.1417
1.0250	-0.0425	1.2414	-0.1418
1.0375	-0.0420	1.2237	-0.1419
1.0500	-0.0415	1.2061	-0.1420
1.0625	-0.0410	1.1886	-0.1421
1.0750	-0.0405	1.1712	-0.1422
1.0875	-0.0400	1.1539	-0.1423
1.1000	-0.0395	1.1366	-0.1424

TABLE 25

SOLUBLE TENSIDES FOR THE CATIONIC CELL METHOD.

\bar{M}_n	\bar{M}_w
1.3	2 572
1.3	2 522
1.4	2 137
1.4	2 381
1.5	1 413
1.7	2 458
1.8	2 752
1.9	1 855
2.0	1 933
2.1	2 222
2.2	2 412
2.3	2 792
4.0	2 452
OH	2 452

APPENDIX

TABLE 45

LOWARD-SCHUBB H-12 PROPERTIES

λ, μ	ϵ/ϵ^0	n/n^0	α/α^0
0.50	+0.0010	1.40	+0.0000
1.00	+0.0040	1.53	+0.0001
1.50	+0.0421	1.56	+0.0014
2.00	+0.0470	1.53	+0.0004
2.50	+0.0879	1.58	+0.0076
3.00	+0.0954	1.58	+0.0177
3.50	+0.0811	1.56	+0.0408
4.00	+0.0807	1.55	+0.0534
4.50	+0.1177	1.56	+0.0000
5.00	+0.1510	1.55	+0.0001
5.50	+0.1679	1.55	+0.0004
6.00	+0.3004	1.55	+0.0001

TABLE III

LARGE- q LIMIT δ - δ POTENTIAL

q	δ	ϵ/μ	ϵ/μ^2
0.50	-0.0000	0.00	-0.0000
0.75	-0.0000	0.00	-0.0000
1.00	-0.0000	0.00	-0.0000
1.25	-0.0000	0.00	-0.0000
1.50	-0.0000	0.00	-0.0000
1.75	-0.0000	0.00	-0.0000
2.00	-0.0000	0.00	-0.0000
2.25	-0.0000	0.00	-0.0000
2.50	-0.0000	0.00	-0.0000
2.75	-0.0000	0.00	-0.0000
3.00	-0.0000	0.00	-0.0000
3.25	-0.0000	0.00	-0.0000
3.50	-0.0000	0.00	-0.0000
3.75	-0.0000	0.00	-0.0000
4.00	-0.0000	0.00	-0.0000

TABLE 82

LEONARD-JONES σ - π POTENTIAL

r/σ	σ/r^{12}	π/r^6	$\sigma - \pi$
0.80	-0.08879	1.35	-1.43879
0.85	-0.08400	1.00	-1.08400
0.90	-0.07939	0.69	-0.79390
0.95	-0.07497	0.49	-0.54970
1.00	-0.07065	0.36	-0.41065
1.05	-0.06643	0.26	-0.33643
1.10	-0.06231	0.19	-0.27231
1.15	-0.05828	0.14	-0.21828

TABLE 64

GEORGETOWN, 1949-50 PERCENTILE

σ^2	$\sigma^2 g^2$	g	$\sigma^2 h^2$	$\sigma^2 a^2$
.00	-0.0704	1.00	-0.0700	-0.0700
.25	-0.0713	1.50	-0.0700	-0.0700
.50	-0.0719	1.50	-0.0700	-0.0700
.75	-0.0719	1.50	-0.0700	-0.0700
1.00	-0.0719	1.50	-0.0700	-0.0700
1.25	-0.0720	1.50	-0.0700	-0.0700
1.50	-0.0720	1.50	-0.0700	-0.0700
1.75	-0.0720	1.50	-0.0700	-0.0700
2.00	-0.0720	1.50	-0.0700	-0.0700
2.25	-0.0720	1.50	-0.0700	-0.0700
2.50	-0.0720	1.50	-0.0700	-0.0700
2.75	-0.0720	1.50	-0.0700	-0.0700
3.00	-0.0720	1.50	-0.0700	-0.0700
3.25	-0.0720	1.50	-0.0700	-0.0700
3.50	-0.0720	1.50	-0.0700	-0.0700

TABLE 10

LIFTING-ORBIT 8-00 POSITION

λ	$\cos \lambda$
0	1.0000
1	0.9998
2	0.9996
3	0.9993
4	0.9989
5	0.9985
6 110	0.9980
6 120	0.9975
6 130	0.9970

TABLE 55

RANKING FORS T-14 ACROSTIC

$\frac{1}{2} \log \frac{1}{2}$	$\frac{1}{2} \log \frac{1}{2}$	$\frac{1}{2} \log \frac{1}{2}$	$\frac{1}{2} \log \frac{1}{2}$
1.48	10.0000	1.48	10.0000
1.49	10.0000	1.49	10.0000
1.50	10.0000	1.50	10.0000
1.51	10.0000	1.51	10.0000
1.52	10.0000	1.52	10.0000
1.53	10.0000	1.53	10.0000
1.54	10.0000	1.54	10.0000
1.55	10.0000	1.55	10.0000
1.56	10.0000	1.56	10.0000
1.57	10.0000	1.57	10.0000
1.58	10.0000	1.58	10.0000
1.59	10.0000	1.59	10.0000
1.60	10.0000	1.60	10.0000
1.61	10.0000	1.61	10.0000
1.62	10.0000	1.62	10.0000
1.63	10.0000	1.63	10.0000
1.64	10.0000	1.64	10.0000
1.65	10.0000	1.65	10.0000
1.66	10.0000	1.66	10.0000
1.67	10.0000	1.67	10.0000
1.68	10.0000	1.68	10.0000
1.69	10.0000	1.69	10.0000
1.70	10.0000	1.70	10.0000
1.71	10.0000	1.71	10.0000
1.72	10.0000	1.72	10.0000
1.73	10.0000	1.73	10.0000
1.74	10.0000	1.74	10.0000
1.75	10.0000	1.75	10.0000
1.76	10.0000	1.76	10.0000
1.77	10.0000	1.77	10.0000
1.78	10.0000	1.78	10.0000
1.79	10.0000	1.79	10.0000
1.80	10.0000	1.80	10.0000
1.81	10.0000	1.81	10.0000
1.82	10.0000	1.82	10.0000
1.83	10.0000	1.83	10.0000
1.84	10.0000	1.84	10.0000
1.85	10.0000	1.85	10.0000
1.86	10.0000	1.86	10.0000
1.87	10.0000	1.87	10.0000
1.88	10.0000	1.88	10.0000
1.89	10.0000	1.89	10.0000
1.90	10.0000	1.90	10.0000
1.91	10.0000	1.91	10.0000
1.92	10.0000	1.92	10.0000
1.93	10.0000	1.93	10.0000
1.94	10.0000	1.94	10.0000
1.95	10.0000	1.95	10.0000
1.96	10.0000	1.96	10.0000
1.97	10.0000	1.97	10.0000
1.98	10.0000	1.98	10.0000
1.99	10.0000	1.99	10.0000
2.00	10.0000	2.00	10.0000

Table 1

Summary of Test Results

Test No.	Test Date	Test Result	Test Location
1	10/10/2020	Pass	Test 1
2	10/10/2020	Pass	Test 2
3	10/10/2020	Pass	Test 3
4	10/10/2020	Pass	Test 4
5	10/10/2020	Pass	Test 5
6	10/10/2020	Pass	Test 6
7	10/10/2020	Pass	Test 7
8	10/10/2020	Pass	Test 8
9	10/10/2020	Pass	Test 9
10	10/10/2020	Pass	Test 10

[illegible]

APPENDIX C

TABLE 17

Values of α and β for various values of γ

Part I		Part II	
γ	α	γ	α
0.00	0.00	0.00	0.00
0.01	0.01	0.01	0.01
0.02	0.02	0.02	0.02
0.03	0.03	0.03	0.03
0.04	0.04	0.04	0.04
0.05	0.05	0.05	0.05
0.06	0.06	0.06	0.06
0.07	0.07	0.07	0.07
0.08	0.08	0.08	0.08
0.09	0.09	0.09	0.09
0.10	0.10	0.10	0.10
0.11	0.11	0.11	0.11
0.12	0.12	0.12	0.12
0.13	0.13	0.13	0.13
0.14	0.14	0.14	0.14
0.15	0.15	0.15	0.15
0.16	0.16	0.16	0.16
0.17	0.17	0.17	0.17
0.18	0.18	0.18	0.18
0.19	0.19	0.19	0.19
0.20	0.20	0.20	0.20
0.21	0.21	0.21	0.21
0.22	0.22	0.22	0.22
0.23	0.23	0.23	0.23
0.24	0.24	0.24	0.24
0.25	0.25	0.25	0.25
0.26	0.26	0.26	0.26
0.27	0.27	0.27	0.27
0.28	0.28	0.28	0.28
0.29	0.29	0.29	0.29
0.30	0.30	0.30	0.30
0.31	0.31	0.31	0.31
0.32	0.32	0.32	0.32
0.33	0.33	0.33	0.33
0.34	0.34	0.34	0.34
0.35	0.35	0.35	0.35
0.36	0.36	0.36	0.36
0.37	0.37	0.37	0.37
0.38	0.38	0.38	0.38
0.39	0.39	0.39	0.39
0.40	0.40	0.40	0.40
0.41	0.41	0.41	0.41
0.42	0.42	0.42	0.42
0.43	0.43	0.43	0.43
0.44	0.44	0.44	0.44
0.45	0.45	0.45	0.45
0.46	0.46	0.46	0.46
0.47	0.47	0.47	0.47
0.48	0.48	0.48	0.48
0.49	0.49	0.49	0.49
0.50	0.50	0.50	0.50

TABLE 2

A6. REFRACTION COEFFICIENT OF CO_2

TABLE 1		TABLE 2	
Temperature, °C	Refractive Index	Temperature 0-1	Refractive Index
°C	Ref.	°C	Ref.
-100	1.4	-1.0000	1.00
-90	1.5	-1.0001	1.01
-80	1.6	-1.0002	1.02
-70	1.7	-1.0003	1.03
-60	1.8	-1.0004	1.04
-50	1.9	-1.0005	1.05
-40	2.0	-1.0006	1.06
-30	2.1	-1.0007	1.07
-20	2.2	-1.0008	1.08
-10	2.3	-1.0009	1.09
0	2.4	-1.0010	1.10
10	2.5	-1.0011	1.11
20	2.6	-1.0012	1.12
30	2.7	-1.0013	1.13
40	2.8	-1.0014	1.14
50	2.9	-1.0015	1.15
60	3.0	-1.0016	1.16
70	3.1	-1.0017	1.17
80	3.2	-1.0018	1.18
90	3.3	-1.0019	1.19
100	3.4	-1.0020	1.20

W.C. CH

THERMAL PROPERTIES CONT. ABOUT 47 °C_g

Reservoir no. 3		Reservoir no. 4	
Thermal conductivity k (W/m·K)	Edge Pressure, psi	Thermal conductivity k (W/m·K)	Edge Pressure, psi
-4.8792	28	-4.8804	34
-4.8793	117	-4.8806	100
-4.8794	123	-4.8807	144
-4.8802	123	-4.8808	200
-4.8803	111	-4.8809	250
-4.8806	125	-4.8810	300
-4.8804	125	-4.8811	350
-4.8805	134	-4.8812	400
-4.8816	124	-4.8813	427
-4.8821	124	-4.8815	500
-4.8824	115	-4.8817	557
-4.8826	140	-4.8818	700
-4.8828	177	-4.8819	750
-4.8837	777	-4.8821	800
-4.8847	120		
-4.8853	102		
-4.8855	114		
-4.8858	102		
-4.8861	90		

DATE OF

NAME, ADDRESS, TELEPHONE NO.

DATE	DESCRIPTION	AMOUNT	BALANCE
1900			
1901			
1902			
1903			
1904			
1905			
1906			
1907			
1908			
1909			
1910			
1911			
1912			
1913			
1914			
1915			
1916			
1917			
1918			
1919			
1920			
1921			
1922			
1923			
1924			
1925			
1926			
1927			
1928			
1929			
1930			
1931			
1932			
1933			
1934			
1935			
1936			
1937			
1938			
1939			
1940			
1941			
1942			
1943			
1944			
1945			
1946			
1947			
1948			
1949			
1950			
1951			
1952			
1953			
1954			
1955			
1956			
1957			
1958			
1959			
1960			
1961			
1962			
1963			
1964			
1965			
1966			
1967			
1968			
1969			
1970			
1971			
1972			
1973			
1974			
1975			
1976			
1977			
1978			
1979			
1980			
1981			
1982			
1983			
1984			
1985			
1986			
1987			
1988			
1989			
1990			
1991			
1992			
1993			
1994			
1995			
1996			
1997			
1998			
1999			
2000			
2001			
2002			
2003			
2004			
2005			
2006			
2007			
2008			
2009			
2010			
2011			
2012			
2013			
2014			
2015			
2016			
2017			
2018			
2019			
2020			
2021			
2022			
2023			
2024			
2025			
2026			
2027			
2028			
2029			
2030			
2031			
2032			
2033			
2034			
2035			
2036			
2037			
2038			
2039			
2040			
2041			
2042			
2043			
2044			
2045			
2046			
2047			
2048			
2049			
2050			
2051			
2052			
2053			
2054			
2055			
2056			
2057			
2058			
2059			
2060			
2061			
2062			
2063			
2064			
2065			
2066			
2067			
2068			
2069			
2070			
2071			
2072			
2073			
2074			
2075			
2076			
2077			
2078			
2079			
2080			
2081			
2082			
2083			
2084			
2085			
2086			
2087			
2088			
2089			
2090			
2091			
2092			
2093			
2094			
2095			
2096			
2097			
2098			
2099			
2100			
2101			
2102			
2103			
2104			
2105			
2106			
2107			
2108			
2109			
2110			
2111			
2112			
2113			
2114			
2115			
2116			
2117			
2118			
2119			
2120			
2121			
2122			
2123			
2124			
2125			
2126			
2127			
2128			
2129			
2130			
2131			
2132			
2133			
2134			
2135			
2136			
2137			
2138			
2139			
2140			
2141			
2142			
2143			
2144			
2145			
2146			
2147			
2148			
2149			
2150			
2151			
2152			
2153			
2154			
2155			
2156			
2157			
2158			
2159			
2160			
2161			
2162			
2163			
2164			
2165			
2166			
2167			
2168			
2169			
2170			
2171			
2172			
2173			
2174			
2175			
2176			
2177			
2178			
2179			
2180			
2181			
2182			
2183			
2184			
2185			
2186			
2187			
2188			
2189			
2190			
2191			
2192			
2193			
2194			
2195			
2196			
2197			
2198			
2199			
2200			
2201			
2202			
2203			
2204			
2205			
2206			
2207			
2208			
2209			
2210			
2211			
2212			
2213			
2214			
2215			
2216			
2217			
2218			
2219			
2220			
2221			
2222			
2223			
2224			
2225			
2226			
2227			
2228			
2229			
2230			
2231			
2232			
2233			
2234			
2235			
2236			
2237			
2238			
2239			
2240			
2241			
2242			
2243			
2244			
2245			
2246			
2247			
2248			
2249			
2250			
2251			
2252			
2253			
2254			
2255			
2256			
2257			
2258			
2259			
2260			
2261			
2262			
2263			
2264			
2265			
2266			
2267			
2268			
2269			
2270			
2271			
2272			
2273			
2274			
2275			
2276			
2277			
2278			
2279			
2280			
2281			
2282			
2283			
2284			
2285			
2286			
2287			
2288			
2289			
2290			
2291			
2292			
2293			
2294			
2295			
2296			
2297			
2298			
2299			
2300			
2301			
2302			
2303			
2304			
2305			
2306			
2307			
2308			
2309			
2310			
2311			
2312			
2313			
2314			
2315			
2316			
2317			
2318			
2319			
2320			
2321			
2322			
2323			
2324			
2325			
2326			
2327			
2328			
2329			
2330			
2331			
2332			
2333			
2334			
2335			
2336			
2337			
2338			
2339			
2340			
2341			
2342			
2343			
2344			
2345			
2346			
2347			
2348			
2349			
2350			
2351			
2352			

TABLE 107

THERMAL-ELASTIC EXPANSION OF P_1

Temperature, °F		Temperature, °C	
Temperature, °F	Area (inches ²)	Temperature, °C	Area (inches ²)
100	0.000	100	0.000
150	0.000	150	0.000
200	0.000	200	0.000
250	0.000	250	0.000
300	0.000	300	0.000
350	0.000	350	0.000
400	0.000	400	0.000
450	0.000	450	0.000
500	0.000	500	0.000
550	0.000	550	0.000
600	0.000	600	0.000
650	0.000	650	0.000
700	0.000	700	0.000
750	0.000	750	0.000
800	0.000	800	0.000
850	0.000	850	0.000
900	0.000	900	0.000
950	0.000	950	0.000
1000	0.000	1000	0.000

TABLE 6.

CALCULATED PERCENT COMPOSITION OF Al_2O_3

Sample No. 7			Sample No. 10	
Wavelength, μ	Wavenumber, cm^{-1}	Transmittance, %	Wavenumber, cm^{-1}	Depth of Absorption, μ
1.25	8000	100	4000	10
1.30	7692	100	3500	100
1.35	7317	100	3000	100
1.40	7143	100	2500	100
1.45	6897	100	2000	100
1.50	6667	100	1800	100
1.55	6452	100	1600	100
1.60	6250	100	1400	100
1.65	6061	100	1200	100
1.70	5882	100	1000	100
1.75	5714	100	900	100
1.80	5556	100	800	100
1.85	5405	100	700	100
1.90	5263	100	600	100
1.95	5128	100	500	100
2.00	5000	100	400	100
2.05	4878	100	300	100
2.10	4762	100	200	100
2.15	4651	100	150	100
2.20	4545	100	100	100
2.25	4444	100	50	100
2.30	4348	100	0	100
2.35	4257	100		
2.40	4170	100		
2.45	4088	100		
2.50	4010	100		
2.55	3937	100		
2.60	3869	100		
2.65	3804	100		
2.70	3743	100		
2.75	3685	100		
2.80	3630	100		
2.85	3578	100		
2.90	3529	100		
2.95	3483	100		
3.00	3440	100		
3.05	3399	100		
3.10	3361	100		
3.15	3325	100		
3.20	3291	100		
3.25	3259	100		
3.30	3229	100		
3.35	3200	100		
3.40	3173	100		
3.45	3148	100		
3.50	3125	100		
3.55	3103	100		
3.60	3083	100		
3.65	3064	100		
3.70	3046	100		
3.75	3029	100		
3.80	3013	100		
3.85	2998	100		
3.90	2984	100		
3.95	2971	100		
4.00	2959	100		
4.05	2948	100		
4.10	2938	100		
4.15	2928	100		
4.20	2919	100		
4.25	2910	100		
4.30	2902	100		
4.35	2894	100		
4.40	2887	100		
4.45	2880	100		
4.50	2873	100		
4.55	2867	100		
4.60	2861	100		
4.65	2855	100		
4.70	2850	100		
4.75	2845	100		
4.80	2840	100		
4.85	2835	100		
4.90	2830	100		
4.95	2826	100		
5.00	2822	100		
5.05	2818	100		
5.10	2814	100		
5.15	2810	100		
5.20	2807	100		
5.25	2804	100		
5.30	2801	100		
5.35	2798	100		
5.40	2795	100		
5.45	2792	100		
5.50	2790	100		
5.55	2787	100		
5.60	2785	100		
5.65	2783	100		
5.70	2781	100		
5.75	2779	100		
5.80	2777	100		
5.85	2775	100		
5.90	2773	100		
5.95	2771	100		
6.00	2770	100		
6.05	2768	100		
6.10	2767	100		
6.15	2766	100		
6.20	2765	100		
6.25	2764	100		
6.30	2763	100		
6.35	2762	100		
6.40	2761	100		
6.45	2760	100		
6.50	2760	100		
6.55	2759	100		
6.60	2758	100		
6.65	2758	100		
6.70	2757	100		
6.75	2757	100		
6.80	2756	100		
6.85	2756	100		
6.90	2755	100		
6.95	2755	100		
7.00	2754	100		
7.05	2754	100		
7.10	2753	100		
7.15	2753	100		
7.20	2753	100		
7.25	2752	100		
7.30	2752	100		
7.35	2752	100		
7.40	2751	100		
7.45	2751	100		
7.50	2751	100		
7.55	2750	100		
7.60	2750	100		
7.65	2750	100		
7.70	2750	100		
7.75	2749	100		
7.80	2749	100		
7.85	2749	100		
7.90	2748	100		
7.95	2748	100		
8.00	2748	100		
8.05	2747	100		
8.10	2747	100		
8.15	2747	100		
8.20	2746	100		
8.25	2746	100		
8.30	2746	100		
8.35	2745	100		
8.40	2745	100		
8.45	2745	100		
8.50	2744	100		
8.55	2744	100		
8.60	2744	100		
8.65	2743	100		
8.70	2743	100		
8.75	2743	100		
8.80	2742	100		
8.85	2742	100		
8.90	2742	100		
8.95	2741	100		
9.00	2741	100		
9.05	2741	100		
9.10	2740	100		
9.15	2740	100		
9.20	2740	100		
9.25	2739	100		
9.30	2739	100		
9.35	2739	100		
9.40	2738	100		
9.45	2738	100		
9.50	2738	100		
9.55	2737	100		
9.60	2737	100		
9.65	2737	100		
9.70	2736	100		
9.75	2736	100		
9.80	2736	100		
9.85	2735	100		
9.90	2735	100		
9.95	2735	100		
10.00	2734	100		

Table 1

Group A		Group B	
Year	Value	Year	Value
1990	100	1990	100
1991	105	1991	105
1992	110	1992	110
1993	115	1993	115
1994	120	1994	120
1995	125	1995	125
1996	130	1996	130
1997	135	1997	135
1998	140	1998	140
1999	145	1999	145
2000	150	2000	150
2001	155	2001	155
2002	160	2002	160
2003	165	2003	165
2004	170	2004	170
2005	175	2005	175
2006	180	2006	180
2007	185	2007	185
2008	190	2008	190
2009	195	2009	195
2010	200	2010	200
2011	205	2011	205
2012	210	2012	210
2013	215	2013	215
2014	220	2014	220
2015	225	2015	225
2016	230	2016	230
2017	235	2017	235
2018	240	2018	240
2019	245	2019	245
2020	250	2020	250

TABLE 1

ANNUAL ENERGY CONSUMPTION, BTU

Consumption by		Consumption by	
Manufacturing and construction	Other	Manufacturing and construction	Other
1949	144	1949	144
1950	144	1950	144
1951	144	1951	144
1952	144	1952	144
1953	144	1953	144
1954	144	1954	144
1955	144	1955	144
1956	144	1956	144
1957	144	1957	144
1958	144	1958	144
1959	144	1959	144
1960	144	1960	144
1961	144	1961	144
1962	144	1962	144
1963	144	1963	144
1964	144	1964	144
1965	144	1965	144
1966	144	1966	144
1967	144	1967	144
1968	144	1968	144
1969	144	1969	144
1970	144	1970	144
1971	144	1971	144
1972	144	1972	144
1973	144	1973	144
1974	144	1974	144
1975	144	1975	144
1976	144	1976	144
1977	144	1977	144
1978	144	1978	144
1979	144	1979	144
1980	144	1980	144
1981	144	1981	144
1982	144	1982	144
1983	144	1983	144
1984	144	1984	144
1985	144	1985	144
1986	144	1986	144
1987	144	1987	144
1988	144	1988	144
1989	144	1989	144
1990	144	1990	144
1991	144	1991	144
1992	144	1992	144
1993	144	1993	144
1994	144	1994	144
1995	144	1995	144
1996	144	1996	144
1997	144	1997	144
1998	144	1998	144
1999	144	1999	144
2000	144	2000	144
2001	144	2001	144
2002	144	2002	144
2003	144	2003	144
2004	144	2004	144
2005	144	2005	144
2006	144	2006	144
2007	144	2007	144
2008	144	2008	144
2009	144	2009	144
2010	144	2010	144
2011	144	2011	144
2012	144	2012	144
2013	144	2013	144
2014	144	2014	144
2015	144	2015	144
2016	144	2016	144
2017	144	2017	144
2018	144	2018	144
2019	144	2019	144
2020	144	2020	144
2021	144	2021	144
2022	144	2022	144
2023	144	2023	144
2024	144	2024	144
2025	144	2025	144
2026	144	2026	144
2027	144	2027	144
2028	144	2028	144
2029	144	2029	144
2030	144	2030	144
2031	144	2031	144
2032	144	2032	144
2033	144	2033	144
2034	144	2034	144
2035	144	2035	144
2036	144	2036	144
2037	144	2037	144
2038	144	2038	144
2039	144	2039	144
2040	144	2040	144
2041	144	2041	144
2042	144	2042	144
2043	144	2043	144
2044	144	2044	144
2045	144	2045	144
2046	144	2046	144
2047	144	2047	144
2048	144	2048	144
2049	144	2049	144
2050	144	2050	144
2051	144	2051	144
2052	144	2052	144
2053	144	2053	144
2054	144	2054	144
2055	144	2055	144
2056	144	2056	144
2057	144	2057	144
2058	144	2058	144
2059	144	2059	144
2060	144	2060	144
2061	144	2061	144
2062	144	2062	144
2063	144	2063	144
2064	144	2064	144
2065	144	2065	144
2066	144	2066	144
2067	144	2067	144
2068	144	2068	144
2069	144	2069	144
2070	144	2070	144
2071	144	2071	144
2072	144	2072	144
2073	144	2073	144
2074	144	2074	144
2075	144	2075	144
2076	144	2076	144
2077	144	2077	144
2078	144	2078	144
2079	144	2079	144
2080	144	2080	144
2081	144	2081	144
2082	144	2082	144
2083	144	2083	144
2084	144	2084	144
2085	144	2085	144
2086	144	2086	144
2087	144	2087	144
2088	144	2088	144
2089	144	2089	144
2090	144	2090	144
2091	144	2091	144
2092	144	2092	144
2093	144	2093	144
2094	144	2094	144
2095	144	2095	144
2096	144	2096	144
2097	144	2097	144
2098	144	2098	144
2099	144	2099	144
2100	144	2100	144

TABLE C30

THERMAL EXPANSION COEFFICIENT OF CO_2

Temperature t		Temperature t	
Temperature t , °C	Thermal Expansion Coeff. β , per cent	Temperature t , °C	Thermal Expansion Coeff. β , per cent
-4.7700	75	-0.0170	80
-4.7600	147.5	-0.0100	147.5
-4.7500	220	-0.0030	220
-4.7400	298	-0.0000	298
-4.7300	384	-0.0070	384
-4.7200	465	-0.0140	465
-4.7100	571.5	-0.0210	571.5
-4.7000	670	-0.0280	670
-4.6900	770	-0.0350	770
-4.6800	875	-0.0420	875
-4.6700	1000.0	-0.0490	1000.0

TABLE VII
THERMAL FREQUENCY COEFFICIENT OF α_1

MEASUREMENT 1		MEASUREMENT 2	
Thermocouple No. 1 in mill. sec.	Seal Pressure, psi.	Thermocouple No. 1 in mill. sec.	Seal Pressure, psi.
14-11145	500	14-11145	75
14-11144	475	14-11141	150
14-11143	500	14-11134	225
14-11142	525	14-11128	300
14-11141	550	14-11125	375
14-11140	575	14-11122	450
14-11139	600	14-11120	525
14-11138	625	14-11114	600
		14-11110	675
		14-11104	750
		14-11098	825
		14-11091	900
		14-11077	975

TABLE C-2

THERMAL EXPANSION COEFFICIENT OF Cu_2S

Experiment 7		Experiment 8	
Temperature (°C)	Exp. Expansion (ppm)	Temperature (°C)	Exp. Expansion (ppm)
-0.1150	20	-0.1700	294
-0.1200	200	-0.1800	302
-0.1300	252	-0.1900	329
-0.1400	277	-0.2000	336
-0.1500	307	-0.2100	374
-0.1600	354	-0.2200	701
-0.1700	477	-0.2300	704
-0.1800	594	-0.2350	674
-0.1900	670	-0.2400	670
-0.2000	750.2		
-0.2100	800		
-0.2200	907		
-0.2300	1000		

TABLE 13.7

THERMAL FREQUENCY COEFFICIENT OF α_2

Experiment 11		Experiment 12	
Temperature (°F)	Gap Frequency, Hz	Temperature (°F)	Gap Frequency, Hz
$t = t_0 \pm \Delta t$		$t = t_0 \pm \Delta t$	
-0.0700	0	-0.1804	0
-0.0704	4	-0.1804	400
-0.0708	80	-0.1800	800
-0.0712	160	-0.1800	1200
-0.0716	240	-0.1800	1600
-0.0720	320	-0.1800	2000
-0.0724	400	-0.1800	2400
-0.0728	480	-0.1800	2800
-0.0732	560	-0.1800	3200
-0.0736	640	-0.1800	3600
-0.0740	720	-0.1800	4000
-0.0744	800	-0.1800	4400

ABBREVIATIONS

α	Number of states of type A in a molecule
β	Reduced rate for state β
γ	Constant in water vapor concentration equation (4) (1000) in Part II. Defined by Equation 42
α'	Number of states of type A in a molecule
β'	Second virial coefficient, also sometimes written as β_2 . Used in Part I and defined by Equation 21
β	Constant in water vapor concentration for liquids in Part II. Defined by Equation 40
β^0, β^1	Reduced second virial coefficients, also written as β_2^0, β_2^1
α	Number of states of type A in a molecule. Also a parameter defined by Equation 17 and used only in Equations (49)
β^0, β^1	First virial coefficients, used in Part I and defined by Equation 20
β	Generalized constant in cell model for constant dielectric used in Part II
α	Part I: Number of states of type A in a molecule. Also a parameter defined by Equation 17 and used only in Equations (49) Part II: Average distance between molecules centers in a liquid
β^0, β^1	Fourth virial coefficients, used in Part I and defined by Equation 22
β	Generalized constant in cell model for constant dielectric used in Part II
α	$\alpha = 1$ of monomers
β	Configurational energy

χ	Value of χ at the minimum in $\chi(\chi)$. Used as a parameter for a molecule
$\chi(\mathbf{R}, \mathbf{T}, \mathbf{T})$	Radial distribution function also written as $\chi(r)$ and $\rho_2(r)$ or $\rho_2(r)/\rho^2$
χ	Helmholtz's constant
χ	Adiabatic constant in the general form of the Lennard-Jones potential
χ	Repulsive constant in the general form of the Lennard-Jones potential
χ	Factor of molecules usually taken as Avogadro's Number
χ	Average number of molecules per unit volume
χ	Pressure
χ_c	Critical pressure
χ	Part I: Distance between centers of atoms or molecules Part II: Distance of a molecule from the center of the cell
χ	Value of χ when $\chi(\chi) = 0$. Usually used as a parameter for an sign
χ	Value of χ at the minimum of $\chi(r)$. Usually used as a parameter for an sign
χ	Statistical short potential; potential that accounts for effects of mutual potential energy function
χ	Distance between molecular centers. Used as the shortest only in Equations (2), (3), and (4)
χ	Value of χ when $\chi(\chi) = 0$. Used as a parameter for a molecule
χ	Value of χ at the minimum in $\chi(r)$. Used as a parameter for a molecule
χ^2/χ_0	
χ	Temperature, $^{\circ}\text{K}$
χ	Relative temperature
χ	Reduced temperature T/T^*
χ	Boyle temperature

δ	Perimeter defined by Equation 4
\bar{r}	Mean position
\bar{r}^2	Value of $\bar{r}(t)$ at the instant is $20\bar{r}$. Usually used as a parameter for noise
ρ	Distance from the center of a molecule to the center of a neighboring one
τ	Time
ω	Angular distance to Pitzer's correlation (22)

- 1385 van der Waals, L., *and* *Verduyn*, *Arch. Sci.*, **11**, 15 (1956).
- 1386 Z. F. Shyns, *J. Gen. Res. Ser.*, *Soviet Union*, **11**, 457 (1955).
- 1387 P. De Groot, "Thermodynamic Functions of Gases," Vol. 1, Butterworths, London (1951).
- 1388 T. H. Keesom, in "Viscosity Calculations," edited J. E. Hilder, Vol. 1, Butterworths Press, New York (1952).
- 1389 J. C. McGarvey and R. E. Kline, *Trans. Faraday Soc.*, **41**, 454 (1945).
- 1390 F. G. Pyrie and R. L. Ballingale, *Trans. Faraday Soc.*, **41**, 793 (1945).
- 1391 R. E. Keesom, R. J. Ballingale, and J. F. Keesom, *Trans. Faraday Soc.*, **41**, 161 (1945).
- 1392 R. G. Treloar, J. E. Leland, and R. E. Thomas, *Australian J. Chem.*, **5**, 149 (1952).
- 1393 International Scientific Association Research Project "Selected Values of Properties of Chemical Compounds," Carnegie Institute of Technology, Pittsburgh (1952).
- 1394 J. E. Perry, editor, "Chemical Engineers' Handbook," McGraw-Hill, New York, New York (1950).
- 1395 Scientific Publications Institute Research Project 44 "Selected Values of Physical and Thermodynamic Properties of Hydrocarbons and Related Compounds," Carnegie Press, Pittsburgh (1954).
- 1396 R. L. Alder, E. W. Depner, J. E. Hilder, and R. Keesom, *J. Chem. Phys.*, **12**, 1036 (1944).
- 1397 R. Keesom and R. L. Keesom, *J. Chem. Phys.*, **12**, 1911 (1944).
- 1398 R. Treloar, R. E. Keesom, and J. E. Hilder, *Phys. Rev.*, **41**, 122 (1943).
- 1399 R. W. Depner, R. J. Alder, and J. E. Hilder, *J. Chem. Phys.*, **12**, 1405 (1944).
- 1400 "NBS Bulletin: Ser. of Scientific Instruments," **11**, 105 (1941).
- 1401 R. J. Candler, *Lectures on Polymer Science*, University of Florida, 1941.
- 1402 R. J. Candler, "The Properties of High Polymers," R. Bell & Sons Ltd., New York (1942).

- 121) National Research Council, "International Critical Tables of Numerical Data, Physics, Chemistry, and Technology," McGraw-Hill Book Co., Inc., New York (1963).
- 122) E. L. Finkle, *Refrigeration Engineering* 22, 364 (1955).
- 123) J. K. Knowlton, "Alcohols and Liquid Mixtures," Butterworths, London, 1955.
- 124) E. S. Rouse and E. L. Lachert, *Refrigeration Engineering* 1, 43 (1948).
- 125) E. S. Rouse, Jr., *American Chemical Society Properties Division of Petroleum Chemistry* 1, No. 2, 108 (1954).
- 126) J. H. Hildebrand and R. L. Scott, "The Solubility of Gas-Liquid Systems," 2nd Edition, Reinhold Publishing Co., New York (1950).
- 127) J. H. Hildebrand and R. L. Scott, *J. Chem. Phys.* 1, 267 (1933).
- 128) J. C. DeCoursey and E. E. Rumpf, *Trans. Faraday Soc.* 22, 377 (1926).
- 129) Text unpublished work.

EDUCATIONAL RECORD

Marvin Lynn Holliday was born March 8, 1937, at Ocala, Florida. In June, 1955, he was graduated from Ben McLarty High School of Fort Pierce, Florida. In June, 1959, Mr. Holliday received the degree of Bachelor of Science Engineering from the University of Florida. He continued his studies at the University of Florida and received the degree of Master of Science in Engineering in August, 1960. From that time until the present, Mr. Holliday has been a National Science Foundation Cooperative Graduate Fellow pursuing his work toward the degree of Doctor of Philosophy.

Marvin Lynn Holliday is married to the former Helen Lynn Mills and has one child, Kathryn Lynn Holliday. Mr. Holliday is a member of Phi Kappa Phi honorary fraternity.

This ~~document~~ was prepared under the direction of the officers of the ~~document's~~ advisory committee and has been approved by all members of said committee. It was submitted to the Dean of the College of Engineering and to the Graduate Council, and was approved as partial fulfillment of the requirements for the degree of Doctor of Philosophy.

June 20, 1963

Josephine A. ...
Dean, College of Engineering

Dean, Graduate School

Department of Physics

L. M. ...
Chairman

John ...
John ...
John ...
Thomas F. ...